

8-27-2009

Shock formation properties of continuum and kinetic models

Pavlo Cherepanov

Follow this and additional works at: https://digitalrepository.unm.edu/math_etds

Recommended Citation

Cherepanov, Pavlo. "Shock formation properties of continuum and kinetic models." (2009). https://digitalrepository.unm.edu/math_etds/10

This Dissertation is brought to you for free and open access by the Electronic Theses and Dissertations at UNM Digital Repository. It has been accepted for inclusion in Mathematics & Statistics ETDs by an authorized administrator of UNM Digital Repository. For more information, please contact disc@unm.edu.

Pavlo Cherepanov

Candidate

Mathematics and Statistics

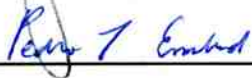
Department

This dissertation is approved, and it is acceptable in quality and form for publication:

Approved by the Dissertation Committee:



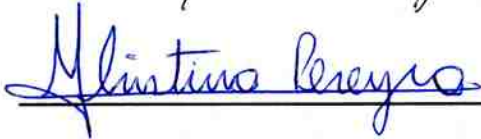
Lorenz, Jens, Chairperson



Embid, Pedro



Hayat, Majeed



Pereyra, Cristina

Shock Formation Properties of Continuum and Kinetic Models

by

Pavlo Cherepanov

B.S., Applied Mathematics, NTUU-KPI, Kiev Ukraine, 2000
M.S., Applied Mathematics, NTUU-KPI, Kiev, Ukraine, 2002
M.S., Pure Mathematics, University of New Mexico, 2003

DISSERTATION

Submitted in Partial Fulfillment of the
Requirements for the Degree of

Doctor of Philosophy
Mathematics

The University of New Mexico

Albuquerque, New Mexico

August, 2009

©2009, Pavlo Cherepanov

Dedication

to mom

Acknowledgments

I am enormously thankful to my adviser Dr. J. Lorenz for his belief in me and without whose guidance and encouragement this dissertation would have never been possible. I want to thank all my family back in Eastern Europe and in the United States whose continuous influx of support has neither ceased nor weakened during my journey in America. I am grateful to all my friends for being patient and understanding of my need to be in seclusion over the last few months of my work.

**Shock Formation Properties
of
Continuum and Kinetic Models**

by

Pavlo Cherepanov

ABSTRACT OF DISSERTATION

Submitted in Partial Fulfillment of the
Requirements for the Degree of

Doctor of Philosophy
Mathematics

The University of New Mexico

Albuquerque, New Mexico

August, 2009

Shock Formation Properties of Continuum and Kinetic Models

by

Pavlo Cherepanov

B.S., Applied Mathematics, NTUU-KPI, Kiev Ukraine, 2000

M.S., Applied Mathematics, NTUU-KPI, Kiev, Ukraine, 2002

M.S., Pure Mathematics, University of New Mexico, 2003

Ph.D., Mathematics, University of New Mexico, 2009

Abstract

Continuum Mechanics and Kinetic Theory are two mathematical theories with fundamentally different approaches to the same physical phenomenon. Continuum Mechanics together with Thermodynamics treat a substance (a gas or a fluid) as a continuous medium and describes the evolution of its macro characteristics via application of the Conservation Laws to small packets of the substance. Kinetic Theory attempts to describe the evolution of the macro parameters by treating a substance as a family of colliding objects. The number of objects must be large enough so a statistical approach can be taken.

In this work we introduce a numerical scheme to solve 1-D Bhatnagar–Gross–Krook model equations and examine the formation of a stationary viscous shock. Obtained results are compared to a stationary numerical solution of 1-D Navier–Stokes equation with a similar set of shock forming conditions.

Contents

List of Figures	xiii
List of Tables	xv
Glossary	xvii
1 Motivation of Study: Thermodynamic Limits	1
1.1 Introduction	1
1.2 Equations of Continuum Mechanics and Thermodynamics	5
1.3 Kinetic Theory	9
1.3.1 Thermodynamic Regimes	9
1.3.2 The Boltzmann Equation	12
1.3.3 The H-Theorem	18
1.3.4 Nondimensionalization of the Boltzmann Equation	20
1.3.5 The Bhatnagar–Gross–Krook Model	23
1.3.6 The Hilbert Procedure	24

Contents

2	Non-dimensionalization of 1-D Euler and Navier-Stokes Systems	32
2.1	The Navier-Stokes System in Physical Variables	32
2.2	The Navier-Stokes System in Generic Variables	36
2.3	The 1-D Navier-Stokes and Euler systems in non-conservative quantities	42
3	The Equations for a Viscous, Heat-Conducting and Inviscid Stationary Shocks	45
3.1	The Rankine-Hugoniot Conditions	45
3.2	An Example of Shock Forming Boundary Conditions	49
4	Numerical Solutions of 1-D Euler and Navier-Stokes Equations	51
4.1	The Numerical Problem Setup	51
4.2	The Upwinding First Order Difference Operator	53
4.3	The Explicit Numerical Scheme for the 1-D Euler System	56
4.4	The Implicit Numerical Scheme for the 1-D Navier-Stokes System	58
4.5	Boundary Conditions	63
4.5.1	Boundary Conditions for the 1-D Euler System	63
4.5.2	Boundary Conditions for the 1-D Navier-Stokes System	68
5	Numerical Solution of the 1-D Bhatnagar–Gross–Krook Model	71
5.1	The Continuous 1-D BGK Model	71
5.2	Numerical Solution of the 1-D BGK Model	73

Contents

5.3	The Boundary Conditions	77
5.4	The Truncation Error	80
5.5	The Reassembling Error	82
6	Numerical Simulations and Results	85
6.1	Numerical Problem Setup	85
6.2	Simulation Results	91
6.3	Analysis of Simulation Results	93
6.3.1	Shock Width	95
6.3.2	Regression Analysis of the Shock Width	110
6.3.3	Conclusions	111
A	Integration Procedures	121
A.1	Moments of the 1-D Maxwellian Distribution	121
A.2	Moments of the 3-D Maxwellian Distribution	123
A.2.1	Additional Moments of Maxwellian Distribution	125
B	Continuum and Kinetic Theory	128
B.1	The Nondimensionalized 3-D Euler System	128
B.2	Proof of Identities (1.56)-(1.58) in Section 1.3.2	130
B.3	Some Details of the Proof of the H-Theorem	132
B.4	Calculation of $D_t \log f_0$	133

Contents

B.5	Certain Orthogonality Relations for Tensors A and B	136
B.6	A Transformation of the Compressible Euler System	138
C	Technical Calculations for Numerical Solutions	142
C.1	Truncation Error Estimation Theorem	142
C.2	Some Technical Result for Section 4.5.1	145
C.3	Computation of the Jacobian for the Implicit Scheme in Sections 4.4 .	146
	References	148

List of Figures

3.1	Inflowing and outflowing characteristics	49
4.1	Stationary Shock Solutions for 1-D Euler System	64
4.2	Direction of propagation of a solution of equation (4.69)	70
5.1	Inflowing and outflowing characteristics of the BGK model	79
6.1	Initial conditions for the 1-D Navier-Stokes and the 1-D Bhatnagar– Gross–Krook models.	91
6.2	Initial distributions	92
6.14	Viscosity and shock profiles	94
6.16	Shock width definition	95
6.3	Numerical stationary solution NS_0RE_r case	98
6.4	Numerical stationary solution NS_1RE_r case	99
6.5	Numerical stationary solution NS_2RE_r case	100
6.6	Numerical stationary solution NS_3RE_r case	101
6.7	Numerical stationary solution NS_4RE_r case	102

List of Figures

6.8	Numerical stationary solution BGK ₀ T _t case	103
6.9	Numerical stationary solution BGK ₁ T _t case	104
6.10	Numerical stationary solution BGK ₂ T _t case	105
6.11	Numerical stationary solution BGK ₃ T _t case	106
6.12	Numerical stationary solution BGK ₄ T _t case	107
6.13	Stationary distributions $f_j(x)$ for BGK ₀ T _t case	108
6.15	Side by side comparison of the macroscopic observables obtained by Navier-Stokes and Bhatnagar–Gross–Krook simulations in the case of BC ₃ set of boundary conditions	109
6.17	Navier-Stokes shock width regression for BC ₀ and BC ₁ sets of bound- ary conditions	115
6.18	Navier-Stokes shock width regression for BC ₂ and BC ₃ sets of bound- ary conditions	116
6.19	Navier-Stokes shock width regression for BC ₄ set of boundary condi- tions	117
6.20	BGK shock width regression for BC ₀ and BC ₁ sets of boundary con- ditions	118
6.21	BGK shock width regression for BC ₂ and BC ₃ sets of boundary con- ditions	119
6.22	BGK shock width regression for BC ₄ set of boundary conditions . . .	120

List of Tables

2.1	List of primary macroscopic observables used in the 1-D Navier-Stokes system	33
2.2	List of secondary macroscopic observables used in the 1-D Navier-Stokes system	33
6.1	Examples of the exact values of shock forming boundary data	87
6.2	Examples of the approximate values of shock forming boundary data	87
6.3	Parameters used in the numerical scheme to solve the 1-D Navier-Stokes system	88
6.4	Computation of truncation error estimate	89
6.5	Parameters used in the numerical scheme to solve the 1-D Bhatnagar-Gross-Krook equation	90
6.6	References to the figures and corresponding pages for results of numerical simulations of the Navier-Stokes and Bhatnagar-Gross-Krook models.	93
6.7	Shock width measurements of numerical solutions	97
6.8	Proportionality coefficients of θ -associated shock width for BGK model	111

List of Tables

6.9	Navier-Stokes and BGK shock width regression results	114
A.1	Moments of Maxwellian Distribution.	126

Glossary

\log	natural logarithm
\mathbb{N}	set of natural numbers
\mathbb{R}	set of real numbers
$C(\mathbb{R}^n)$	set of continuous functions defined on \mathbb{R}^n , n can be $1, 2, \dots$, etc.
$\text{Mat}_n(\mathbb{R})$	space of real n -by- n matrices
\mathbb{S}	unit sphere $\{\vec{x} \in \mathbb{R}^3 : \vec{x} = 1\}$
\oplus	direct sum of linear subspaces
\otimes	dyadic product, outer product, $\vec{u} \otimes \vec{v} = \vec{u} \cdot \vec{v}^T$
$\otimes 2$	dyadic square, $\vec{v}^{\otimes 2} = \vec{v} \otimes \vec{v}$
:	scalar product of matrices (see formula 1.117 on p.1.117)
*	reverse-order notation for matrix-vector multiplication (p.29)
\perp	orthogonal subspaces, orthogonal compliment
∂_t	partial derivative with respect to t
D_t	material derivative (see definition on p.25)

Glossary

Div	divergence applied to a tensor field (formula 1.44, p.15)
tr	trace of a square matrix
\mathcal{Ker}	null space of a linear operator
$\mathcal{I}m$	image space of a linear operator
l.s.	linear span
BGK	Bhatnagar–Gross–Krook
NS	Navier-Stokes

Chapter 1

Motivation of Study: Thermodynamic Limits

1.1 Introduction

There are two approaches to studying the dynamic theory of gases. One can consider a set of macroscopic equations in terms of independent macroscopic variables such as density ρ , velocity \vec{v} and temperature θ . A classic example of such equations is the set compressible Navier-Stokes equations or inviscid Euler equations. On the other hand one can address the problem from the more fundamental point of view involving microscopic one particle distribution function $f = f(t, \vec{x}, \vec{v})$ known as the microscopic state. Its evolution is described by the Boltzmann Equation. The first approach is a combination of the Theory of Fluid Dynamics and Thermodynamics. The later one is known as the Kinetic Theory. There have been a significant amount of effort to demonstrate that these two fundamentally different approaches lead to the same result as far as the macroscopic behavior of a gas concerned.

Development of Fluid Dynamics started with Euler by his introduction of inviscid

Chapter 1. Motivation of Study: Thermodynamic Limits

flow equations in 1755. Claude Louis Marie Henri Navier derived the famous Navier-Stokes equations in 1822 when he first introduced viscous effects. The derivations of equation of motions were further refined by Cauchy in 1828 and Poisson in 1829. Finally in 1843 George Gabriel Stokes published a derivation of the equations that is well understood and is known until today.

Development of the Kinetic Theory started as early as 1738 when Daniel Bernoulli proposed the idea that a gas consists of a finite number of elastic particles with non-zero radii colliding and bouncing at high speeds. Bernoulli suggested that the motion of such a system is governed by the laws of elementary mechanics. The idea of discrete matter was not completely new, because a few Greek Philosophers asserted that the splitting of matter onto two equal parts can be repeated only until the smallest possible quantity of matter is achieved. The fresh taste to the old idea was imparted by the hypothesis that macro properties of gas such as pressure and temperature can be attributed to the mechanical motion of the colliding spheres. Although Bernoulli Theory can qualitatively explain elementary properties of gases such as temperature, compressibility, etc., its rigorous quantitative verification was not possible until much later – during the formation of Kinetic Theory in the beginning of 19th century.

Although the laws of mechanics are relatively simple, understanding the overall behavior of the family may prove to be a very challenging task, especially when long time behavior or thermodynamical limits are of interest. One should expect that the resolution of simple mechanical laws will provide a complete description of the dynamics of the system. Although true, this is an infeasible practical challenge. Indeed, when one accounts for the number of the members in the ensemble it becomes clear that this is not a feasible computational problem. Namely, the order of magnitude of the ensemble whose members need to be tracked individually is related to the Avogadro Number (6.022×10^{23}). It becomes clear that at the present state of

Chapter 1. Motivation of Study: Thermodynamic Limits

computer and applied science¹ there is not enough computational power available to address a problem of such magnitude.

Position and velocity of each of the spheres (\vec{x}_i, \vec{v}_i) is called a microscopic state. Provided the number of all microscopic states is very large, an attempt to describe the behavior of the gas through microscopic states of its molecules is doomed to fail. Thus probabilistic methods of what is presently known as Statistical Mechanics should be employed. This should prove a fruitful approach since a change in a small number of micro-states of particles will not affect the macro-state of the gas. Moreover, in reality, the only observable variables one can detect are macroscopic parameters of the gas such as temperature, density, velocity, stresses and heat flow. These observables should depend on some statistical averages of microscopic states. The average quantities is all that matters in determining the macroscopic state. Thus solving for microscopic states is not only a complex but also an unnecessary problem.

The original idea for statistical treatment of an ensemble belongs to Ludwig Boltzmann who laid out the foundation of modern Statistical Mechanics. He introduced [2] the distribution function f that statistically describes the behavior of gases. After neglecting trinary and higher order collisions and assuming the Molecular Chaos Hypothesis (Stosszahlansatz) Boltzmann wrote down a partial differential equation describing an evolution of f .

$$\partial_t f + \vec{v} \cdot \vec{\nabla} f = \mathcal{B}(f, f) \tag{1.1}$$

This famous equation is known as The Boltzmann Equation or the Maxwell-Boltzmann Equation. In the same paper of 1872 [2] he introduced an important consequence of his equation known as The H-Theorem. The H-Theorem explains the irreversibility of natural process in gases by showing that the molecular collisions tend to increase chaos inside a gas. Appearance of this theorem resulted in a big turmoil in the scien-

¹year 2009

Chapter 1. Motivation of Study: Thermodynamic Limits

tific community of that time. The result seemed to produce a number of paradoxes and hence it was rejected by many mathematicians and physicists by the end of the 19th century.

However, shortly after Boltzmann's death in 1906 the existence of atoms had been established experimentally and detailed heuristic analysis of the Boltzmann Equation by Paulus and Tatiana Ehrenfest reinstated [11] its credibility and the Kinetic Theory regained much popularity among scientists.

The Boltzmann Equation has become a universal tool in investigating a behavior of dilute gases (Kinetic Regime)² where the continuum approach of Fluid Dynamics is incapable of producing reliable simulations. Significant efforts were applied to obtain its approximate and exact solutions. David Hilbert first obtained [10] a result expressing a solution of the Boltzmann Equation as a series expansion³. S. Chapman [9] and D. Enskog [12] obtained a series solution valid for dense gases. Global existence and uniqueness were proved by T. Carleman [5, 6, 7] in certain restricting assumption which were removed in the following papers. H. Grad [15] developed a systematic method of expanding a solution of the Boltzmann Equation in a series of orthogonal polynomials.

Even in the most simple physical applications solving the Boltzmann equation is rather a cumbersome task due to the complexity of its nonlinear right hand side term $\mathcal{B}(f, f)$, which is known as the Collision Integral. A modification of the collision integral was proposed by P. L. Bhatnagar, E. P. Gross, M. Krook in [1] and is known as the BGK Model.

$$\mathcal{B}_{\text{BGK}}(f, f) = -\frac{1}{\tau}(f - f_e) \tag{1.2}$$

The modified collision term is designed to conserve mass, momentum and energy as

²see Section 1.3.1.

³see Section 1.3.6 for a review

well as to ensure that the microscopic one particle density function is close to the equilibrium distribution f_e provided by the H-Theorem. The corresponding BGK-Boltzmann equation has been known to adequately model properties of gases both in Fluid Regime as well as Knudsen Regime where applicability of the Navier-Stokes equations are limited.

In this dissertation we consider the particular situation of one-dimensional viscous flow in the Fluid Regime. The general comparison of the Kinetic Theory and Fluid Dynamics is a major undertaking of Statistical Mechanics and cannot be addressed within a scope of this work. However we consider one single aspect of the problem. Due to its strong non-linearity, the Navier-Stokes system it has been known [19, 22] to exhibit shock layer solutions under certain conditions. The author investigates whether it is possible to obtain a comparable viscous shock layer profile by developing and applying similar conditions to the BGK-Boltzmann model. The BGK-Boltzmann model is set up and numerically solved. The solution is then compared to the solution of the corresponding compressible Navier-Stokes system.

1.2 Equations of Continuum Mechanics and Thermodynamics

Consider a system of partial equations that describes a viscous heat conducting flow subject to external force \vec{f} and external heat source Q [20]:

$$\begin{aligned}
 \partial_t \rho + \operatorname{div}(\rho \vec{u}) &= 0, \\
 \partial_t(\rho \vec{u}) + \operatorname{Div}(\rho \vec{u} \otimes \vec{u}) &= \rho \vec{f} + \operatorname{div} \sigma, \\
 \partial_t \left(\frac{1}{2} \rho |\vec{u}|^2 + \rho e \right) + \operatorname{div} \left[\rho \vec{u} \left(\frac{1}{2} |\vec{u}|^2 + e \right) \right] + \operatorname{div}(\vec{q}) &= \rho \vec{f} \cdot \vec{u} + \operatorname{div}(\sigma \vec{u}) + \rho Q,
 \end{aligned} \tag{1.3}$$

Chapter 1. Motivation of Study: Thermodynamic Limits

where ρ , \vec{u} , e are local quantities characterizing the density, velocity, and internal energy per unit mass; $\sigma = -pI + \tau$ is the stress tensor, τ is the shear stress and p is the pressure. The capitalized divergence operator (Div) is the extension of the regular divergence from vector fields to matrix fields. The definition of Div is given by (1.44). For the purposes of this chapter we will assume that the flow is subject to no external influences i.e.

$$\begin{aligned}\vec{f} &= 0, \\ Q &= 0\end{aligned}\tag{1.4}$$

and, furthermore we will neglect viscous and heat conducting effects in the flow

$$\begin{aligned}\tau &= 0, \\ \vec{q} &= 0.\end{aligned}\tag{1.5}$$

After the assumptions (1.4,1.5) system (1.3) reduces to the system of Euler equations describing 3-D inviscid compressible flow

$$\begin{aligned}\partial_t \rho + \text{div}(\rho \vec{u}) &= 0, \\ \partial_t(\rho \vec{u}) + \text{Div}(\rho \vec{u} \otimes \vec{u}) + \vec{\nabla} p &= 0, \\ \partial_t \left(\frac{1}{2} \rho |\vec{u}|^2 + \rho e \right) + \text{div} \left[\rho \vec{u} \left(\frac{1}{2} |\vec{u}|^2 + e \right) + p \vec{u} \right] &= 0.\end{aligned}\tag{1.6}$$

We will assume the following equations of state

$$\begin{aligned}p &= \frac{R}{M} \rho \theta, \\ e &= \frac{C_V}{M} \theta,\end{aligned}\tag{1.7}$$

where θ is the temperature, M , R , and C_V are gas specific and universal constants described in Table 2.2. Equations (1.6) are provided in physical variables therefore

Chapter 1. Motivation of Study: Thermodynamic Limits

we rewrite the system in terms of generic variables $\hat{\rho}$, $\hat{\vec{u}}$, \hat{e} and $\hat{\theta}$ such that

$$\begin{aligned}\vec{x} &= L\hat{\vec{x}}, & \vec{u} &= u_0\hat{\vec{u}}, \\ t &= t_0\hat{t}, & e &= e_0\hat{e}, \\ \rho &= \rho_0\hat{\rho}, & \theta &= \theta_0\hat{\theta}, \\ p &= p_0\hat{p}.\end{aligned}\tag{1.8}$$

We assume the following four normalization identities that regulate the characteristic quantities

$$u_0 = Lt_0^{-1}\tag{1.9}$$

$$e_0 = u_0^2\tag{1.10}$$

$$R\theta_0 = Mu_0^2\tag{1.11}$$

$$p_0 = \rho_0u_0^2\tag{1.12}$$

After applying transformations (1.8) to system (1.6) and implementing state equations (1.7), the resulting system will depend on variables $\hat{\rho}$, $\hat{\vec{u}}$, and $\hat{\theta}$. For simplicity of notations, hats ($\hat{\cdot}$) above the variables will be dropped. The resulting system is given by (1.13), where γ is a gas specific constant⁴ (2.33). The details of rescaling procedure are provided in Appendix B.1.

$$\begin{aligned}\partial_t\rho + \text{div}(\rho\vec{u}) &= 0, \\ \partial_t(\rho\vec{u}) + \text{Div}(\rho\vec{u} \otimes \vec{u}) + \vec{\nabla}(\rho\theta) &= 0, \\ \partial_t\left(\frac{1}{2}\rho|\vec{u}|^2 + \frac{1}{\gamma-1}\rho\theta\right) + \text{div}\left[\rho\vec{u}\left(\frac{1}{2}|\vec{u}|^2 + \frac{\gamma}{\gamma-1}\theta\right)\right] &= 0.\end{aligned}\tag{1.13}$$

⁴In general γ depends on the temperature of the gas. We will assume that the medium is *calorically perfect*, i.e. $\gamma = \text{const}$

Chapter 1. Motivation of Study: Thermodynamic Limits

Let us consider a few specific examples of the Euler system. For a gas whose molecules have d degrees of freedom, it has been calculated [20]⁵ that γ can be given by

$$\gamma = \frac{d+2}{d}. \quad (1.14)$$

We will further consider a monoatomic gas whose molecules are modeled by hard spheres (Section 1.3.1). In this case a molecule has $d = 3$ degrees of freedom and hence $\gamma = \frac{5}{3}$. In this case the Euler system takes form

$$\begin{aligned} \partial_t \rho + \operatorname{div}(\rho \vec{u}) &= 0, \\ \partial_t(\rho \vec{u}) + \operatorname{Div}(\rho \vec{u} \otimes \vec{u}) + \vec{\nabla}(\rho \theta) &= 0, \\ \partial_t \left(\frac{1}{2} \rho |\vec{u}|^2 + \frac{3}{2} \rho \theta \right) + \operatorname{div} \left[\rho \vec{u} \left(\frac{1}{2} |\vec{u}|^2 + \frac{5}{2} \theta \right) \right] &= 0, \end{aligned} \quad (1.15)$$

which coincides with (Section 1.3.6). Starting Chapter 2 our efforts will be concentrated on one-dimensional Euler and Navier-Stokes systems. In order to obtain a 1-D version of (1.13) we eliminate dependance on coordinates x_2 and x_3 i.e. it is assumed that $\partial_{x_2} = \partial_{x_3} = 0$ and therefore the state variable can be treated as

$$\begin{aligned} \rho &= \rho(t, x_1), \\ \vec{u} &= [u_1(x_1, t) \ 0 \ 0]^T, \\ \theta &= \theta(x_1, t) \end{aligned} \quad (1.16)$$

To simplify notations x_1 is denoted by x , and u_1 is denoted by u . The system (1.13) reduces to

$$\begin{aligned} \partial_t \rho + \partial_x(\rho u) &= 0, \\ \partial_t(\rho u) + \partial_x(\rho u^2 + \rho \theta) &= 0, \\ \partial_t \left(\frac{1}{2} \rho u^2 + \frac{1}{\gamma-1} \rho \theta \right) + \partial_x \left[\rho u \left(\frac{1}{2} u^2 + \frac{\gamma}{\gamma-1} \theta \right) \right] &= 0. \end{aligned} \quad (1.17)$$

⁵p.43, formula 3-20

Chapter 1. Motivation of Study: Thermodynamic Limits

In the case of “one-dimensional gas”, a member-molecule possesses $d = 1$ degree of freedom, and therefore according to (1.14) the adiabatic ratio for a monoatomic hard sphere gas must be set

$$\gamma = 3, \tag{1.18}$$

and the 1-D equations of inviscid flow become

$$\begin{aligned} \partial_t \rho + \partial_x (\rho u) &= 0, \\ \partial_t (\rho u) + \partial_x (\rho u^2 + \rho \theta) &= 0, \\ \partial_t \left(\frac{1}{2} \rho u^2 + \frac{1}{2} \rho \theta \right) + \partial_x \left[\rho u \left(\frac{1}{2} u^2 + \frac{3}{2} \theta \right) \right] &= 0. \end{aligned} \tag{1.19}$$

We have discussed 1-D and 3-D cases of inviscid flow. The 3-D Euler system (1.15) will be obtained from a solution of the Boltzmann Equation (see Section 1.3.6). The 1-D case was discussed to justify $\gamma = 3$ value. This case will be addressed as the main subject of study of this dissertation starting Chapter 2.

1.3 Kinetic Theory

1.3.1 Thermodynamic Regimes

Consider a gas confined in a vessel with characteristic length L and volume V . Assume that the vessel contains \mathcal{N} molecules colliding with each other. We will assume that a molecule is a spherical hard object with radius $r > 0$. Let l be the average distance between two collisions of a typical molecule. Quaintly l is called the *mean free path*. We resort to an intuitive meaning of mean free path⁶. The volume that is not available for molecular motion is called *the excluded volume*. The

⁶For the exact definition of mean free path see [25, 24]

excluded volume V_e can be calculated as the volume of all the molecules once they are tightly packed. It is clear that

$$\mathcal{N} \cdot \frac{4\pi}{3} r^3 < V_e < \mathcal{N} \cdot (2r)^3 \quad (1.20)$$

The mean free path l can be expressed (see [24]) in terms of the excluded volume and the size of a molecule by

$$l \simeq \frac{1}{\frac{\mathcal{N}}{V - V_e} \cdot 4\mathcal{A}} \quad (1.21)$$

where $\mathcal{A} = \pi r^2$ is the cross section of a molecule. A gas is called rarified when the mean free path is comparable to the characteristic length. The rarefication degree is measured by dimensionless number called the Knudsen number $\mathcal{K}n$

$$\mathcal{K}n = \frac{l}{L} \quad (1.22)$$

Gas dynamics identifies two regimes:

1. **Fluid Regime.** A fluid regime is characterized by the mean free path that is negligible with respect to the characteristic length of the container. A fluid regime is characterized in terms of of Knudsen number as

$$\mathcal{K}n \ll 1 \quad (1.23)$$

In this case the gas is said to be in the state of local thermodynamic equilibrium and its state can be adequately characterized by a few continuum variables such as pressure $p = p(t, \vec{x}) \geq 0$, temperature $\theta = \theta(t, \vec{x}) > 0$, and velocity $\vec{u} = \vec{u}(t, \vec{x}) \in \mathbb{R}^3$. Evolution of the continuum variables is described by equations of continuum mechanics and thermodynamics such as Navier-Stokes or Euler equations.

2. **Kinetic Regime.** In the case the gas is more rarefied i.e. there is not enough collisions happening between molecules of for a local equilibrium to be achieved. The gas is said to be in the Kinetic Regime. The average path traveled between two consecutive collisions is comparable to the characteristic length of the vessel or equivalently

$$\mathcal{K}n = \mathcal{O}(1). \quad (1.24)$$

In this case the state of the gas can be described by a single-particle phase space density function

$$f = f(t, \vec{x}, \vec{v}) \geq 0. \quad (1.25)$$

Function f provides a statistical distribution of the molecules by their velocities \vec{v} and locations \vec{x} at any time $t \geq 0$. Thus the total momentum of the gas can be calculated by averaging over all velocities and coordinates with respect to the density $f(t, \vec{x}, \vec{v})$

$$\vec{M}(t) = \int_{\mathbb{R}^3} \int_{\mathbb{R}^3} m\vec{v}f(t, \vec{x}, \vec{v})d\vec{v}d\vec{x} \quad (1.26)$$

Similarly, the local macroscopic distribution of momentum is given by

$$\vec{\rho}_M(t, \vec{x}) = \int_{\mathbb{R}^3} m\vec{v}f(t, \vec{x}, \vec{v})d\vec{v}d\vec{x} \quad (1.27)$$

where m is the mass of one molecule. Momentum density defined by (1.27) is one of the *macroscopic observables* that can be obtained as an image of mapping

$$\phi \mapsto \int_{\mathbb{R}^3} \phi(\vec{v})f(t, \vec{x}, \vec{v})d\vec{v} \quad (1.28)$$

applied to a scalar or vector field $\phi = \phi(\vec{v})$. Statistical approach is valid in the a fluid regime as well. Thus we have two descriptions of the state of a gas. One that

involves a set of two scalar and one vector field and that is valid for fluid regimes. The other description is statistical and it adequate for both fluid and kinetic regimes. A natural and the most general question is to describe how these two approaches to the same physical phenomenon relate to each other.

1.3.2 The Boltzmann Equation

In the absence of external forces, the evolution of one-particle density functions f is described by the *Boltzmann Equation*

$$\partial_t f + \vec{v} \cdot \vec{\nabla}_{\vec{x}} f = \mathcal{B}(f, f) \quad (1.29)$$

The left hand side $\partial_t f + \vec{v} \cdot \vec{\nabla}_{\vec{x}} f$ of the Boltzmann Equation is called the streaming part and the right hand side $\mathcal{B}(f, f)$ is called the collision integral. The streaming part can be expressed in terms of the material derivative defined as

$$D_t f = \partial_t f + \vec{v} \cdot \vec{\nabla}_{\vec{x}} f = \partial_t f + \text{div}_{\vec{x}}(\vec{v}f) \quad (1.30)$$

Using (1.30) the Boltzmann Equation can be written in an alternative form

$$\partial_t f + \text{div}_{\vec{x}}(\vec{v}f) = \mathcal{B}(f, f) \quad (1.31)$$

The derivation of the Boltzmann Equation is provided in [4, 13, 16]. Before giving an expression of the collision integral we will briefly discuss the idea involved in its derivation.

Let us consider two colliding molecules A and A_* with the same masses m and radii r . Let (\vec{v}', \vec{v}'_*) and (\vec{v}, \vec{v}_*) be pre- and post-collision velocities of the molecules.

Chapter 1. Motivation of Study: Thermodynamic Limits

Due to the assumption that all molecules of the gas have the same mass, the laws of conservation of momentum and energy read

$$\begin{aligned}\vec{v} + \vec{v}_* &= \vec{v}' + \vec{v}'_* \\ |\vec{v}|^2 + |\vec{v}_*|^2 &= |\vec{v}'|^2 + |\vec{v}'_*|^2\end{aligned}\tag{1.32}$$

If we treat the pre-collision velocities \vec{v}' and \vec{v}'_* as functions of the post-collision ones \vec{v} and \vec{v}_* , equations (1.32) constitute a homogeneous system of five equations an six unknowns whose all solutions are [18]

$$\begin{aligned}\vec{v}' &= \vec{v}'(\vec{v}, \vec{v}_*, \vec{\omega}) = \vec{v} - [(\vec{v} - \vec{v}_*) \cdot \vec{\omega}] \vec{\omega} \\ \vec{v}'_* &= \vec{v}'_*(\vec{v}, \vec{v}_*, \vec{\omega}) = \vec{v}_* + [(\vec{v} - \vec{v}_*) \cdot \vec{\omega}] \vec{\omega}\end{aligned}\tag{1.33}$$

where $\vec{\omega} \in \mathbb{S}^2$ is a free parameter.

For a hard sphere gas with elastic collisions⁷, collision integral $\mathcal{B}(f, f)$ takes form [18]

$$\mathcal{B}(f, f)(\vec{v}) = 2r^2 \int_{\mathbb{R}^3} \int_{\mathbb{S}^2} [f(\vec{v}')f(\vec{v}'_*) - f(\vec{v})f(\vec{v}_*)] |(\vec{v} - \vec{v}_*) \cdot \vec{\omega}| d\vec{\omega} d\vec{v}_* \tag{1.34}$$

Following the standard notation adopted in the Kinetic theory, we set

$$\begin{aligned}f_* &= f(t, \vec{x}, \vec{v}_*), \\ f' &= f(t, \vec{x}, \vec{v}'), \\ f'_* &= f(t, \vec{x}, \vec{v}'_*),\end{aligned}\tag{1.35}$$

where \vec{v}' and \vec{v}'_* are defined by (1.33). The notation for the collision integral (1.34) reduces to

$$\mathcal{B}(f, f)(\vec{v}) = 2r^2 \int_{\mathbb{R}^3} \int_{\mathbb{S}^2} [f'f'_* - ff_*] |(\vec{v} - \vec{v}_*) \cdot \vec{\omega}| d\vec{\omega} d\vec{v}_* \tag{1.36}$$

⁷Momentum and energy are preserved

Chapter 1. Motivation of Study: Thermodynamic Limits

The inner integral $\int_{\mathbb{S}^2}$ is the surface integral over unit sphere defined by

$$\int_{\mathbb{S}^2} f(\vec{\omega}) d\vec{\omega} = \oint_{\omega_1^2 + \omega_2^2 + \omega_3^2 = 1} f(\omega_1, \omega_2, \omega_3) dS \quad (1.37)$$

Proposition 1. *Assume that f is a locally L_1 -integrable and faster than polynomially decaying function on \mathbb{R}^3 . Assume that $\phi \in C(\mathbb{R}^3)$ has at most polynomial growth on infinity. Then the following formula is true:*

$$\begin{aligned} \int_{\mathbb{R}^3} \mathcal{B}(f, f) \phi(v) d\vec{v} &= \\ &= \frac{2r^2}{4} \int_{\mathbb{R}^3} \int_{\mathbb{R}^3} \int_{\mathbb{S}^3} [f' f'_* - f f_*] (\phi + \phi_* - \phi' - \phi'_*) |(\vec{v} - \vec{v}_*) \cdot \vec{\omega}| d\vec{\omega} d\vec{v} d\vec{v}_* \end{aligned} \quad (1.38)$$

For a proof of Proposition 1 see [18].

Definition 1. *The continuous function $\phi : \mathbb{R}^3 \rightarrow \mathbb{R}$ is called a collision invariant if $\forall \vec{v}, \vec{v}_* \in \mathbb{R}^3$ and $\forall \vec{\omega} \in \mathbb{S}^2$ the following is true*

$$\phi(\vec{v}) + \phi(\vec{v}_*) = \phi(\vec{v}') + \phi(\vec{v}'_*) \quad (1.39)$$

where \vec{v} and \vec{v}'_* are defined by (1.33).

Due to (1.33), examples of collision invariants include

$$\begin{aligned} \phi_0(\vec{v}) &= 1 \\ \phi_k(\vec{v}) &= v_k, \quad k = 1, 2, 3 \\ \phi_4(\vec{v}) &= \frac{1}{2} |\vec{v}|^2 \end{aligned} \quad (1.40)$$

It follows from Definition 1, that any linear combination of ϕ_k , $k = 0, 1, \dots, 4$ is a collision invariant as well. The next proposition provides a description of all collision invariants. A proof of Proposition 2 is given in [8].

Proposition 2. *Any collision invariant must be of the form*

$$\phi(\vec{v}) = a + \vec{b} \cdot \vec{v} + c |\vec{v}|^2 \quad (1.41)$$

where $a, c \in \mathbb{R}$ and $\vec{b} \in \mathbb{R}^3$

Corollary 1. *For any collision invariant ϕ and for any rapidly decaying measurable f the following is true*

$$\int_{\mathbb{R}^3} \mathcal{B}(f, f) \phi(\vec{v}) d\vec{v} = 0 \quad (1.42)$$

Proof. The proof follows from Proposition 2 and Definition 1. Since ϕ is a collision invariant we have

$$\phi + \phi_* - \phi' - \phi'_* = 0 \quad (1.43)$$

and therefore the integral in the right hand side of (1.38) is zero. Thus the conclusion follows. \square

Before we proceed with the next corollary we extend the definition of the divergence to a matrix field. Let $A : \mathbb{R}^3 \rightarrow \text{Mat}_3(\mathbb{R})$ be a matrix field, then

$$\text{Div}_{\vec{x}} A = \begin{bmatrix} \text{div}_{\vec{x}} A_1^T \\ \text{div}_{\vec{x}} A_2^T \\ \text{div}_{\vec{x}} A_3^T \end{bmatrix} \quad (1.44)$$

where A_k are rows of A . Definition of Div allows us to state the following corollary in a compact form.

Corollary 2. *Let $f = f(t, \vec{x}, \vec{v})$ be a locally integrable and rapidly decaying in \vec{v} solution of the Boltzmann Equation (1.29). Then for $k = 1, 2, 3$*

$$\int_{\mathbb{R}^3} \mathcal{B}(f, f) d\vec{v} = \int_{\mathbb{R}^3} \mathcal{B}(f, f) v_k d\vec{v} = \int_{\mathbb{R}^3} \mathcal{B}(f, f) \frac{1}{2} |\vec{v}|^2 d\vec{v} = 0 \quad (1.45)$$

Chapter 1. Motivation of Study: Thermodynamic Limits

Moreover the following local conservation laws hold:

$$\partial_t \int_{\mathbb{R}^3} f(t, \vec{x}, \vec{v}) d\vec{v} + \operatorname{div}_{\vec{x}} \int_{\mathbb{R}^3} \vec{v} f(t, \vec{x}, \vec{v}) d\vec{v} = 0 \quad (1.46)$$

$$\partial_t \int_{\mathbb{R}^3} \vec{v} f(t, \vec{x}, \vec{v}) d\vec{v} + \operatorname{div}_{\vec{x}} \int_{\mathbb{R}^3} \vec{v} \otimes \vec{v} f(t, \vec{x}, \vec{v}) d\vec{v} = 0 \quad (1.47)$$

$$\partial_t \int_{\mathbb{R}^3} \frac{1}{2} |\vec{v}|^2 f(t, \vec{x}, \vec{v}) d\vec{v} + \operatorname{div}_{\vec{x}} \int_{\mathbb{R}^3} \vec{v} \frac{1}{2} |\vec{v}|^2 f(t, \vec{x}, \vec{v}) d\vec{v} = 0 \quad (1.48)$$

Proof. Since ϕ_k , defined by (1.40), are collision invariants, according to Corollary 1

$$\int_{\mathbb{R}^3} \mathcal{B}(f, f) \phi_k(\vec{v}) d\vec{v} = 0, \quad \forall k = 0, 1, \dots, 4 \quad (1.49)$$

and thus (1.45) is obtained.

In order to obtain (1.46)-(1.48) we multiply Boltzmann Equation in (1.31) by each of the collision invariants ϕ_k defined by (1.40) and integrate over \mathbb{R}^3 :

$$\partial_t \int_{\mathbb{R}^3} \phi_k f d\vec{v} + \operatorname{div}_{\vec{x}} \int_{\mathbb{R}^3} \vec{v} \phi_k f d\vec{v} = \int_{\mathbb{R}^3} \mathcal{B}(f, f) \phi_k d\vec{v} \quad (1.50)$$

We notice that $\int_{\mathbb{R}^3} \mathcal{B}(f, f) \phi_k d\vec{v} = 0$ because of (1.45) and therefore (1.46) and (1.48) follow. It becomes clear that (1.47) holds as well after $\operatorname{div}_{\vec{x}} \int_{\mathbb{R}^3} \vec{v} \otimes \vec{v} f d\vec{v}$ is written in the component form

$$\left[\operatorname{Div}_{\vec{x}} \int_{\mathbb{R}^3} \vec{v} \otimes \vec{v} f d\vec{v} \right]_k = \operatorname{div}_{\vec{x}} \int_{\mathbb{R}^3} v_k \vec{v} f d\vec{v} \quad (1.51)$$

and this finalizes the proof. □

Chapter 1. Motivation of Study: Thermodynamic Limits

We define the following fields

$$\rho(t, \vec{x}) = \int_{\mathbb{R}} f d\vec{v} \quad (1.52)$$

$$u(t, \vec{x}) = \rho^{-1} \int_{\mathbb{R}} \vec{v} f d\vec{v} \quad (1.53)$$

$$P(t, \vec{x}) = \int_{\mathbb{R}} (\vec{v} - \vec{u})^{\otimes 2} f d\vec{v} \quad (1.54)$$

$$C(t, \vec{x}) = \int_{\mathbb{R}} (\vec{v} - \vec{u}) |\vec{v} - \vec{u}|^2 f d\vec{v} \quad (1.55)$$

It can be shown (see Appendix B.2) that the moments of the distribution function are

$$\int_{\mathbb{R}^3} \vec{v}^{\otimes 2} f d\vec{v} = \rho \vec{u}^{\otimes 2} + P \quad (1.56)$$

$$\int_{\mathbb{R}^3} |\vec{v}|^2 f d\vec{v} = \rho |\vec{u}|^2 + \text{tr } P \quad (1.57)$$

$$\int_{\mathbb{R}^3} \vec{v} |\vec{v}|^2 f d\vec{v} = [\rho |\vec{u}|^2 + \text{tr } P] \vec{u} + 2P\vec{u} + C \quad (1.58)$$

and therefore equations (1.46)-(1.48) take form

$$\begin{aligned} \partial_t \rho + \text{div}(\rho \vec{u}) &= 0 \\ \partial_t(\rho \vec{u}) + \text{Div}(\rho \vec{u} \otimes \vec{u} + P) &= 0 \\ \partial_t \frac{1}{2}(\rho |\vec{u}|^2 + \text{tr } P) + \text{div} \frac{1}{2}[(\rho |\vec{u}|^2 + \text{tr } P) \vec{u} + 2P\vec{u} + C] &= 0 \end{aligned} \quad (1.59)$$

One can observe that if we take

$$\begin{aligned} P &= pI, \\ C &= 0, \end{aligned} \quad (1.60)$$

with pressure p subject to the Ideal Gas Law (1.7)⁸, then system (1.59) will become the 3-D Euler system with the adiabatic ratio $\gamma = \frac{5}{3}$ that corresponds to a gas with $d = 3$ degrees of freedom (see formula 1.14):

$$\begin{aligned} \partial_t \rho + \operatorname{div}(\rho \vec{u}) &= 0, \\ \partial_t(\rho \vec{u}) + \operatorname{Div}(\rho \vec{u} \otimes \vec{u}) + \vec{\nabla}(\rho \theta) &= 0, \\ \partial_t \left(\frac{1}{2} \rho |\vec{u}|^2 + \frac{3}{2} \rho \theta \right) + \operatorname{div} \left[\rho \vec{u} \left(\frac{1}{2} |\vec{u}|^2 + \frac{5}{2} \theta \right) \right] &= 0. \end{aligned} \tag{1.61}$$

The resulting system is the same as provided by (1.15) in Section 1.2. Despite of this remarkable coincidence, assumptions (1.60) are unsubstantiated and cannot be accepted.

1.3.3 The H-Theorem

The most famous form of the Boltzmann's H-Theorem allows to solve the following integral equation

$$\mathcal{B}(f, f) = 0 \tag{1.62}$$

as well as it provides an expression for the entropy production rate. We will state only a part of the H-Theorem to the extent that suffices to proceed with our consideration. A complete version of the H-Theorem can be found in [18].

Theorem 1. *Let $f : \mathbb{R}^3 \rightarrow \mathbb{R}$ be a locally integrable function with at most polynomial decay on infinity. Then the following statements are equivalent:*

$$(a) \quad \mathcal{B}(f, f) = 0 \text{ a.e.}, \tag{1.63}$$

⁸The Ideal Gas Law in nondimensionalized variables takes form $p = \rho \theta$. See Appendix B.1 formula (B.5)

Chapter 1. Motivation of Study: Thermodynamic Limits

$$(b) \quad \int_{\mathbb{R}} \mathcal{B}(f, f) \log f d\vec{v} = 0, \quad (1.64)$$

(c) the distribution f is a Maxwellian density $f = f_{(\rho, u, \theta)}^e$, i.e.

$$f = f_{(\rho, u, \theta)}^e(\vec{v}) = \frac{\rho}{\sqrt{(2\pi\theta)^3}} \exp \left\{ -\frac{|\vec{v} - \vec{u}|^2}{2\theta} \right\}, \quad (1.65)$$

for some $\rho, \theta > 0$ and $\vec{u} \in \mathbb{R}^3$.

Proof. Implication (a) \implies (b) follows from the properties of the Lebesgue integral.

Assume that statement (b) holds. We apply Proposition 1 for $\phi = f$ and we get

$$\begin{aligned} 0 &= \int_{\mathbb{R}} \mathcal{B}(f, f) \log f d\vec{v} = \\ &= \frac{2r^2}{4} \int_{\mathbb{R}^3} \int_{\mathbb{R}^3} \int_{\mathbb{S}^3} [f' f'_* - f f_*] \log \frac{f f_*}{f' f'_*} |(\vec{v} - \vec{v}_*) \cdot \vec{\omega}| d\vec{\omega} d\vec{v} d\vec{v}_* \end{aligned} \quad (1.66)$$

Trivially

$$(b - a) \log \frac{a}{b} \leq 0 \quad \forall a, b > 0 \quad (1.67)$$

therefore it follows from (1.66) that for a continuous f

$$f' f'_* - f f_* = 0 \text{ a.e.} \iff \log f' + \log f'_* = \log f + \log f_* \text{ a.e.} \quad (1.68)$$

If f is a continuous function then $\log f$ is a collision invariant (Definition 1) and therefore, by Proposition 2, it must be of the form

$$\log f = a + \vec{b} \cdot \vec{v} + c |\vec{v}|^2 \quad (1.69)$$

Conclusion (1.69) still can be achieved without assuming continuity of f (see for details in [18, 3, 23]). Since f is a decaying function, c must be negative. Statement (c) follows after setting

$$\begin{aligned}\rho &= \sqrt{-\frac{\pi^3}{c^3}} \exp \left\{ a - \frac{|\vec{b}|^2}{4c} \right\}, \\ \vec{u} &= -\frac{\vec{b}}{2c}, \\ \theta &= -\frac{1}{2c}.\end{aligned}\tag{1.70}$$

Implication (c) \implies (a) can be verified directly. We refer to Appendix B.3 for the details. \square

1.3.4 Nondimensionalization of the Boltzmann Equation

Consider the original Boltzmann Equation as given by (1.29) with the collision term define by (1.34). We apply the following scaling transformations to obtain the nondimensionalized Boltzmann Equation :

$$\begin{aligned}x &= L\hat{x}, \quad \vec{v} = v_0\hat{v}, \\ t &= t_0\hat{t}, \quad f = f_0\hat{f}.\end{aligned}\tag{1.71}$$

After substituting (1.71) into the collision term (1.34) we obtain

$$\mathcal{B}(f, f) = B_0 \int_{\mathbb{R}^3} \int_{\mathbb{S}^2} (\hat{f}'\hat{f}'_* - \hat{f}\hat{f}_*) |(\hat{v} - \hat{v}_*)\vec{\omega}| d\vec{\omega} d\vec{v}_* = B_0 \hat{\mathcal{B}}(\hat{f}, \hat{f}),\tag{1.72}$$

where

$$B_0 = 2r^2 f_0^2 v_0^4.\tag{1.73}$$

Equation (1.29) takes form

$$\frac{f_0}{t_0} \partial_i \hat{f} + \frac{v_0 f_0}{L} \hat{v} \cdot \vec{\nabla}_x \hat{f} = B_0 \hat{\mathcal{B}}(\hat{f}, \hat{f}). \quad (1.74)$$

As usual, we will omit the hat-notation above the variables. All variables will be assumed to be nondimensional. We note that the only difference between $\hat{\mathcal{B}}$ and \mathcal{B} is the scaling constant B_0 . Hence all previously described machinery for treating \mathcal{B} is available for $\hat{\mathcal{B}}$ without change. We also assume that the scaling parameters L , t_0 , and v_0 are related via $\frac{L}{t_0 v_0} = 1$. After simplifying equation 1.74 we arrive to the nondimensional Boltzmann Equation

$$\partial_t f + \vec{v} \cdot \vec{\nabla}_x f = \mathcal{B}_0 \mathcal{B}(f, f), \quad (1.75)$$

where

$$\mathcal{B}_0 = 2r^2 L f_0 v_0^3 \quad (1.76)$$

We recall that f is the number density i.e. $\rho = \rho_0 \hat{\rho} = \int_{\mathbb{R}^3} f_0 \hat{f} v_0^3 d\vec{v}$, where the characteristic density must be $\rho_0 = \frac{\mathcal{N}}{L^3}$; and \mathcal{N} is the characteristic number of molecules.⁹ From this we deduce that

$$f_0 = \frac{\mathcal{N}}{L^3 v_0^3} \quad (1.77)$$

After substituting (1.77) into (1.76) the expression for \mathcal{B}_0 becomes

$$\mathcal{B}_0 = \frac{2r^2}{L^2} \mathcal{N} \quad (1.78)$$

We recall, that according to (1.21) the mean free path can be calculated as

$$l = \frac{\Delta V}{4\mathcal{N}\pi r^2}, \quad (1.79)$$

⁹It can be the Avogadro Number for example.

Chapter 1. Motivation of Study: Thermodynamic Limits

where $\Delta V = \text{const}$ is the difference between the characteristic volume V and the excluded volume V_e . Here we recall that by the definition of the collision integral, r is the radius of a molecule and therefore $\mathcal{A} = \pi r^2$ is the cross section of one molecule. Using the expression for the mean free path (1.79) we obtain

$$l = \frac{L^2}{2r^2\mathcal{N}} \cdot \frac{\Delta V}{2\pi} \cdot \frac{1}{L^2} = \frac{1}{\mathcal{B}_0} \frac{\Delta V}{2\pi L^2}. \quad (1.80)$$

The quotient of the mean free path and the characteristic length is referred to by the Knudsen number, and therefore (1.22) yields

$$\mathcal{B}_0 = \frac{\alpha}{\mathcal{K}n} =: \frac{1}{\mathcal{E}}. \quad (1.81)$$

The scaled Boltzmann Equation takes form

$$\partial_t f_\mathcal{E} + \vec{v} \cdot \vec{\nabla} f_\mathcal{E} = \frac{1}{\mathcal{E}} \mathcal{B}(f_\mathcal{E}, f_\mathcal{E}) \quad (1.82)$$

From now on we assume that the gas is in the *fluid regime* (see Section 1.3.1). In the *fluid regime* collision between molecules occur with a high frequency and therefore according to (1.23) Knudsen number $\mathcal{K}n$ must be close to zero. This enables us to consider the behavior of solutions of the family of equations (1.82) when $\mathcal{E} \rightarrow 0$. We will proceed formally without explaining modes of convergence and existence of the limiting distribution.

Assume that the limit in certain sense when \mathcal{E} goes to zero exists and

$$\lim_{\mathcal{E} \rightarrow 0} f_\mathcal{E} = f. \quad (1.83)$$

It follows from the existence of the limit (provided that passing to the limit in (1.82) is justified), that

$$\mathcal{B}(f, f) = 0. \quad (1.84)$$

According to the H-Theorem (Theorem 1) a solution of (1.84) exists and must be of the form of the Maxwellian distribution (1.65). Thus we have arrived to the following conclusion: for the fluid regimes the solution of the Boltzmann Equation is close to a Maxwellian distribution for some $\rho, \theta > 0$ and $\vec{u} \in \mathbb{R}^3$:

$$f \simeq f_{(\rho, \vec{u}, \theta)}^e(\vec{v}) = \frac{\rho}{\sqrt{(2\pi\theta)^3}} \exp\left\{-\frac{|\vec{v} - \vec{u}|^2}{2\theta}\right\} \quad (1.85)$$

1.3.5 The Bhatnagar–Gross–Krook Model

P. L. Bhatnagar, E. P. Gross, and M. Krook in 1954 proposed to modify the collision term of (1.29) or (1.82) so that the collisions conserve particle number, momentum and energy as well as the convergence of the type $f \rightarrow f^e$ is preserved. The following model was suggested [1]:

$$\partial_t f + \vec{v} \cdot \vec{\nabla}_{\vec{x}} f = -\frac{1}{\tau} (f - f^e), \quad (1.86)$$

where f_e is defined by (1.65) and (ρ, \vec{u}, θ) are chosen so that

$$\begin{aligned} \int_{\mathbb{R}^3} f^e(\vec{v}) d\vec{v} &= \int_{\mathbb{R}^3} f(\vec{v}) d\vec{v} \\ \int_{\mathbb{R}^3} f^e(\vec{v}) \vec{v} d\vec{v} &= \int_{\mathbb{R}^3} f(\vec{v}) \vec{v} d\vec{v} \\ \int_{\mathbb{R}^3} f^e(\vec{v}) |\vec{v}|^2 d\vec{v} &= \int_{\mathbb{R}^3} f(\vec{v}) |\vec{v}|^2 d\vec{v} \end{aligned} \quad (1.87)$$

Let us introduce a notation $\langle \phi, f \rangle = \int_{\mathbb{R}^3} f(\vec{v}) \phi(\vec{v}) d\vec{v}$. It is easy to verify that (see Appendix A.2 for the details)

$$\begin{aligned} \langle 1, f^e \rangle &= \rho \\ \langle \vec{v}, f^e \rangle &= \rho \vec{u} \\ \langle |\vec{v}|^2, f^e \rangle &= \rho(\theta + 3|\vec{u}|^2) \end{aligned} \quad (1.88)$$

Therefore

$$\begin{aligned}\rho &= \langle 1, f \rangle \\ \vec{u} &= \frac{\langle \vec{v}, f \rangle}{\langle 1, f \rangle} \\ \theta &= \frac{\langle |\vec{v}|^2, f \rangle}{\langle 1, f \rangle} - 3 \frac{|\langle \vec{v}, f \rangle|^2}{\langle 1, f \rangle^2}.\end{aligned}\tag{1.89}$$

Equations (1.89) together with (1.86) constitute the 3-D Bhatnagar–Gross–Krook model. The parameter $\tau > 0$ is called relaxation time it is usually function of \vec{v} , however for the numerical simulations (Section 5.1) we will assume that τ is a small positive constant. The 1-D BGK model can be obtained similarly to (1.86,1.89)

$$\frac{\partial f}{\partial t} + v \frac{\partial f}{\partial x} = -\frac{1}{\tau}(f - f^e).\tag{1.90}$$

The Maxwellian distribution in this case needs to be adjusted to reflect the proper dimensionality i.e. the Maxwellian must be taken to be

$$f_{(\rho,u,\theta)}^e(v) = \frac{\rho(t,x)}{\sqrt{2\pi\theta(t,x)}} \exp\left\{-\frac{(u(t,x) - v)^2}{2\theta(t,x)}\right\}.\tag{1.91}$$

Details conserving the 1-D BGK model are provided in Chapter 5, Section 5.1.

1.3.6 The Hilbert Procedure

Consider the Boltzmann Equation as given by (1.82). Although we do not attach the subscript \mathcal{E} to the distribution function f , we still bare in mind that a solution of the Boltzmann Equation depends on \mathcal{E} :

$$\partial_t f + \vec{v} \cdot \vec{\nabla} f = \frac{1}{\mathcal{E}} \mathcal{B}(f, f),\tag{1.92}$$

Chapter 1. Motivation of Study: Thermodynamic Limits

where \mathcal{B} is nondimensionalized collision operator defined in (1.72). The quadratic operator $f \mapsto \mathcal{B}(f, f)$ can be extended [8] to a bilinear map by

$$\mathcal{B}(f, g) = \frac{1}{2} \int_{\mathbb{R}^2} \int_{\mathbb{S}^2} [f'g'_* + g'f'_* - fg_* - gf_*] |\vec{\omega} \cdot (\vec{v} - \vec{v}_*)| d\vec{\omega} d\vec{v}_*, \quad (1.93)$$

where $f', f_*, f'_*, g', g_*, f'_*$ are defined by (1.35) and the inner integral is given by (1.37). It follows from the definition (1.93) that the bilinear map \mathcal{B} is symmetric, i.e.

$$\mathcal{B}(f, g) = \mathcal{B}(g, f). \quad (1.94)$$

Let D_t denote the following differential operator

$$D_t = \partial_t + \vec{v} \cdot \vec{\nabla}_{\vec{x}} \quad (1.95)$$

The idea of the Hilbert procedure is to seek a solution of the Boltzmann Equation in the form of a power series in \mathcal{E} :

$$f = \sum_{n=0}^{\infty} \mathcal{E}^n f_n. \quad (1.96)$$

Although each of $\{f_n\}$ may be dependent on \mathcal{E} , we assume that $f_n = \mathcal{O}(1)$ if $\mathcal{E} \rightarrow 0$. After substituting (1.96) into (1.92) we get

$$\sum_{n=0}^{\infty} \mathcal{E}^n D_t f_n = \frac{1}{\mathcal{E}} \sum_{m,n=0}^{\infty} \mathcal{E}^{m+n} \mathcal{B}(f_n, f_m) \quad (1.97)$$

Using the symmetry of \mathcal{B} (1.94) and after matching corresponding powers of \mathcal{E} we get

$$\begin{aligned} 0 &= \mathcal{B}(f_0, f_0), \\ D_t f_0 &= 2\mathcal{B}(f_0, f_1), \\ D_t f_1 &= 2\mathcal{B}(f_0, f_2) + \mathcal{B}(f_1, f_1), \\ &\dots \end{aligned} \quad (1.98)$$

Chapter 1. Motivation of Study: Thermodynamic Limits

We will consider only the first two terms of (1.98). By the H-Theorem (Theorem 1) the first equation $\mathcal{B}(f_0, f_0) = 0$ implies that f_0 must be a Maxwellian distribution of the form (1.65). Thus for some (ρ, \vec{u}, θ)

$$f_0 = f_{(\rho, \vec{u}, \theta)}^e(\vec{v}) = \frac{\rho}{\sqrt{(2\pi\theta)^3}} \exp\left\{-\frac{|\vec{v} - \vec{u}|^2}{2\theta}\right\}. \quad (1.99)$$

Let \mathcal{W}_{f_0} be a set of measurable $L_2(f_0 d\mu)$ -integrable functions on \mathbb{R}^3 equipped with a scalar product:

$$\mathcal{W}_{f_0} = \left\{ f : \mathbb{R}^3 \longrightarrow \mathbb{R} : \int_{\mathbb{R}^3} |f|^2 f_0 d\vec{v} < +\infty \right\} \quad (1.100)$$

$$f, g \in \mathcal{W}_{f_0}, \quad \langle f, g \rangle = \int_{\mathbb{R}^3} f(\vec{v})g(\vec{v})f_0(\vec{v})d\vec{v} \quad (1.101)$$

The scalar product is well defined due to the Cauchy-Schwarz inequality $|fg| \leq \frac{1}{2}(|f|^2 + |g|^2)$. The linear space \mathcal{W}_{f_0} is also complete [18, 8] and thus \mathcal{W}_{f_0} is a Hilbert space. Linear operator $L_{f_0} : \mathcal{W}_{f_0} \longrightarrow \mathcal{W}_{f_0}$ is defined as follows

$$L_{f_0} h = -2f_0^{-1}\mathcal{B}(f_0, f_0 h) \quad (1.102)$$

Properties of operator L_{f_0} are described in detail in [18] and [8]. We will present the properties that concern our further consideration.

1. L_{f_0} is a self-adjoint operator i.e.

$$L_{f_0}^* = L_{f_0} \quad (1.103)$$

2. The null space of L_{f_0} consists of linear combinations of the collision invariants ϕ_k defined by (1.40):

$$\text{Ker } L_{f_0} = \text{l.s. } \{\phi_k : k = 0, \dots, 4\}. \quad (1.104)$$

3. The Hilbert space \mathcal{W}_{f_0} can be represented as a sum of the image space of L_{f_0} and its orthogonal complement: $\mathcal{W}_{f_0} = \mathcal{I}m L_{f_0} \oplus (\mathcal{I}m L_{f_0})^\perp$. Since $(\mathcal{I}m L_{f_0})^\perp = \mathcal{K}er L_{f_0}^*$ and $L_{f_0} = L_{f_0}^*$, we have that

$$\mathcal{W}_{f_0} = \mathcal{I}m L_{f_0} \oplus \mathcal{K}er L_{f_0} \quad (1.105)$$

and

$$\mathcal{I}m L_{f_0} \perp \mathcal{K}er L_{f_0}. \quad (1.106)$$

Let

$$h = \frac{f_1}{f_0}, \quad (1.107)$$

where f_0 and f_1 are the first two members of the expansion (1.96); moreover f_0 is a Maxwellian of the form (1.99). Then the second equation of (1.98) can be written as

$$\frac{D_t f_0}{f_0} = 2f_0^{-1} \mathcal{B}(f_0, f_0 h) \quad (1.108)$$

It is easy to verify that differentiation D_t complies with the Chain Rule and hence $D_t \log f_0 = \frac{D_t f_0}{f_0}$. The right hand side of (1.108) can be represented in terms of L_{f_0} . Equation (1.108) takes form of an operator equation

$$L_{f_0} h = -D_t \log f_0 \quad (1.109)$$

Equation (1.109) has a solution if and only if $D_t \log f_0 \in \mathcal{I}m L_{f_0}$ which is, according to (1.105,1.106), equivalent to

$$D_t \log f_0 \perp \mathcal{K}er L_{f_0} \quad (1.110)$$

Chapter 1. Motivation of Study: Thermodynamic Limits

We assumed that the expansion (1.96) is valid, therefore equation (1.109) must have a solution (1.107). Since a solution exists the orthogonality relation (1.110) holds. The null space $\mathcal{Ker} L_{f_0}$ is spanned by five collision invariants ϕ_k . This means that

$$\langle D_t \log f_0, \phi_k \rangle_{\mathcal{W}_{f_0}} = 0, \quad k = 0, \dots, 4. \quad (1.111)$$

It is demonstrated in Appendix B.4 that

$$\begin{aligned} D_t \log f_0 &= \frac{1}{\rho} \underbrace{\left[\partial_t \rho + \vec{u} \cdot \vec{\nabla} \rho + \rho \operatorname{div} \vec{u} \right]}_{E_1} + \\ &+ \frac{\vec{v} - \vec{u}}{\theta} \cdot \underbrace{\left[\partial_t \vec{u} + \vec{u} * \vec{\nabla} \vec{u} + \vec{\nabla} \theta + \frac{\theta}{\rho} \vec{\nabla} \rho \right]}_{\vec{E}_2} + \\ &+ \frac{1}{2\theta} \left[\frac{|\vec{v} - \vec{u}|^2}{\theta} - 3 \right] \underbrace{\left[\partial_t \theta + \vec{u} \cdot \vec{\nabla} \theta + \frac{2}{3} \theta \operatorname{div} \vec{u} \right]}_{E_3} + \\ &+ A \left(\frac{\vec{v} - \vec{u}}{\sqrt{\theta}} \right) : \vec{\nabla} \vec{u} + 2B \left(\frac{\vec{v} - \vec{u}}{\sqrt{\theta}} \right) \cdot \vec{\nabla} \sqrt{\theta}, \end{aligned} \quad (1.112)$$

where tensors A and B are defined by

$$A(\vec{V}) = \vec{V} \otimes \vec{V} - \frac{1}{3} |\vec{V}|^2 I, \quad (1.113)$$

$$B(\vec{V}) = \frac{1}{2} \left(|\vec{V}|^2 - 5 \right) \vec{V}. \quad (1.114)$$

Gradient $\vec{\nabla}$ is extended to a vector field by

$$\vec{\nabla} \vec{u} = \begin{bmatrix} \vec{\nabla}^T u_1 \\ \vec{\nabla}^T u_2 \\ \vec{\nabla}^T u_3 \end{bmatrix}, \quad (1.115)$$

and operations $*^{10}$ and $:$ are defined by

$$\vec{u} * \vec{\nabla} \vec{u} = \begin{bmatrix} \vec{u} \cdot \vec{\nabla} u_1 \\ \vec{u} \cdot \vec{\nabla} u_2 \\ \vec{u} \cdot \vec{\nabla} u_3 \end{bmatrix}. \quad (1.116)$$

and

$$P, Q \in \text{Mat}_{m,n}(\mathbb{R}) \implies P : Q = \sum_{j,k} P_{ij} Q_{ij} \in \mathbb{R}. \quad (1.117)$$

Let

$$\psi_1(\vec{v}) = \frac{1}{\rho} \quad (1.118)$$

$$\psi_2^k(\vec{v}) = \frac{v_k - u_k}{\theta} \quad (1.119)$$

$$\psi_3(\vec{v}) = \frac{1}{2\theta} \left[\frac{|\vec{v} - \vec{u}|^2}{\theta} - 3 \right] \quad (1.120)$$

The functions ψ_j , $j = 1, 2, 3$ are linear combinations of the collision invariants
(1.40)

$$\begin{aligned} \psi_1(\vec{v}) &= \frac{1}{\rho} \phi_0(\vec{v}), \\ \psi_2^k(\vec{v}) &= \frac{1}{\theta} \phi_k(\vec{v}) - \frac{u_k}{\theta} \phi_0(\vec{v}), \\ \psi_3(\vec{v}) &= \frac{1}{\theta^2} \phi_4(\vec{v}) - \frac{1}{\theta^2} \sum_{j=1}^4 u_j \phi_j(\vec{v}) + \left[\frac{|\vec{u}|^2}{2\theta^2} - \frac{3}{2\theta} \right] \phi_0(\vec{v}); \end{aligned} \quad (1.121)$$

¹⁰ $\vec{b} * A$ can be viewed as $A\vec{b}$

Chapter 1. Motivation of Study: Thermodynamic Limits

and therefore, because of (1.104), $\phi_1, \phi_2^k, \phi_3 \in \mathcal{Ker} L_{f_0}$. Expression of $D_t \log f_0$ can be rewritten in terms of $\phi_1, \vec{\phi}_2, \phi_3$ and E_1, \vec{E}_2, E_3 defined by (1.112) as

$$D_t \log f_0 = E_1 \psi_1(\vec{v}) + \vec{E}_2 \cdot \vec{\phi}_2(\vec{v}) + E_3 \psi_3(\vec{v}) + A : \vec{\nabla} \vec{u} + 2B \cdot \vec{\nabla} \sqrt{\theta} \quad (1.122)$$

It is demonstrated in Appendix B.5 that

$$A_{ij} \left(\frac{\vec{v} - \vec{u}}{\sqrt{\theta}} \right) \perp \mathcal{Ker} L_{f_0}, \quad (1.123)$$

$$B_k \left(\frac{\vec{v} - \vec{u}}{\sqrt{\theta}} \right) \perp \mathcal{Ker} L_{f_0}; \quad (1.124)$$

and, therefore because of (1.110), $E_1 = E_2^k = E_3 = 0$ must be met. These conditions imply

$$\begin{aligned} \partial_t \rho + \vec{u} \cdot \vec{\nabla} \rho + \rho \operatorname{div} \vec{u} &= 0, \\ \partial_t \vec{u} + \vec{u} * \vec{\nabla} \vec{u} + \vec{\nabla} \theta + \frac{\theta}{\rho} \vec{\nabla} \rho &= 0, \\ \partial_t \theta + \vec{u} \cdot \vec{\nabla} \theta + \frac{2}{3} \theta \operatorname{div} \vec{u} &= 0. \end{aligned} \quad (1.125)$$

System (1.125) is equivalent to the compressible Euler system (1.15) (the details are provided in Appendix B.6):

$$\begin{aligned} \partial_t \rho + \operatorname{div}(\rho \vec{u}) &= 0, \\ \partial_t(\rho \vec{u}) + \operatorname{Div}(\rho \vec{u} \otimes \vec{u}) + \vec{\nabla}(\rho \theta) &= 0, \\ \partial_t \left(\frac{1}{2} \rho |\vec{u}|^2 + \frac{3}{2} \rho \theta \right) + \operatorname{div} \left[\rho \vec{u} \left(\frac{1}{2} |\vec{u}|^2 + \frac{5}{2} \theta \right) \right] &= 0. \end{aligned} \quad (1.126)$$

The compressible Euler System (1.126) was obtained assuming the possibility of asymptotic expansion (1.96) of a solution of the Boltzmann Equation (1.92). The resulting system coincides with the Euler system obtained in Section 1.2 with adiabatic ratio $\gamma = \frac{5}{3}$. This value of γ is related to the number of degrees of freedom

Chapter 1. Motivation of Study: Thermodynamic Limits

of the hard sphere gas (see formula 1.14). The equations of state used are given by (1.7) whose nondimensionalized versions for $\gamma = \frac{5}{3}$ are

$$\begin{aligned} p &= \rho\theta, \\ e &= \frac{3}{2}\theta. \end{aligned} \tag{1.127}$$

Details for the derivation of (1.127) are give in Appendix B.1 (see formulas B.5 and B.6).

Chapter 2

Non-dimensionalization of 1-D Euler and Navier-Stokes Systems

2.1 The Navier-Stokes System in Physical Variables

Consider the one-dimensional Navier-Stokes system given as in [14]:

$$\rho_t + (\rho u)_x = 0 \tag{2.1}$$

$$(\rho u)_t + (\rho u^2)_x = \sigma_x \tag{2.2}$$

$$\left(\frac{1}{2}\rho u^2 + \rho e\right)_t + \left(\rho u\left(\frac{1}{2}u^2 + e\right)\right)_x + q_x = (\sigma u)_x \tag{2.3}$$

The macroscopic variables that are used in the Navier-Stokes system (2.1)-(2.3) are listed in Table 2.1.

Chapter 2. Non-dimensionalization of 1-D Euler and Navier-Stokes Systems

ρ	$kg \cdot m^{-3}$	density
u	$m \cdot s^{-1}$	velocity
e	$m^2 \cdot s^{-2}$	internal energy per unit mass
q	$kg \cdot s^{-3}$	heat flux
σ	Pa^1	stress tensor

Table 2.1: List of primary macroscopic observables used in the 1-D Navier-Stokes system (2.1)-(2.3)

We chose to express the system (2.1)-(2.3) in terms of three major thermodynamic variables: the density ρ , the velocity u , and the temperature θ . In order to accomplish this we introduce some important physical quantities (see Table 2.2) and relationship among them.

θ	K	temperature
p	Pa	pressure
τ	Pa	shear stress
λ	$Pa \cdot s$	first viscosity coefficient
μ	$Pa \cdot s$	second viscosity coefficient
$\tilde{\mu}$	$Pa \cdot s$	dynamic viscosity
k	$kg \cdot m \cdot s^{-3} \cdot K$	heat conductivity
R	$J \cdot K^{-1}$	The Universal Gas Constant
C_V	$J \cdot K^{-1}$	volume specific heat capacity
C_P	$J \cdot K^{-1}$	pressure specific heat capacity
M	$mol \cdot kg^{-1}$	molar mass

Table 2.2: List of secondary macroscopic observables used in the 1-D Navier-Stokes system (2.1)-(2.3)

¹ $Pa = N \cdot m^{-2} = kg \cdot m^{-1} \cdot s^{-2}$

Chapter 2. Non-dimensionalization of 1-D Euler and Navier-Stokes Systems

We assume Stokes' relation

$$\lambda = -\frac{2}{3}\mu \quad (2.4)$$

then the dynamic viscosity becomes

$$\tilde{\mu} = \lambda + 2\mu = \frac{4}{3}\mu. \quad (2.5)$$

The stress tensor σ can be obtained as follows

$$\sigma = -p + \tau \quad (2.6)$$

$$\tau = \tilde{\mu}u_x. \quad (2.7)$$

Therefore

$$\sigma = -p + \tilde{\mu}u_x. \quad (2.8)$$

The heat flux q and temperature θ are related by Fourier's Law

$$q = -k\theta_x. \quad (2.9)$$

It remains to express internal energy per unit mass e and pressure p in terms of the chosen thermodynamic variables ρ , u , and θ . We adopt the following equations of state

$$p = \frac{R}{M}\rho\theta \quad (2.10)$$

$$e = \frac{C_V}{M}\theta \quad (2.11)$$

Chapter 2. Non-dimensionalization of 1-D Euler and Navier-Stokes Systems

After substituting (2.10) into (2.8) and we obtain

$$\sigma_x = (-p + \tau)_x = \left(-\frac{R}{M}\rho\theta + \tilde{\mu}u_x \right)_x = \tilde{\mu}u_{xx} - \frac{R}{M}(\rho\theta)_x, \quad (2.12)$$

$$(\sigma u)_x = (\tau u - pu)_x = \left(\tilde{\mu}uu_x - \frac{R}{M}\rho u\theta \right)_x = \frac{1}{2}\tilde{\mu}u_{xx}^2 - \frac{R}{M}(\rho u\theta)_x. \quad (2.13)$$

From (2.11) and (2.9) we obtain

$$\frac{1}{2}u^2 + e = \frac{1}{2}u^2 + \frac{C_V}{M}\theta \quad (2.14)$$

$$q_x = -k\theta_{xx}. \quad (2.15)$$

After utilizing (2.12), (2.13), (2.14) and (2.15) and noticing that $uu_x = \frac{1}{2}u_{xx}^2$ equations (2.1)-(2.3) take form

$$\rho_t + (\rho u)_x = 0$$

$$(\rho u)_t + (\rho u^2)_x = \tilde{\mu}u_{xx} - \frac{R}{M}(\rho\theta)_x \quad (2.16)$$

$$\left(\frac{1}{2}\rho u^2 + \frac{C_V}{M}\rho\theta \right)_t + \left(\rho u \left(\frac{1}{2}u^2 + \frac{C_V}{M}\theta \right) \right)_x + \left(\frac{R}{M}\rho u\theta \right)_x = k\theta_{xx} + \frac{1}{2}\tilde{\mu}u_{xx}^2$$

We simplify the system above by keeping all first order derivative on the left hand side and all second order ones on the right hand side. We also recall that specific heat capacities and the universal gas constant are related as

$$R = C_P - C_V \quad (2.17)$$

Finally the 1-D Navier-Stokes system of three equations in three thermodynamic variables takes form

$$\rho_t + (\rho u)_x = 0 \quad (2.18)$$

$$(\rho u)_t + \left(\rho u^2 + \frac{R}{M} \rho \theta \right)_x = \tilde{\mu} u_{xx} \quad (2.19)$$

$$\left(\frac{1}{2} \rho u^2 + \frac{C_V}{M} \rho \theta \right)_t + \left(\rho u \left(\frac{1}{2} u^2 + \frac{C_P}{M} \theta \right) \right)_x = k \theta_{xx} + \frac{1}{2} \tilde{\mu} u_{xx}^2 \quad (2.20)$$

2.2 The Navier-Stokes System in Generic Variables

In this section we will remove units from the equations (2.18)-(2.19). We will start with introducing some characteristics quantities and unitless parameters that the nondimensionalized equations will depend upon. Let t_0 and L be the characteristic time and length then

$$t = t_0 \hat{t} \quad (2.21)$$

$$x = L \hat{x} \quad (2.22)$$

where \hat{t} and \hat{x} are a generic time and coordinate. Similarly, nondimensional versions of the density, the velocity, and the temperature are

$$\rho = \rho_0 \hat{\rho} \quad (2.23)$$

$$u = u_0 \hat{u} \quad (2.24)$$

$$\theta = \theta_0 \hat{\theta} \quad (2.25)$$

We require that

$$\frac{L}{t_0} = u_0 \quad (2.26)$$

Chapter 2. Non-dimensionalization of 1-D Euler and Navier-Stokes Systems

The differential operators in dimensionless variables become

$$\frac{\partial}{\partial t} = \frac{1}{t_0} \frac{\partial}{\partial \hat{t}} \quad (2.27)$$

$$\frac{\partial}{\partial x} = \frac{1}{L} \frac{\partial}{\partial \hat{x}} \quad (2.28)$$

$$\frac{\partial^2}{\partial x^2} = \frac{1}{L^2} \frac{\partial^2}{\partial \hat{x}^2} \quad (2.29)$$

The nondimensionalized system will contain the four standard dimensionless parameters: Mach Number $\mathcal{M}a$, Prandtl number $\mathcal{P}r$, Reynolds Number $\mathcal{R}e$, and the Adiabatic Ratio γ .

$$\mathcal{M}a^2 = \frac{u_0^2 M}{\gamma R \theta_0} \quad (2.30)$$

$$\mathcal{P}r = \frac{\tilde{\mu} C_P}{Mk} \quad (2.31)$$

$$\mathcal{R}e = \frac{L u_0 \rho_0}{\tilde{\mu}} \quad (2.32)$$

$$\gamma = \frac{C_P}{C_V} > 1 \quad (2.33)$$

In order to simplify the notation we agree to drop the hats ($\hat{}$) above the dimensionless variables. We proceed with nondimensionalization applied to the each of the equation of the system (2.18)-(2.20)

Equation (2.18): Since we adopted normalization (2.26) equation (2.18) in terms of generic variables has the same form as the original one in physical quantities:

$$\rho_t + (\rho u)_x = 0$$

Chapter 2. Non-dimensionalization of 1-D Euler and Navier-Stokes Systems

Equation (2.19): After substituting (2.23)-(2.29) into (2.19) we obtain

$$\frac{\rho_0 u_0}{t_0} (\rho u)_t + \frac{1}{L} \left(\rho_0 u_0^2 \rho u^2 + \frac{\rho_0 R \theta_0}{M} \rho \theta \right)_x = \frac{\tilde{\mu} u_0}{L^2} u_{xx} \quad (2.34)$$

According to (2.30)

$$\frac{\rho_0 \theta_0 R}{M} = \frac{\rho_0 u_0^2}{\gamma \mathcal{M} a^2} \quad (2.35)$$

therefore

$$(\rho u)_t + \frac{\rho_0 u_0^2}{L} \frac{t_0}{\rho_0 u_0} (\rho u^2 + \gamma^{-1} \mathcal{M} a^{-2} \rho \theta)_x = \frac{\tilde{\mu} u_0}{L^2} \frac{L}{\rho_0 u_0^2} u_{xx} \quad (2.36)$$

Due to the normalization in (2.26) and by the definition of the Reynolds Number (2.32) we obtain that $\frac{\rho_0 u_0^2}{L} \frac{t_0}{\rho_0 u_0} = 1$ and $\frac{\tilde{\mu} u_0}{L^2} \frac{L}{\rho_0 u_0^2} = \mathcal{R}e^{-1}$. Thus the nondimensional version of equation (2.18) is

$$(\rho u)_t + (\rho u^2 + \gamma^{-1} \mathcal{M} a^{-2} \rho \theta)_x = \mathcal{R}e^{-1} u_{xx} \quad (2.37)$$

Equation (2.20): We will nondimensionalize equation (2.20) step by step due to its complexity.

The time derivative term is transformed as

$$\begin{aligned} \frac{1}{2} \rho u^2 + \frac{C_V}{M} \rho \theta &\mapsto \frac{1}{2} \rho_0 u_0^2 \rho u^2 + \frac{C_V}{M} \rho_0 \theta_0 \rho \theta = \\ &\rho_0 u_0^2 \left(\frac{1}{2} \rho u^2 + \frac{C_V}{\gamma R} \frac{\gamma R \theta_0}{M u_0^2} \rho \theta \right) \end{aligned}$$

It follows from (2.17) and (2.33) that $\frac{C_V}{\gamma R} = \gamma^{-1}(\gamma - 1)^{-1}$, and after applying the definition of the Mach Number (2.30) we obtain

$$\frac{1}{2} \rho u^2 + \frac{C_V}{M} \rho \theta \mapsto \rho_0 u_0^2 \left(\frac{1}{2} \rho u^2 + \gamma^{-1}(\gamma - 1)^{-1} \mathcal{M} a^{-2} \rho \theta \right) \quad (2.38)$$

The space derivative term is dimensionalized similarly:

$$\rho u \left(\frac{1}{2} u^2 + \frac{C_P}{M} \theta \right) \mapsto \rho_0 u_0 \rho u \left(\frac{1}{2} u_0^2 u^2 + \frac{C_P \theta_0}{M} \theta \right) =$$

Chapter 2. Non-dimensionalization of 1-D Euler and Navier-Stokes Systems

$$\rho u \rho_0 u_0^3 \left(\frac{1}{2} u^2 + \frac{C_P \gamma R \theta_0}{\gamma R M u_0^2} \theta \right) = \rho u \rho_0 u_0^3 \left(\frac{1}{2} u^2 + (\gamma - 1)^{-1} \mathcal{M} a^{-2} \theta \right)$$

since by (2.17) and (2.33) $\frac{C_P}{\gamma R} = (\gamma - 1)^{-1}$ Therefore we obtain

$$\rho u \left(\frac{1}{2} u^2 + \frac{C_P}{M} \theta \right) \mapsto \rho_0 u_0^3 \rho u \left(\frac{1}{2} u^2 + (\gamma - 1)^{-1} \mathcal{M} a^{-2} \theta \right) \quad (2.39)$$

The second order terms are translated as follows

$$k \theta_{xx} \mapsto \frac{k \theta_0}{L^2} \theta_{xx} \quad (2.40)$$

$$\frac{1}{2} \tilde{\mu} u_{xx}^2 \mapsto \frac{1}{2} \frac{\tilde{\mu} u_0^2}{L^2} u_{xx}^2 \quad (2.41)$$

Incorporating transformations (2.38), (2.39), (2.40), and (2.41) into one equation we obtain

$$\begin{aligned} & \frac{\rho_0 u_0^2}{t_0} \left(\frac{1}{2} \rho u^2 + \gamma^{-1} (\gamma - 1)^{-1} \mathcal{M} a^{-2} \rho \theta \right)_t + \\ & + \frac{\rho_0 u_0^3}{L} \left(\frac{1}{2} \rho u^3 + (\gamma - 1)^{-1} \mathcal{M} a^{-2} \rho u \theta \right)_x = \frac{k \theta_0}{L^2} \theta_{xx} + \frac{1}{2} \frac{\tilde{\mu} u_0^2}{L^2} u_{xx}^2 \end{aligned} \quad (2.42)$$

After simplifying, equation (2.41) reduces to

$$\begin{aligned} & \left(\frac{1}{2} \rho u^2 + \frac{\rho \theta}{\gamma (\gamma - 1) \mathcal{M} a^2} \right)_t + \left(\frac{1}{2} \rho u^3 + \frac{\rho u \theta}{(\gamma - 1) \mathcal{M} a^2} \right)_x = \\ & = \frac{k \theta_0}{L^2} \frac{t_0}{\rho u_0^2} \theta_{xx} + \frac{1}{2} \frac{\tilde{\mu} u_0^2}{L^2} \frac{t_0}{\rho u_0^2} u_{xx}^2 \end{aligned} \quad (2.43)$$

According to (2.32) the coefficient preceding u_{xx} can be expressed in terms of the Reynolds Number

$$\frac{\tilde{\mu} u_0^2 t_0}{2 L^2 \rho u_0^2} = \frac{\tilde{\mu}}{2 L u_0 \rho_0} = \frac{1}{2 \mathcal{R}e} \quad (2.44)$$

Chapter 2. Non-dimensionalization of 1-D Euler and Navier-Stokes Systems

The constant in θ_{xx} requires some manipulations. Consider

$$\frac{1}{(\gamma - 1)\mathcal{M}a^2\mathcal{P}r\mathcal{R}e} = \frac{1}{\gamma - 1} \cdot \frac{\gamma R\theta_0}{u_0^2 M} \cdot \frac{Mk}{\tilde{\mu}C_P} \cdot \frac{\tilde{\mu}}{Lu_0\rho_0} = \frac{k\theta_0}{Lu_0^3\rho_0} = \frac{k\theta_0 t_0}{L^2\rho_0 u_0^2} \quad (2.45)$$

Thus, one can see that the θ_{xx} coefficient is exactly the quantity on the left hand side of the equation (2.45) Here we used the identity

$$\frac{\gamma R}{(\gamma - 1)C_P} = \frac{\gamma(C_P - C_V)}{(\gamma - 1)C_P} = 1$$

that follows from (2.17) and (2.33). Therefore equation the energy conservation equation (2.20) takes form

$$\begin{aligned} & \left(\frac{1}{2}\rho u^2 + \frac{\rho\theta}{\gamma(\gamma - 1)\mathcal{M}a^2} \right)_t + \left(\frac{1}{2}\rho u^3 + \frac{\rho u\theta}{(\gamma - 1)\mathcal{M}a^2} \right)_x = \\ & = \frac{1}{(\gamma - 1)\mathcal{M}a^2\mathcal{P}r\mathcal{R}e}\theta_{xx} + \frac{1}{2\mathcal{R}e}u_{xx}^2 \end{aligned} \quad (2.46)$$

As a result we obtain the 1-D Navier-Stokes system of PDE in nondimensionalized variables

$$\left\{ \begin{array}{l} \rho_t + (\rho u)_x = 0 \\ (\rho u)_t + \left(\rho u^2 + \frac{\rho\theta}{\gamma\mathcal{M}a^2} \right)_x = \frac{1}{\mathcal{R}e}u_{xx} \\ \left(\frac{1}{2}\rho u^2 + \frac{\rho\theta}{\gamma(\gamma-1)\mathcal{M}a^2} \right)_t + \left(\frac{1}{2}\rho u^3 + \frac{\rho u\theta}{(\gamma-1)\mathcal{M}a^2} \right)_x = \frac{\theta_{xx}}{(\gamma-1)\mathcal{M}a^2\mathcal{P}r\mathcal{R}e} + \frac{u_{xx}^2}{2\mathcal{R}e} \end{array} \right. \quad (2.47)$$

Without losing generality one can assume that $\gamma\mathcal{M}a^2 = 1$ which, according to (2.30), is equivalent to $\frac{Mu_0^2}{R\theta_0} = 1$. This can be achieved by further rescaling the temperature θ by setting $\tilde{\theta} = \frac{\theta}{\gamma\mathcal{M}a^2}$. In this case system (2.47) takes the simpler form:

$$\left\{ \begin{array}{l} \rho_t + (\rho u)_x = 0 \\ (\rho u)_t + (\rho u^2 + \rho\theta)_x = \frac{1}{\mathcal{R}e}u_{xx} \\ \left(\frac{1}{2}\rho u^2 + \frac{\rho\theta}{\gamma - 1} \right)_t + \left(\frac{1}{2}\rho u^3 + \frac{\gamma\rho u\theta}{\gamma - 1} \right)_x = \frac{\gamma}{(\gamma - 1)\mathcal{P}r\mathcal{R}e}\theta_{xx} + \frac{1}{2\mathcal{R}e}u_{xx}^2 \end{array} \right. \quad (2.48)$$

or equivalently

$$\begin{bmatrix} \rho \\ \rho u \\ \frac{1}{2}\rho u^2 + \frac{\rho\theta}{\gamma-1} \end{bmatrix}_t + \begin{bmatrix} \rho u \\ \rho u^2 + \rho\theta \\ \frac{1}{2}\rho u^3 + \frac{\gamma\rho u\theta}{\gamma-1} \end{bmatrix}_x = \frac{1}{\mathcal{R}e} \begin{bmatrix} 0 \\ u \\ \frac{\gamma}{(\gamma-1)\mathcal{P}r}\theta + \frac{1}{2}u^2 \end{bmatrix}_{xx} \quad (2.49)$$

In order to obtain the Euler system one has to consider the inviscid case of the corresponding Navier-Stokes system as well as the heat conductivity k must be set to zero. Thus from (2.45) we get

$$\frac{\gamma}{(\gamma-1)\mathcal{P}r\mathcal{R}e} = \frac{k\theta_0 t_0}{L^2\rho u_0} = 0 \quad (2.50)$$

and using the definition of the Reynolds Number (2.32) it follows that zero viscosity $\tilde{\mu} = 0$ implies

$$\mathcal{R}e = +\infty \quad (2.51)$$

After substituting (2.50) and (2.51) into (2.48) we arrive to 1-D Euler System describing an inviscid compressible flow:

$$\begin{bmatrix} \rho \\ \rho u \\ \frac{1}{2}\rho u^2 + \frac{\rho\theta}{\gamma-1} \end{bmatrix}_t + \begin{bmatrix} \rho u \\ \rho u^2 + \rho\theta \\ \frac{1}{2}\rho u^3 + \frac{\gamma\rho u\theta}{\gamma-1} \end{bmatrix}_x = \vec{0} \quad (2.52)$$

It has been shown in Sections 1.2 and 1.3.6 that in order to obtain the 3-D Euler system from the 3-D Boltzmann Equation one has to choose γ according to formula (1.13) on page 7. In order to be consistent with the 3-D case, the value for γ in the 1-D situation must be chosen according to the same formula. Thus we take $\gamma = 3$ that corresponds to $d = 1$ degree of freedom for a one-dimensional gas. In this case the Navier-Stokes and Euler systems become:

$$\begin{bmatrix} \rho \\ \rho u \\ \frac{1}{2}\rho u^2 + \frac{1}{2}\rho\theta \end{bmatrix}_t + \begin{bmatrix} \rho u \\ \rho u^2 + \rho\theta \\ \frac{1}{2}\rho u^3 + \frac{3}{2}\rho u\theta \end{bmatrix}_x = \frac{1}{\mathcal{R}e} \begin{bmatrix} 0 \\ u \\ \frac{3}{2\mathcal{P}r}\theta + \frac{1}{2}u^2 \end{bmatrix}_{xx} \quad (2.53)$$

$$\begin{bmatrix} \rho \\ \rho u \\ \frac{1}{2}\rho u^2 + \frac{1}{2}\rho\theta \end{bmatrix}_t + \begin{bmatrix} \rho u \\ \rho u^2 + \rho\theta \\ \frac{1}{2}\rho u^3 + \frac{3}{2}\rho u\theta \end{bmatrix}_x = \vec{0} \quad (2.54)$$

2.3 The 1-D Navier-Stokes and Euler systems in non-conservative quantities

The quantities ρu and $\frac{1}{2}\rho u^2 + \frac{\rho\theta}{\gamma-1}$ represent the momentum and the total energy of the substance (gas or fluid), therefore equations (2.48) and (2.54) are said to be in conservative variables. In the following we present the same equations in non-conservative variables ρ , u , and θ :

$$\begin{aligned} & \begin{bmatrix} \rho \\ \rho u \\ \frac{1}{2}\rho u^2 + \frac{\rho\theta}{\gamma-1} \end{bmatrix}_t = \begin{bmatrix} \rho_t \\ \rho_t u + \rho u_t \\ \frac{1}{2}\rho_t u^2 + \rho u u_t + \frac{\rho_t \theta}{\gamma-1} + \frac{\rho \theta_t}{\gamma-1} \end{bmatrix} \\ & = \underbrace{\begin{bmatrix} 1 & 0 & 0 \\ u & \rho & 0 \\ \frac{1}{2}u^2 + \frac{\theta}{\gamma-1} & \rho u & \frac{\rho}{\gamma-1} \end{bmatrix}}_{C_{(\rho,u,\theta)}} \begin{bmatrix} \rho \\ u \\ \theta \end{bmatrix}_t = C_{(\rho,u,\theta)} \begin{bmatrix} \rho \\ u \\ \theta \end{bmatrix}_t \end{aligned} \quad (2.55)$$

$$\begin{aligned} & \begin{bmatrix} \rho u \\ \rho u^2 + \rho\theta \\ \frac{1}{2}\rho u^3 + \frac{\gamma\rho u\theta}{\gamma-1} \end{bmatrix}_x = \begin{bmatrix} \rho_x u + \rho u_x \\ \rho_x(u^2 + \theta) + \rho(2uu_x + \theta_x) \\ \rho_x\left(\frac{1}{2}u^3 + \frac{\gamma\theta u}{\gamma-1}\right) + \rho\left(\frac{3}{2}u^2 u_x + \frac{\gamma}{\gamma-1}\theta_x u + \frac{\gamma}{\gamma-1}\theta u_x\right) \end{bmatrix}_x = \\ & = \underbrace{\begin{bmatrix} u & \rho & 0 \\ u^2 + \theta & 2\rho u & \rho \\ \frac{1}{2}u^3 + \frac{\gamma\theta u}{\gamma-1} & \frac{3}{2}\rho u^2 + \frac{\gamma\rho\theta}{\gamma-1} & \frac{\gamma\rho u}{\gamma-1} \end{bmatrix}}_{D_{(\rho,u,\theta)}} \begin{bmatrix} \rho \\ u \\ \theta \end{bmatrix}_x = D_{(\rho,u,\theta)} \begin{bmatrix} \rho \\ u \\ \theta \end{bmatrix}_x \end{aligned} \quad (2.56)$$

After substituting (2.55) and (2.56) into (2.48) we obtain

$$C(\vec{w}) \cdot \vec{w}_t + D(\vec{w}) \cdot \vec{w}_x = \frac{1}{\mathcal{R}e} F(\vec{w})_{xx} \quad (2.57)$$

Chapter 2. Non-dimensionalization of 1-D Euler and Navier-Stokes Systems

where

$$\vec{w} = [\rho \quad u \quad \theta]^T; \quad (2.58)$$

and $C(\vec{w})$ and $D(\vec{w})$ are defined by (2.55) and (2.56) and

$$F(\vec{w}) = \begin{bmatrix} 0 \\ u \\ \frac{\gamma\theta}{(\gamma-1)\mathcal{P}r} + \frac{1}{2}u^2 \end{bmatrix} \quad (2.59)$$

Further simplification yields

$$\vec{w}_t + C^{-1}D \cdot \vec{w}_x = \frac{1}{\mathcal{R}e} C^{-1}F(\vec{w})_{xx} \quad (2.60)$$

where C^{-1} exist and can be computed analytically as well as $C^{-1}D$:

$$Q := C^{-1} = \begin{bmatrix} 1 & 0 & 0 \\ -\frac{u}{\rho} & \frac{1}{\rho} & 0 \\ \frac{u^2(\gamma-1)}{2\rho} - \frac{\theta}{\rho} & -\frac{u(\gamma-1)}{\rho} & \frac{\gamma-1}{\rho} \end{bmatrix} \quad (2.61)$$

$$A := C^{-1}D = \begin{bmatrix} u & \rho & 0 \\ \frac{\theta}{\rho} & u & 1 \\ 0 & (\gamma-1)\theta & u \end{bmatrix} \quad (2.62)$$

Substituting (2.61) and (2.62) into (2.60) we obtain

$$\vec{w}_t + A(\vec{w})\vec{w}_x = \frac{1}{\mathcal{R}e} Q(\vec{w})F(\vec{w})_{xx} \quad (2.63)$$

One can verify that the advection matrix $A(\vec{w})$ has three distinct real eigenvalues

$$\begin{aligned} \lambda_1 &= u + \sqrt{\gamma\theta} \\ \lambda_2 &= u - \sqrt{\gamma\theta} \\ \lambda_3 &= u \end{aligned} \quad (2.64)$$

Chapter 2. Non-dimensionalization of 1-D Euler and Navier-Stokes Systems

thus it can be diagonalized using transformation T whose columns are eigenvectors of A :

$$T^{-1}AT = \Lambda = \begin{bmatrix} \lambda_1 & 0 & 0 \\ 0 & \lambda_2 & 0 \\ 0 & 0 & \lambda_3 \end{bmatrix}, \quad (2.65)$$

where T and T^{-1} are given by

$$T = \begin{bmatrix} 1 & 1 & -\frac{\rho}{\theta} \\ \frac{\sqrt{\gamma\theta}}{\rho} & -\frac{\sqrt{\gamma\theta}}{\rho} & 0 \\ \frac{\theta(\gamma-1)}{\rho} & \frac{\theta(\gamma-1)}{\rho} & 1 \end{bmatrix} \quad (2.66)$$

$$T^{-1} = \begin{bmatrix} \frac{1}{2\gamma} & \frac{\rho}{2\sqrt{\gamma\theta}} & \frac{\rho}{2\sqrt{\gamma\theta}} \\ \frac{1}{2\gamma} & -\frac{\rho}{2\sqrt{\gamma\theta}} & \frac{\rho}{2\sqrt{\gamma\theta}} \\ -\frac{\theta(\gamma-1)}{\rho\gamma} & 0 & \frac{1}{\gamma} \end{bmatrix} \quad (2.67)$$

This property of the advection matrix A will be used later in designing a numerical solver for (2.63).

Chapter 3

The Equations for a Viscous, Heat-Conducting and Inviscid Stationary Shocks

3.1 The Rankine-Hugoniot Conditions

Consider the 1-D Navier-Stokes system as derived in section 2.2

$$\begin{cases} \rho_t + (\rho u)_x = 0 \\ (\rho u)_t + (\rho u^2 + \rho \theta)_x = \frac{1}{\mathcal{R}e} u_{xx} \\ \left(\frac{1}{2} \rho u^2 + \frac{\rho \theta}{\gamma - 1} \right)_t + \left(\frac{1}{2} \rho u^3 + \frac{\gamma \rho u \theta}{\gamma - 1} \right)_x = \frac{\gamma}{(\gamma - 1) \mathcal{P}r \mathcal{R}e} \theta_{xx} + \frac{1}{2 \mathcal{R}e} u_{xx}^2 \end{cases} \quad (3.1)$$

For the purpose of deriving the shock conditions we disregard all second order terms and set the time derivatives to zeros.

$$\begin{cases} (\rho u)_x = 0 \\ (\rho u^2 + \rho \theta)_x = 0 \\ \left(\frac{1}{2} \rho u^3 + \frac{\gamma}{\gamma - 1} \rho u \theta \right)_x = 0 \end{cases} \quad (3.2)$$

By assuming that the range of nondimensionalized space coordinate x is the interval $[0, 1]$, the left and the right boundaries are $x = 0$ and $x = 1$ correspondingly. Let

$$\vec{w}(t, x) = [\rho(t, x) \ u(t, x) \ \theta(t, x)]^T$$

then $\vec{w}_L = \vec{w}(+\infty, 0) = [\rho_L \ u_L \ \theta_L]^T$ and $\vec{w}_R = \vec{w}(+\infty, 1) = [\rho_R \ u_R \ \theta_R]^T$ represent left and right boundary values for of the stationary shock solution.

According to Rankine-Hugoniot conditions the following equations must be satisfied:

$$\begin{cases} \rho_L u_L = \rho_R u_R \\ \rho_L u_L^2 + \rho_L \theta_L = \rho_R u_R^2 + \rho_R \theta_R \\ \frac{1}{2} \rho_L u_L^3 + \frac{\gamma}{\gamma-1} \rho_L u_L \theta_L = \frac{1}{2} \rho_R u_R^3 + \frac{\gamma}{\gamma-1} \rho_R u_R \theta_R \end{cases} \quad (3.3)$$

Equivalently

$$\begin{cases} \rho_L u_L = \rho_R u_R \\ \rho_L u_L^2 + \rho_L \theta_L = \rho_R u_R^2 + \rho_R \theta_R \\ \frac{1}{2} u_L^2 + \frac{\gamma}{\gamma-1} \theta_L = \frac{1}{2} u_R^2 + \frac{\gamma}{\gamma-1} \theta_R \end{cases} \quad (3.4)$$

This is an algebraic system of three equations and six variables. In order to successfully solve it one has the freedom of choosing and fixing three variables. Following [14] we assume that the following values are provided

$$\rho_L > 0, \quad 0 < u_R < u_L \quad (3.5)$$

From the first equation we have $\rho_R = \rho_L \frac{u_L}{u_R}$ and let $k = \frac{u_R}{u_L}$ then we have

$$k = \frac{u_R}{u_L} = \frac{\rho_L}{\rho_R} \quad (3.6)$$

where all five parameters are known. The last two equation of (3.4) can be rewritten as

$$\begin{cases} \rho_L \theta_L - \rho_R \theta_R = \rho_R u_R^2 - \rho_L u_L^2 \\ \theta_L - \theta_R = \frac{\gamma-1}{2\gamma} (u_R^2 - u_L^2) \end{cases} \quad (3.7)$$

From (3.7) we find θ_L and θ_R by solving the linear system above:

$$\begin{bmatrix} \theta_L \\ \theta_R \end{bmatrix} = \begin{bmatrix} -1 & \rho_R \\ -1 & \rho_L \end{bmatrix} \begin{bmatrix} \frac{\rho_R u_R^2 - \rho_L u_L^2}{\rho_R - \rho_L} \\ \frac{\gamma - 1}{2\gamma} \frac{u_R^2 - u_L^2}{\rho_R - \rho_L} \end{bmatrix} \quad (3.8)$$

$$\begin{aligned} \theta_L &= \frac{\gamma - 1}{2\gamma} \frac{\rho_R (u_R^2 - u_L^2)}{\rho_R - \rho_L} - \frac{\rho_R u_R^2 - \rho_L u_L^2}{\rho_R - \rho_L} = u_L^2 \frac{k^{+1}(\gamma + 1) - (\gamma - 1)}{2\gamma} \\ \theta_R &= \frac{\gamma - 1}{2\gamma} \frac{\rho_L (u_R^2 - u_L^2)}{\rho_R - \rho_L} - \frac{\rho_R u_R^2 - \rho_L u_L^2}{\rho_R - \rho_L} = u_R^2 \frac{k^{-1}(\gamma + 1) - (\gamma - 1)}{2\gamma} \end{aligned} \quad (3.9)$$

In order for the boundary values to yield a shock there must be two restrictions imposed on the ratio k . Firstly, we require the temperature to be always positive $\theta_L, \theta_R > 0$. Secondly, in order for the shock to occur one has to make sure that the number of inflowing and outflowing characteristics of the system (3.1) are different. The characteristics are given by¹

$$\begin{aligned} \lambda^0 &= u \\ \lambda^\pm &= u \pm \sqrt{\gamma\theta} \end{aligned} \quad (3.10)$$

λ^0 and λ^+ are always positive since we consider $u > 0$. The only sign change that may occur for λ^- . Thus in order to privies a set of shock favorable conditions one requests four inflows into the domain $[0, 1]$ and two outflows:

$$\lambda_L^0 > 0 \quad (3.11)$$

$$\lambda_L^+ > 0 \quad (3.12)$$

$$\lambda_L^- > 0 \quad (3.13)$$

¹see formula (2.64) on page 43.

$$\lambda_R^0 > 0 \tag{3.14}$$

$$\lambda_R^+ > 0 \tag{3.15}$$

$$\lambda_R^- < 0 \tag{3.16}$$

Inequalities (3.11), (3.12), (3.14), and (3.15) are automatically satisfied. (3.13) and (3.16) will impose further constrain on the ratio k :

$$\begin{aligned} u_L - u_L \sqrt{\frac{k(\gamma+1) - (\gamma-1)}{2}} &> 0 \\ u_R - u_R \sqrt{\frac{\gamma+1 - k(\gamma-1)}{2k}} &< 0 \end{aligned} \tag{3.17}$$

Thus we get ($\gamma > 1$):

$$k(\gamma + 1) - (\gamma - 1) > 0 \tag{3.18}$$

$$\gamma + 1 - k(\gamma - 1) > 0 \tag{3.19}$$

$$\frac{k(\gamma + 1) - (\gamma - 1)}{2} < 1 \tag{3.20}$$

$$\frac{\gamma + 1 - k(\gamma - 1)}{2k} > 1 \tag{3.21}$$

Inequalities (3.18) and (3.19) are equivalent to

$$\frac{\gamma - 1}{\gamma + 1} < k < \frac{\gamma + 1}{\gamma - 1} \tag{3.22}$$

and (3.20) and (3.21) are satisfied if and only if $k < 1 \quad \forall \gamma > 1$. The later one is satisfied automatically since $u_R < u_L$ according to (3.5).

3.2 An Example of Shock Forming Boundary Conditions

In this section we consider a few examples of sets of boundary conditions that yields a stationary shock profile in the stationary solution of the Navier-Stokes and Euler systems.

The following is an algorithm to obtain a stationary shock solution. For given $\gamma > 1$ we choose values of ρ_L , u_L , and u_R so that (3.5) and (3.22) are met. Then ρ_R is obtained from (3.6) and formulas (3.9) are used to obtain θ_L and θ_R

Consider an example when $\gamma = 3$. Choose $\rho_L = 1.5$, $u_L = 2$, and $u_R = 1.5$. In this case $k = \frac{u_R}{u_L} = 0.75$. Condition (3.22) requires that $\frac{2}{3} < k < \frac{4}{3}$, thus $k = 0.75$ is within the admissible range. $\rho_R = 2$ is obtained from (3.6). Formulas in (3.9) yield $\theta_L = \frac{2}{3}$ and $\theta_R = \frac{5}{4}$. The values summarized in (3.23) are one set among several sets of boundary conditions used to simulate viscous and inviscid shocks (see Chapter 6).

$$\begin{aligned} \rho_L &= \frac{3}{2} & \rho_R &= 2 \\ u_L &= 2 & u_R &= \frac{3}{2} \\ \theta_L &= \frac{2}{3} & \theta_R &= \frac{5}{4} \end{aligned} \tag{3.23}$$

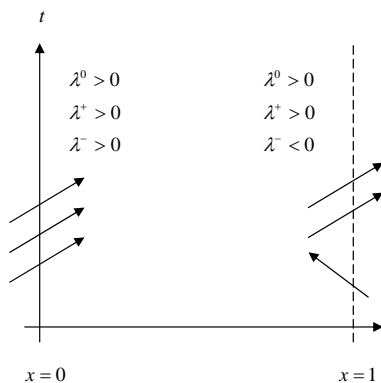


Figure 3.1: Inflowing and outflowing characteristics

The eigenvalues on the left and right boundaries are calculated based on (3.23) and (3.10). Sign counting reveals that there are four inflowing characteristics into the domain and two outflowing characteristics from the domain (Figure 3.1). This indicates that, indeed, the stationary solution must possess a shock layer profile as prescribed by the Rankine-Hugoniot conditions (3.3).

$$\begin{aligned}\lambda_L^0 &= +2.00 > 0 & \lambda_R^0 &= +1.50 > 0 \\ \lambda_L^+ &\approx +3.41 > 0 & \lambda_R^+ &\approx +3.44 > 0 \\ \lambda_L^- &\approx +0.59 > 0 & \lambda_R^- &\approx -0.44 < 0\end{aligned}\tag{3.24}$$

Other examples of boundary data that are consistent with the Rankine-Hugoniot equations are provided in Tables 6.1 and 6.2 on page 87.

Chapter 4

Numerical Solutions of 1-D Euler and Navier-Stokes Equations

4.1 The Numerical Problem Setup

In this section we develop numerical schemes to solve a system of partial differential equations in the form:

$$\vec{w}_t + A(\vec{w})\vec{w}_x = \frac{1}{\mathcal{R}e}Q(\vec{w})F(\vec{w})_{xx} \quad (4.1)$$

where A and Q are 3-by-3 matrix valued functions and F is a vector field. All functions are defined on $\Omega = [0, +\infty) \times [0, 1]$. Additionally we require that $A(\vec{w})$ be diagonalizable $\forall \vec{w} \in \Omega$. For \vec{w} defined by (2.58) and A , Q , and F defined by (2.59)-(2.62) the system (4.1) becomes the Navier-Stokes System ($\mathcal{R}e > 0$) or the Euler System ($\mathcal{R}e = +\infty$).

Chapter 4. Numerical Solutions of 1-D Euler and Navier-Stokes Equations

Let $\{(t^k, x_j) : k = 0, 1, 2, \dots; j = 1, 2, \dots, N\}$ be an infinite uniform mesh in Ω , such that $t^0 = 0$, $x_1 = 0$, $x_N = 1$, and

$$\Delta x = x_{j+1} - x_j, \quad \Delta t = t^{k+1} - t^k. \quad (4.2)$$

Let \vec{w}_t^k be an approximation of $\vec{w}(t^k, x_j)$. We introduce two difference schemes for system (4.1):

$$\frac{\vec{w}_j^{k+1} - \vec{w}_j^k}{\Delta t} + A_{j,k} \frac{\hat{\Delta} \vec{w}_j^k}{\Delta x} = \frac{1}{\mathcal{R}e} Q_{j,k} \frac{\Delta^2 F_j^k}{\Delta x^2} \quad (4.3)$$

and

$$\frac{\vec{w}_j^{k+1} - \vec{w}_j^k}{\Delta t} + A_{j,k} \frac{\hat{\Delta} \vec{w}_j^k}{\Delta x} = \frac{1}{\mathcal{R}e} Q_{j,k} \frac{\Delta^2 F_j^{k+1}}{\Delta x^2}, \quad (4.4)$$

where $A_{j,k} = A(w_j^k)$, $Q_{j,k} = Q(w_j^k)$, and

$$\Delta^2 F_j^k = \frac{F(\vec{w}_{j-1}^k) - 2F(\vec{w}_j^k) + F(\vec{w}_{j+1}^k)}{\Delta x^2} = \frac{F_{j-1}^k - 2F_j^k + F_{j+1}^k}{\Delta x^2} \quad (4.5)$$

The first order upwinding difference operator $\hat{\Delta}$ will be introduced shortly.

Equations (4.3) can be readily solved for \vec{w}_j^{k+1} , therefore (4.3) is classified as a finite volume explicit difference scheme. The main disadvantage for explicit schemes is that in the case $\mathcal{R}e < +\infty$ the stability restrictions imposed on Δt and Δx are of the type

$$\frac{\Delta t}{\Delta x^2} \leq \mathcal{O}(1)$$

Equations (4.4) are not readily solvable for \vec{w}_j^{k+1} . Resolving (4.4) requires solving a non-linear system of equations. Thus (4.4) represents an implicit finite difference scheme which is known to poses better stability characteristics [17]:

$$\frac{\Delta t}{\Delta x} \leq \mathcal{O}(1)$$

The only difference between (4.3) and (4.4) is the level of time at which second order difference operator Δ^2 is evaluated. Thus we will write these two schemes in the same form

$$\frac{\vec{w}_j^{k+1} - \vec{w}_j^k}{\Delta t} + A_{j,k} \frac{\hat{\Delta} \vec{w}_j^k}{\Delta x} = \frac{1}{\mathcal{R}e} Q_{j,k} \frac{\Delta^2 F_j}{\Delta x^2}, \quad (4.6)$$

The superscript k is intentionally omitted inside Δ^2 . We bare in mind that whenever k is used in reference to Δ^2 , the explicit version of (4.6) is implied. Similarly, if Δ^2 is evaluated at the time level $k + 1$, then we consider the implicit version of (4.6), namely (4.4).

The difference scheme described by (4.6) is not complete since it is invalid for $j = 1$ and $j = N$. Thus the provided equations need to be supplemented by additional equations that describe the behavior of \vec{w} on the boundary $x = 0$ and $x = 1$. The treatment of the boundary will greatly vary with respect to the type of the system considered $\mathcal{R}e < +\infty$ (the Navier-Stokes case) or $\mathcal{R}e = +\infty$ (the Euler case). This discussion is laid out in Section 4.5 on page 63.

4.2 The Upwinding First Order Difference Operator $\hat{\Delta}$

The discussion in this section is valid for both explicit and implicit methods. In order to insure stability of (4.6) we use the upwinding approach based on the characteristics method. According to the problem set up, matrix function A is required to have three distinct eigenvalues $\lambda_i(t, x)$, $i = 1, 2, 3$. This will ensure that A is diagonalizable. Let T be the diagonalizable transformation of A then

$$AT = \Lambda T, \quad (4.7)$$

where

$$\Lambda = \begin{bmatrix} \lambda_1 & 0 & 0 \\ 0 & \lambda_2 & 0 \\ 0 & 0 & \lambda_3 \end{bmatrix} \quad (4.8)$$

The dependence of (t, x) in all quantities is implied. Let \vec{v}_j^k be the characteristic variables defined by

$$\vec{v}_j^k = T_{j,k} \vec{w}_j^k \text{ and } \vec{v}_{j\pm 1}^k = T_{j,k} \vec{w}_{j\pm 1}^k \quad (4.9)$$

Then according to the upwinding method [21, 26] for $i = 1, 2, 3$ we have:

$$\Delta \vec{v}_{j,i}^k = \begin{cases} \vec{v}_{j,i}^k - \vec{v}_{j-1,i}^k, & \lambda_{j,k}^i > 0 \\ \vec{v}_{j+1,i}^k - \vec{v}_{j,i}^k, & \lambda_{j,k}^i \leq 0 \end{cases} \quad (4.10)$$

Let

$$\alpha_{j,i}^k = \text{sign } \lambda_{j,i}^k \quad (4.11)$$

then we notice that the definition (4.10) can be written as

$$\Delta \vec{v}_{j,i}^k = \frac{1}{2}(\alpha_{j,i}^k + 1)(\vec{v}_{j,i}^k - \vec{v}_{j-1,i}^k) - \frac{1}{2}(\alpha_{j,i}^k - 1)(\vec{v}_{j+1,i}^k - \vec{v}_{j,i}^k)$$

After simplifying the expression above we arrive to a more convenient equivalent definition of the upwinding difference

$$\Delta \vec{v}_{j,i}^k = -\frac{1}{2}(\alpha_{j,i}^k + 1)\vec{v}_{j-1,i}^k - \frac{1}{2}(\alpha_{j,i}^k - 1)\vec{v}_{j+1,i}^k + \alpha_{j,i}^k \vec{v}_{j,i}^k,$$

which in the vector form can be written as

$$\Delta \vec{v}_j^k = -\frac{1}{2}(\alpha_j^k + I)\vec{v}_{j-1}^k - \frac{1}{2}(\alpha_j^k - I)\vec{v}_{j+1}^k + \alpha_j^k \vec{v}_j^k, \quad (4.12)$$

where I is the 3-by-3 identity matrix and $\alpha_j^k = \text{diag}(\alpha_{j,1}^k, \alpha_{j,2}^k, \alpha_{j,3}^k)$. By substituting (4.9) into (4.12) $\Delta \vec{v}_j^k$ can be expressed in terms of generic variables \vec{w}_j^k :

$$\Delta \vec{v}_j^k = -\frac{1}{2}(\alpha_j^k + I)T_{j,k}^{-1}\vec{w}_{j-1}^k - \frac{1}{2}(\alpha_j^k - I)T_{j,k}^{-1}\vec{w}_{j+1}^k + \alpha_j^k T_{j,k}^{-1}\vec{w}_j^k. \quad (4.13)$$

According to the upwinding principle [21, 26] $\hat{\Delta} \vec{w}_j^k$ must be defined as

$$\hat{\Delta} \vec{w}_j^k = T_{j,k} \Delta \vec{v}_j^k. \quad (4.14)$$

The final expression is obtained by substituting (4.13) into (4.14):

$$\hat{\Delta} \vec{w}_j^k = -\frac{1}{2}T_{j,k}(\alpha_j^k + I)T_{j,k}^{-1}\vec{w}_{j-1}^k - \frac{1}{2}T_{j,k}(\alpha_j^k - I)T_{j,k}^{-1}\vec{w}_{j+1}^k + T_{j,k}\alpha_j^k T_{j,k}^{-1}\vec{w}_j^k.$$

Further simplification yields

$$\hat{\Delta} \vec{w}_j^k = -\frac{1}{2}T_{j,k}\alpha_j^k T_{j,k}^{-1}(\vec{w}_{j+1}^k - 2\vec{w}_j^k + \vec{w}_{j-1}^k) + \frac{1}{2}(\vec{w}_{j+1}^k - \vec{w}_{j-1}^k)$$

or

$$\hat{\Delta} \vec{w}_j^k = -\frac{1}{2}T_{j,k}\alpha_j^k T_{j,k}^{-1}\Delta^2 \vec{w}_j^k + \frac{1}{2}\overset{\circ}{\Delta} \vec{w}_j^k$$

where Δ^2 is the second order difference defined similarly to (4.5) and

$$\overset{\circ}{\Delta} \vec{w}_j^k = \vec{w}_{j+1}^k - \vec{w}_{j-1}^k.$$

Furthermore

$$A_{j,k}\hat{\Delta} \vec{w}_j^k = -\frac{1}{2}A_{j,k}T_{j,k}\alpha_j^k T_{j,k}^{-1}\Delta^2 \vec{w}_j^k + \frac{1}{2}A_{j,k}\overset{\circ}{\Delta} \vec{w}_j^k \quad (4.15)$$

Let

$$|\Lambda_{i,j}| = \Lambda_{i,j}\alpha_j^k = \begin{bmatrix} |\lambda_1| & 0 & 0 \\ 0 & |\lambda_2| & 0 \\ 0 & 0 & |\lambda_3| \end{bmatrix} \quad (4.16)$$

then according to (4.7)

$$A_{j,k}T_{j,k}\alpha_j^k T_{j,k}^{-1} = T_{j,k}\Lambda_{j,k}\alpha_j^k T_{j,k}^{-1} = T_{j,k}|\Lambda_{j,k}|T_{j,k}^{-1} \quad (4.17)$$

To simplify formula (4.17) we adopt the following “natural” notation

$$|A_{j,k}| = T_{j,k}|\Lambda_{j,k}|T_{j,k}^{-1} \quad (4.18)$$

By substituting this expression into (4.17) and then into (4.15) we obtain the final form of the first order upwinding operator

$$A_{j,k} \frac{\hat{\Delta} \vec{w}_j^k}{\Delta x} = -\frac{1}{2} T_{j,k} |\Lambda_{j,k}| T_{j,k}^{-1} \frac{\Delta^2 \vec{w}_j^k}{\Delta x} + \frac{1}{2} A_{j,k}^k \overset{\circ}{\Delta} \vec{w}_j^k \quad (4.19)$$

or equivalently

$$A_{j,k} \hat{\Delta} \vec{w}_j^k = -\frac{1}{2} T_{j,k} |\Lambda_{j,k}| T_{j,k}^{-1} \Delta^2 \vec{w}_j^k + \frac{1}{2} A_{j,k}^k \overset{\circ}{\Delta} \vec{w}_j^k \quad (4.20)$$

4.3 The Explicit Numerical Scheme for the 1-D Euler System

For the explicit version of the numerical scheme (4.6) we evaluate the second order difference operator Δ^2 at time level t_k :

$$\frac{\vec{w}_j^{k+1} - \vec{w}_j^k}{\Delta t} + A_{j,k} \frac{\hat{\Delta} \vec{w}_j^k}{\Delta x} = \frac{1}{\mathcal{R}e} Q_{j,k} \frac{\Delta^2 F_j^k}{\Delta x^2}. \quad (4.21)$$

which can be transformed into

$$\vec{w}_j^{k+1} = \vec{w}_j^k - \sigma_1 A_{j,k} \hat{\Delta} \vec{w}_j^k + \sigma_2 \Delta^2 F_j^k, \quad (4.22)$$

where

$$\sigma_1 = \frac{\Delta t}{2\Delta x} \tag{4.23}$$

$$\sigma_2 = \frac{\Delta t}{\mathcal{R}e\Delta x^2} \tag{4.24}$$

and $A_{j,k}\hat{\Delta}$ is defined by (4.19) or (4.20)

For the Euler case we set $\mathcal{R}e = +\infty$ and therefore $\sigma_2 = 0$. In the case of the Euler System we obtain a numerical scheme that involves first difference operators. Due to the hyperbolic type of the problem the stability of such scheme is related to the Courant-Friedrichs-Lewy necessary stability condition

$$\frac{\Delta t}{\Delta x} < \frac{\nu}{|\lambda|_{\max}}, \tag{4.25}$$

where ν is the CFL constant independent of $(\Delta x, \Delta t)$ and is determined experimentally. For the hyperbolic case ($\mathcal{R}e = +\infty$) the stability condition (4.25) is not hard to satisfy since the rate of growth of Δx is the same as for Δt .

In the case of the Navier-Stokes equations the system becomes parabolic. In this case the key stability condition takes form

$$\frac{\Delta t}{\Delta x^2} = \mathcal{O}(1) \tag{4.26}$$

For small values of Δx (4.26) is computationally more challenging to satisfy and we must resort to an implicit numerical approach whose stability will be determined by a CFL-type condition.

4.4 The Implicit Numerical Scheme for the 1-D Navier-Stokes System

An explicit numerical scheme can be obtained from (4.6) by taking the second order difference operator Δ^2 at time t_{k+1} :

$$\frac{\vec{w}_j^{k+1} - \vec{w}_j^k}{\Delta t} + A_{j,k} \frac{\hat{\Delta} \vec{w}_j^k}{\Delta x} = \frac{1}{\mathcal{R}e} Q_{j,k} \frac{\Delta^2 \vec{F}_j^{k+1}}{\Delta x^2} \quad (4.27)$$

Let us assume that the values of \vec{w} at time t_k have been calculated and known. The transition to the next time step t_{k+1} is accomplished by solving equation (4.27) with respect to \vec{w}^{k+1} . We keep all the unknowns on the left hand side and the rest of the terms is moved to the right hand side:

$$\vec{w}_j^{k+1} - \sigma_2 Q_{j,k} \Delta^2 \vec{F}_j^{k+1} = \vec{w}_j^k - \sigma_1 A_{j,k} \hat{\Delta} \vec{w}_j^k \quad (4.28)$$

where σ_1 and σ_2 are defined by (4.23) and (4.24). In addition we define vectors \vec{u}_j^k as

$$\vec{u}_j^k = \vec{w}_j^k - \sigma_1 A_{j,k} \hat{\Delta} \vec{w}_j^k. \quad (4.29)$$

To avoid an overload of notation the following conventions are adopted. We drop the subscript k from equation (4.29). Vector \vec{u}_j refers to \vec{u}_j^k and is treated as a known parameter. Vector \vec{w}_j is an unknown variable and it refers to \vec{w}_j^{k+1} . Similarly Q_j should be regarded as $Q_{j,k}$ as well as F_j should refer to F_j^{k+1} .

In the light of the aforementioned simplifications we obtain

$$\vec{w}_j - \sigma_2 Q_j (\vec{F}_{j-1} - 2\vec{F}_j + \vec{F}_{j+1}) = \vec{u}_j, \quad (4.30)$$

where $\vec{F}_j = \vec{F}(\vec{w}_j)$.

From this point on we will address the 1-D Navier-Stokes system written in the form of equation (2.63) page 43 whose discretization scheme is given by (4.21) and reduced to (4.30). For such system of PDEs Q and F are known functions given by (2.61) and (2.59) on page 43.

Here, as in Section 4.1, we assume that the coordinate space $[0, 1]$ is split by N equidistant points that create a mesh with the step Δx . Therefore system (4.30) is a set of $3N$ equations and $3N$ variables ($\vec{u}_j, \vec{w}_j \in \mathbb{R}^3$)

Let $\vec{U}, \vec{W} \in \mathbb{R}^{3N}$ be vectors based on \vec{u}_j and \vec{w}_j , and whose definitions are provided below

$$\vec{W} = [w_1^1 \quad w_2^1 \quad w_3^1 \quad \dots \quad w_1^N \quad w_2^N \quad w_3^N]^T \quad (4.31)$$

$$\vec{U} = [u_1^1 \quad u_2^1 \quad u_3^1 \quad \dots \quad u_1^N \quad u_2^N \quad u_3^N]^T \quad (4.32)$$

Variable w_j^i refers to the i^{th} component of vector \vec{w} approximated at the j^{th} node of the space mesh x_j . A similar agreement is in affect for \vec{u} or any other \mathbb{R}^{3N} vector under consideration.

Let $\mathcal{F} : \mathbb{R}^{3N} \longrightarrow \mathbb{R}^{3N}$ be a function whose definition is based on function F and defined by

$$\mathcal{F}(\vec{z}_1, \vec{z}_2, \dots, \vec{z}_N) = \left[\vec{F}(\vec{z}_1) \quad \vec{F}(\vec{z}_2) \quad \dots \quad \vec{F}(\vec{z}_N) \right]^T \quad (4.33)$$

Here we treat $(\vec{z}_1, \vec{z}_2, \dots, \vec{z}_N)$ as a long vector Z from \mathbb{R}^{3N} for purposes of reducing complexity of notation. Thus $\mathcal{F}(Z)$ is the same as $\mathcal{F}(\vec{z}_1, \vec{z}_2, \dots, \vec{z}_N)$.

Chapter 4. Numerical Solutions of 1-D Euler and Navier-Stokes Equations

Before we write down a vector form of system (4.30) we assume that a set of adequate boundary conditions is provided by (4.72) and (4.73) on page 70

$$\vec{u}_1 = \vec{w}_1 = \vec{w}_1^{k+1} \tag{4.34}$$

$$\vec{u}_N = \vec{w}_N = \vec{w}_N^{k+1}$$

A method to obtain proper boundary conditions is discussed in Section 4.5.2. After incorporating the boundary data into vector U a set of vector equations (4.30) maybe written as

$$W - \sigma_2 \mathcal{Q} \mathcal{J} \mathcal{F}(W) = U \tag{4.35}$$

Block sparse diagonal matrix \mathcal{Q} and sparse block tri-diagonal matrix \mathcal{J} are defined as

$$\mathcal{Q} = \begin{bmatrix} O & & & & & \\ & Q_2 & & & & \\ & & Q_3 & & & \\ & & & \ddots & & \\ & & & & Q_{N-1} & \\ & & & & & O \end{bmatrix} \tag{4.36}$$

$$\mathcal{J} = \begin{bmatrix} O & O & O & & & \\ I & -2I & I & & & \\ O & I & -2I & I & & \\ & & & \ddots & & \\ & & & & I & -2I & I \\ & & & & O & O & O \end{bmatrix} \tag{4.37}$$

where I and O are the identity and zero 3×3 matrices correspondingly. We recall that according to (4.33)

$$\mathcal{F}(W) = \left[\vec{F}(\vec{w}_1) \quad \vec{F}(\vec{w}_2) \quad \dots \quad \vec{F}(\vec{w}_N) \right]^T \tag{4.38}$$

Chapter 4. Numerical Solutions of 1-D Euler and Navier-Stokes Equations

Let \mathbb{G}_U be a nonlinear mapping of \mathcal{R}^{3N} into itself defined as

$$\mathbb{G}_U : W \mapsto W - \sigma_2 \mathcal{QJF}(W) - U \quad (4.39)$$

Finding a solution of (4.35) is equivalent to finding a solution of

$$\mathbb{G}_U(W) = 0 \quad (4.40)$$

In order to solve (4.40) we use the Newtonian Iteration Method:

$$W_{m+1} = W_m - [\mathbb{G}'(W_m)]^{-1} \mathbb{G}_U(W_m) \quad (4.41)$$

The initial iteration W_0 was taken as a solution of (4.40) in the previous time step. Jacobian \mathbb{G}' does not depend on the right hand side vector U for obvious reasons, therefore the subscript U was omitted. Due to the special structure of mapping F the computation of the Jacobian can be simplified.

Let us recall that for the Navier-Stokes system function $F : \mathbb{R}^3 \longrightarrow \mathbb{R}^3$ (2.59) is given by

$$F(\vec{w}) = \begin{bmatrix} 0 \\ w_2 \\ \kappa w_3 + \frac{1}{2} w_2^2 \end{bmatrix}, \quad (4.42)$$

where

$$\kappa = \frac{\gamma}{(\gamma - 1)Pr}. \quad (4.43)$$

Function \vec{F} can be represented as the sum of a linear and non-linear terms

$$F_L(\vec{w}) = \begin{bmatrix} 0 \\ w_2 \\ \kappa w_3 \end{bmatrix} = \underbrace{\begin{bmatrix} 0 & 0 & 0 \\ 0 & 1 & 0 \\ 0 & 0 & \kappa \end{bmatrix}}_{\Omega} \vec{w} = \Omega \vec{w} \quad (4.44)$$

$$F_{NL}(\vec{w}) = \frac{1}{2}w_2^2 \begin{bmatrix} 0 \\ 0 \\ 1 \end{bmatrix} \quad (4.45)$$

$$\vec{F}(\vec{w}) = \Omega\vec{w} + \vec{F}_{NL}(\vec{w}) \quad (4.46)$$

Because of the definition (4.33) will inherit the same structure as \vec{F}

$$\mathcal{F}(W) = \Omega W + \mathcal{F}_{NL}(W) \quad (4.47)$$

where ω is a sparse $3N \times 3N$ block-diagonal matrix:

$$\Omega = \text{diag}(\underbrace{\Omega, \Omega, \dots, \Omega}_N) \quad (4.48)$$

Expression for mapping \mathbb{G}_U (4.39) can be simplified using (4.47) and (4.48)

$$\mathbb{G}_U = (I - \mathcal{Q}\mathcal{I})W - \sigma_2\mathcal{Q}\mathcal{J}\mathcal{F}_{NL}(W) - U \quad (4.49)$$

Here product $\sigma_2\mathcal{J}\Omega$ was substituted by \mathcal{I} which is a constant tri-diagonal matrix that needs to be calculated only once:

$$\mathcal{I} = \mathcal{J}\Omega = \begin{bmatrix} O & O & O & & & & \\ \sigma_2\Omega & -2\sigma_2\Omega & \sigma_2\Omega & & & & \\ O & \sigma_2\Omega & -2\sigma_2\Omega & \sigma_2\Omega & & & \\ & & & \ddots & & & \\ & & & & \sigma_2\Omega & -2\sigma_2\Omega & \sigma_2\Omega \\ & & & & O & O & O \end{bmatrix} \quad (4.50)$$

The jacobian of \mathbb{G}_U , given in the form of equation (4.49), can be written as

$$\mathbb{G}'(W) = I - \mathcal{Q}\mathcal{I} - \mathcal{Q}\mathcal{J}\mathcal{F}'_{NL}(W) \quad (4.51)$$

Although the non-linear part of \mathcal{F} is a simple quadratic function, writing it is rather a cumbersome task. Therefore we provide its exact expression $\mathcal{J}\mathcal{F}_{NL}$ and the jacobian of $\mathcal{J}\mathcal{F}'_{NL}(W)$ in Appendix C.3 on page 146 formulae (C.22) and (C.26). It is worth mentioning that due to the fact that function \vec{F} , and therefore \mathcal{F} as well, is quadratic, the Newtonian Iteration is supposed to converge no later than the second iteration, which was confirmed by numerical simulations.

4.5 Boundary Conditions

The structure of the boundary conditions for the systems (4.1) may vary greatly depending on the structure of the righthand side of (4.1). For $Re = +\infty$, (4.1) represents a hyperbolic system of PDEs (provided certain requirements on the eigenvalues of matrix A are met). For $Re = < +\infty$ system (4.1) may become of the parabolic type or mixed parabolic-hyperbolic type. The different classes of systems of PDEs require different approaches to designing boundary conditions. Thus we will only consider two specific cases: The 1-D Euler System and The 1-D Navier-Stokes System of equations. Moreover we will consider only the case of shock forming conditions described in Section 3.1 This type of boundary conditions is required for the numerical algorithms discussed in Sections 4.4 and 4.3.

4.5.1 Boundary Conditions for the 1-D Euler System

By substituting $Re = +\infty$ into (2.63) we obtain 1-D Euler System that describes an inviscid flow:

$$\vec{w}_t + A(\vec{w})\vec{w}_x = 0, \tag{4.52}$$

where $A(\vec{w})$ is given by (2.62) and $\vec{w} = [\rho, u, \theta]^T$

According to the discussion in Section 3.1 the stationary solution of (4.52) must have a stationary shock profile (see Figure 4.5.1) with values on the boundary that satisfy (3.11)-(3.16).

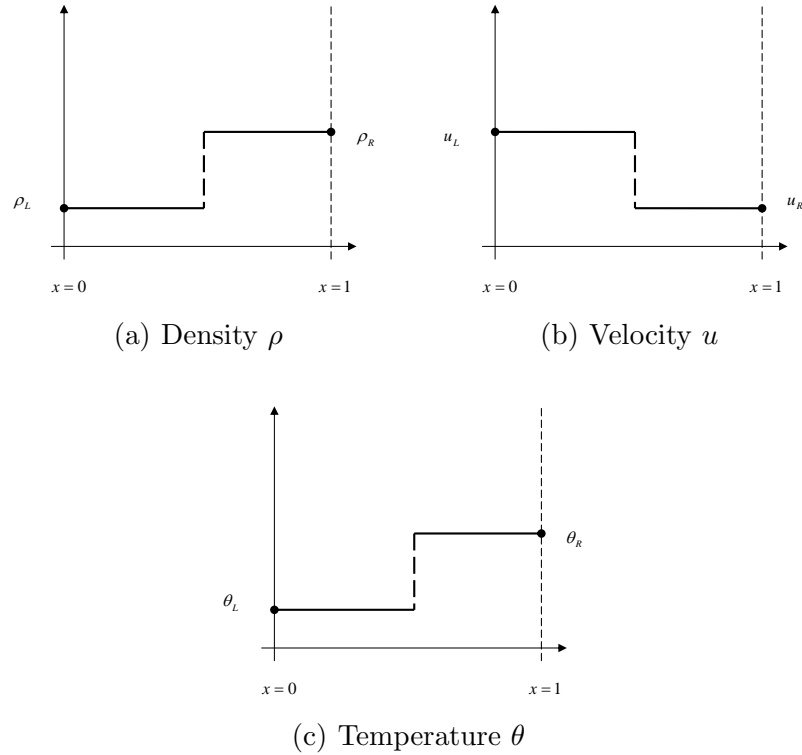


Figure 4.1: Stationary shock profiles

Since the characteristics $\lambda_1, \lambda_2, \lambda_3$ on the left boundary are positive, the left boundary behavior is characterized as inflows into the domain $[0, 1]$. Therefore the left boundary admits three rigid constraints on $\rho, u,$ and θ . Thus the boundary condition for $x = 0$ takes form

$$\begin{aligned} \rho(t, 0) &= \rho_L \\ u(t, 0) &= u_L \\ \theta(t, 0) &= \theta_L \end{aligned} \tag{4.53}$$

The equivalent discrete boundary condition on the left is given by

$$\vec{w}_1^k = \begin{bmatrix} \rho_L \\ u_L \\ \theta_L \end{bmatrix} \quad (4.54)$$

According to (3.14)-(3.16) the right boundary characteristics are chosen so that $\lambda_1 > 0$, $\lambda_2 > 0$, and $\lambda_3 < 0$. Thus two characteristics are outflowing and one characteristic provides an inflow into the domain. Such boundary situation admits only one rigid constrain on ρ , u , and θ . It can be formulated as

$$\phi_1 w_1(t, 1) + \phi_2 w_2(t, 1) + \phi_3 w_2(t, 1) = \phi_0 \quad (4.55)$$

or equivalently

$$\vec{\phi}^T \vec{w} = \phi_0, \quad (4.56)$$

where $\vec{\phi} = \begin{bmatrix} \phi_1 \\ \phi_2 \\ \phi_3 \end{bmatrix} \in \mathbb{R}^3$ and $\phi_0 \in \mathbb{R}$ are constants.

A numerical implementation of (4.56) is not as straightforward as in the case of the left boundary. Our goal here is to develop an algorithms that will allow us to compute values \vec{w}_N^{k+1} without boundary layer effects. Since we are interested in the time level t_{k+1} we assume that values of \vec{w}^k have already been calculated and available for any $x = x_j$. Moreover values of the local linearization transformations $T_{j,k}$ and eigenvalues $\Lambda_{j,k}$ are available as well. Thus the characteristic variables \vec{v}_j^k can be calculated in a straightforward manner:

$$\vec{v}_j^k = T_{j,k}^{-1} \vec{w}_j^k, \quad j = 1 \dots N \quad (4.57)$$

Chapter 4. Numerical Solutions of 1-D Euler and Navier-Stokes Equations

The first two components of \vec{v}_j^{k+1} can be advected using the diagonalized numerical procedure:

$$\begin{aligned} \frac{v_{1,N}^{k+1} - v_{1,N}^k}{\Delta t} + \lambda_{N,k}^1 \frac{v_{1,N}^k - v_{1,N-1}^k}{\Delta x} &= 0 \\ \frac{v_{2,N}^{k+1} - v_{2,N}^k}{\Delta t} + \lambda_{N,k}^2 \frac{v_{2,N}^k - v_{2,N-1}^k}{\Delta x} &= 0 \end{aligned} \quad (4.58)$$

No such equation can be obtained for the third component $v_{3,N}^{k+1}$ since $\lambda_3 < 0$ on the right boundary. One would have to use the backwards difference $\frac{v_{3,N+1}^k - v_{3,N}^k}{\Delta x}$ which is not available since $x = x_{n+1}$ is outside the domain. Thus the values for $v_{3,N}^{k+1}$ must be obtained using the information about the values of the generic variables \vec{w}_N^{k+1} on the right boundary - equations (4.55)-(4.56). At this moment we accept that the values of $v_{1,N}^{k+1}$ and $v_{2,N}^{k+1}$ are calculated from (4.58) and we denote them as \hat{v}_1 and \hat{v}_2 :

$$\begin{aligned} \hat{v}_1 &= v_{1,N}^k - \frac{\Delta t}{\Delta x} (v_{1,N}^k - v_{1,N-1}^k) \\ \hat{v}_2 &= v_{2,N}^k - \frac{\Delta t}{\Delta x} (v_{2,N}^k - v_{2,N-1}^k) \end{aligned} \quad (4.59)$$

In what follows we design a method to calculate $v_{3,N}^{k+1}$. First we relate \vec{w}_N^{k+1} and \vec{v}_N^{k+1} through the local diagonalization transformation T . However T is not available at time level t^{k+1} therefore we approximate $T_{N,k+1}$ by $T_{N,k}$:

$$\vec{w}_N^{k+1} = T_{N,k} \vec{v}_N^{k+1} \quad (4.60)$$

Discretized version of equation (4.56) takes form

$$\vec{\phi}^T \vec{w}_N^{k+1} = \phi_0 \quad (4.61)$$

Chapter 4. Numerical Solutions of 1-D Euler and Navier-Stokes Equations

Let us treat variables \vec{w}_N^{k+1} and \vec{v}_N^{k+1} as unknowns. Then we obtain a linear system with six equations and six variables:

$$\begin{aligned}
 \vec{w}_j^{k+1} &= T_{N,k} \vec{v}_j^{k+1} \\
 \vec{\phi}^T \vec{w}_N^{k+1} &= \phi_0 \\
 \vec{v}_{1,N}^{k+1} &= \hat{v}_1 \\
 \vec{v}_{2,N}^{k+1} &= \hat{v}_2
 \end{aligned} \tag{4.62}$$

If we organize the unknown variables $w_{1,N}^{k+1}$, $w_{2,N}^{k+1}$, $w_{3,N}^{k+1}$, $v_{1,N}^{k+1}$, $v_{2,N}^{k+1}$, and $v_{3,N}^{k+1}$ as a six-by-one vector we obtain the following linear system in the matrix form:

$$\underbrace{\begin{bmatrix} & & & & & \\ & & & & & \\ & & & & & \\ \hline \phi_1 & \phi_2 & \phi_3 & 0 & 0 & 0 \\ 0 & 0 & 0 & 1 & 0 & 0 \\ 0 & 0 & 0 & 0 & 1 & 0 \end{bmatrix}}_M \begin{bmatrix} w_{1,N}^{k+1} \\ w_{2,N}^{k+1} \\ w_{3,N}^{k+1} \\ v_{1,N}^{k+1} \\ v_{2,N}^{k+1} \\ v_{3,N}^{k+1} \end{bmatrix} = \begin{bmatrix} 0 \\ 0 \\ 0 \\ \phi_0 \\ \hat{v}_1 \\ \hat{v}_2 \end{bmatrix}, \tag{4.63}$$

where \hat{v}_1 and \hat{v}_2 are provided by (4.59).

It can be shown (see Appendix C.2 p.145) that $\det M = -(\phi_3 + \phi_1 \rho \theta^{-1})$. Thus by manipulating constants ϕ_1 and ϕ_2 one can always ensure that $0 \neq \det M = \mathcal{O}(1)$ and therefore the system (4.63) is non-singular and well posed.

The following is a summary of a set of adequate boundary conditions required for a numerical solution of the Euler System in the continuous and discretized data.

Continuous case:

$$\begin{cases} \vec{w}(t, 0) = [\rho_L, u_L, \theta_L]^T \\ \vec{\phi}^T \vec{w}(t, 1) = \phi_0 \end{cases} \tag{4.64}$$

Discretized case:

$$\begin{cases} \vec{w}_1^{k+1} = [\rho_L, u_L, \theta_L]^T \\ \vec{w}_N^{k+1} = PM^{-1}[0, 0, 0, \phi_0, \hat{v}_1, \hat{v}_2]^T, \end{cases} \quad (4.65)$$

where $P = \begin{bmatrix} 1 & 0 & 0 & 0 & 0 & 0 \\ 0 & 1 & 0 & 0 & 0 & 0 \\ 0 & 0 & 1 & 0 & 0 & 0 \end{bmatrix}$ and M is defined by (4.63).

Quantities $\vec{\phi}$ and ϕ_0 must satisfy

$$\vec{\phi}^T[\rho_R, u_R, \theta_R] = \phi_0,$$

where $[\rho_L, u_L, \theta_L]$ and $[\rho_R, u_R, \theta_R]$ are values consistent with the Rankine-Hugoniot system (3.4).

4.5.2 Boundary Conditions for the 1-D Navier-Stokes System

The 1-D Navier-Stokes system of partial differential equations fits the general framework of equation (4.1) with A , F , and Q given by (2.62), (2.59), and (2.61) on p.43 correspondingly and whose component form is provided by (3.1) on p.45:

$$\rho_t + (\rho u)_x = 0 \quad (4.66)$$

$$(\rho u)_t + (\rho u^2 + \rho \theta)_x = \frac{1}{\mathcal{R}e} u_{xx} \quad (4.67)$$

$$\left(\frac{1}{2} \rho u^2 + \frac{\rho \theta}{\gamma - 1} \right)_t + \left(\frac{1}{2} \rho u^3 + \frac{\gamma \rho u \theta}{\gamma - 1} \right)_x = \frac{\gamma}{(\gamma - 1) \mathcal{P}r \mathcal{R}e} \theta_{xx} + \frac{1}{2 \mathcal{R}e} u_{xx}^2 \quad (4.68)$$

For $\mathcal{R}e < +\infty$ this is a mixed type system. Indeed equations (4.68) and (4.67) are of the parabolic type and equation (4.66) is hyperbolic. There must be a set

of two boundary conditions for each side of the boundary for each of the parabolic equation.

Due to the hyperbolic type of equation (4.66) we must examine its characteristic to determine a proper behavior on the boundary. To accomplish this we rewrite equation (4.66) in a different form where we assume that function u is known and, in the greatest generality, it depends on ρ , x , and t :

$$\rho_t + u\rho_x = -\rho u_x \quad (4.69)$$

For the moment let us disregard the lower order term $-\rho u_x$ in the equation above:

$$\rho_t + u\rho_x = 0 \quad (4.70)$$

Equation (4.70) is a homogeneous hyperbolic equation whose solution is a wave, the direction of propagation of which depends solely upon the sign of the function u in the advection term $u\rho_x$. According to the initial assumption on the boundary conditions described in Section 3.1 page 45 inequality (3.5) u must be a positive quantity. In this case one and the only characteristic of (4.70) is positive. The original equation (4.69) exhibits an equivalent behavior as far as the direction of propagation of their wave-like solutions is concerned. Thus (4.69) has an inflow on the left boundary and an outflow on the right boundary. This situation requires a boundary condition for $x = 0$ and the value of ρ at $x = 1$ must be advected from the interior of the domain (see Figure 4.2).

Discretization of equation (4.69) around the right boundary takes form

$$\frac{\rho_N^{k+1} - \rho_N^k}{\Delta t} + u_N^k \frac{\rho_N^k - \rho_{N-1}^k}{\Delta x} = -\rho_N^k \frac{u_N^k - u_{N-1}^k}{\Delta x} \quad (4.71)$$

The following is a summary of a set of adequate boundary conditions required for a numerical solution of the Navier-Stokes System in the continuous and discretized

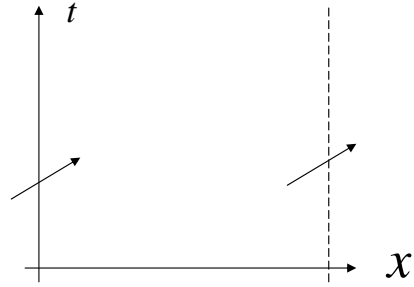


Figure 4.2: Direction of propagation of a solution of equation (4.69)

data.

Continuous case:

$$\begin{cases} \vec{w}(t, 0) = [\rho_L, u_L, \theta_L]^T \\ w_2(t, 1) = u_R \\ w_3(t, 1) = \theta_R \end{cases} \quad (4.72)$$

Discretized case:

$$\begin{cases} \vec{w}_1^{k+1} = [\rho_L, u_L, \theta_L]^T \\ \vec{w}_N^{k+1} = [\hat{\rho}_R, u_R, \theta_R]^T \end{cases} \quad (4.73)$$

where $\hat{\rho}_R = \rho_N^{k+1}$, which is obtained from solving (4.71):

$$\rho_N^{k+1} = \rho_N^k - \sigma_1 [u_N^k (\rho_N^k - \rho_{N-1}^k) + \rho_N^k (u_N^k - u_{N-1}^k)] \quad (4.74)$$

where σ_1 defined by (4.23) on page 57.

Chapter 5

Numerical Solution of the 1-D Bhatnagar–Gross–Krook Model

5.1 The Continuous 1-D BGK Model

Consider the 1-D Bhatnagar–Gross–Krook equation discussed in Section 1.3.5:

$$\frac{\partial f}{\partial t} + v \frac{\partial f}{\partial x} = -\frac{1}{\tau}(f - f^e), \quad (5.1)$$

where $f = f(t, x, v)$, f^e is a 1-D local Maxwellian parametrized by functions $\rho, u, \theta : [0, +\infty] \times [0, 1] \rightarrow \mathbb{R}$, and τ is a small parameter called a relaxation time ($0 < \tau \ll 1$). The expression for a 1-D local Maxwellian is given by (5.2).

$$f_{(\rho, u, \theta)}^e(v) = \frac{\rho(t, x)}{\sqrt{2\pi\theta(t, x)}} \exp \left\{ -\frac{(u(t, x) - v)^2}{2\theta(t, x)} \right\} \quad (5.2)$$

We require that the one particle distribution function f possess the same moments as the equilibrium distribution f^e does. This requirement is a part of the BGK model

and it is written as

$$\int_{\mathbb{R}} f(v) \begin{bmatrix} 1 \\ v \\ v^2 \end{bmatrix} dv = \int_{\mathbb{R}} f^e(v) \begin{bmatrix} 1 \\ v \\ v^2 \end{bmatrix} dv \quad (5.3)$$

The moments of the Maxwellian distribution can be calculated analytically. Corresponding computations are provided in Appendix A.1 on page 121. It follows from the definition (A.1) that

$$\int_{\mathbb{R}} f^e(v) \begin{bmatrix} 1 \\ v \\ v^2 \end{bmatrix} dv = \frac{\rho}{\sqrt{2\pi\theta}} \begin{bmatrix} I_0 \\ I_1 \\ I_2 \end{bmatrix} = \begin{bmatrix} \rho \\ \rho u \\ \rho(u^2 + \theta) \end{bmatrix} \quad (5.4)$$

To obtain (5.4) we used (A.6), (A.8), and (A.10). From (5.4) we obtain a set of conditions that provide closure of model (5.1)-(5.2). To simplify notations we introduce the averaging operator.

Let \mathcal{P} be the space of continuous functions with at most polynomial growth on infinity¹:

$$\mathcal{P} = \left\{ \phi \in C(\mathbb{R}) \mid \exists n \in \mathbb{N} : \limsup_{v \rightarrow \infty} \frac{\phi(v)}{|v|^n} < +\infty \right\} \quad (5.5)$$

For $\phi \in \mathcal{P}$ we define its average with respect to distribution function f (or simply f -average) as

$$\langle \phi \rangle_f = \int_{\mathbb{R}} f(v) \phi(v) dv \quad (5.6)$$

¹This is a technical assumption required to establish convergence of improper integral (5.6). We also assume that, similarly to f^e , distribution function f decays exponentially in v .

Formula (5.6) defines a linear functional on \mathcal{P} . From now on whenever the subscript is not specified it is assumed to be f i.e. $\langle \cdot \rangle = \langle \cdot \rangle_f$. After substituting (5.4) into (5.3) moments of distribution function f can be expressed as

$$\begin{aligned}\langle 1 \rangle &= \rho \\ \langle v \rangle &= \rho u \\ \langle v^2 \rangle &= \rho(u^2 + \theta)\end{aligned}\tag{5.7}$$

Furthermore parameters ρ , u , and θ can be expressed in terms of the f -averages of 1, v , and v^2 by solving (5.7):

$$\begin{aligned}\rho &= \langle 1 \rangle \\ u &= \frac{\langle v \rangle}{\langle 1 \rangle} \\ \theta &= \frac{\langle v^2 \rangle}{\langle 1 \rangle} - \frac{\langle v \rangle^2}{\langle 1 \rangle^2}\end{aligned}\tag{5.8}$$

Equations (5.1), (5.2) together with (5.7) provide closed Bhatnagar–Gross–Krook model.

5.2 Numerical Solution of the 1-D BGK Model

We proceed in a similar manner as for the implicit and explicit approaches discussed in Sections 4.4 and 4.3.

Let $\{x_i : i = 1 \dots N\} \subset [0, 1]$ be a mesh with N equispaced nodes and step Δx such that $x_1 = 0$ and $x_N = 1$. Let $\{t_k : k = 0, 1, \dots\}$ be the time discretization nodes such that $\Delta t = t_{k+1} - t_k, \forall k \geq 0$. In addition to the space and time discretization

we have to introduce the velocity space² discretization as well. According to the Bhatnagar–Gross–Krook model, the moments are calculated as improper integrals over \mathbb{R} (5.3),(5.7). For the numerical purposes we substitute the integration over all real number by the numerical integration over finite symmetrical interval $[-V, V]$. Such approximation will result in truncation error \mathcal{E}_T and reassembling error \mathcal{E}_R that we require to be of the order of magnitude that does not exceed the order of magnitude of error resulted from a numerical scheme itself:

$$\max \{ \mathcal{E}_T, \mathcal{E}_R \} \leq \mathcal{E} \quad (5.9)$$

In the best case scenario the truncation and reassembling errors should be of the order of the discretization noise, typically $\mathcal{E}_D = 10^{-16}$. However it may be computationally too expensive to implement. The discussion of the truncation and reassembling errors and the methods to choose the values for V and the number of nodes $2M + 1$ are given in Sections 5.4 and 5.5. For now we will assume that these parameters have been chosen.

Let $\{v_j : j = -M, \dots, M\} \subset [-V, V]$ be a uniform mesh of $2M + 1$ nodes with step $\Delta v = v_{j+1} - v_j$, such that $v_{-M} = -V$ and $v_M = +V$. We assume that V and M have been chosen appropriately to satisfy (5.9).

We arrange the nodes of the phase space mesh in vector $\vec{v} \in \mathbb{R}^{2M+1}$:

$$\vec{v} = [v_{-M}, v_{-M+1}, \dots, v_M]^T \quad (5.10)$$

The discretization of (5.1) takes form

$$\frac{f_{i,j}^{k+1} - f_{i,j}^k}{\Delta t} + v_j \frac{\hat{\Delta} f_{i,j}^k}{\Delta x} = -\frac{1}{\tau} (f_{i,j}^k - f_{i,j}^{e,k}) \quad (5.11)$$

²The velocity space is often referred as the phase space [18].

Let

$$\begin{aligned} I^+ &= \{j : v_j \geq 0\} \\ I^- &= \{j : v_j < 0\} \end{aligned} \tag{5.12}$$

then the upwinding first order operator $\hat{\Delta}$ is defined by

$$\hat{\Delta} f_{i,j}^k = \begin{cases} f_{i,j}^k - f_{i-1,j}^k, & i \in I^+ \\ f_{i,j+1}^k - f_{i,j}^k, & i \in I^- \end{cases} \tag{5.13}$$

Discretized equilibrium $f_{i,j}^{e,k}$ is calculated using the Maxwellian distribution (5.2):

$$f_{i,j}^{k,e} = f_{(\rho_j^k, u_j^k, \theta_j^k)}^e(v_i) = \frac{\rho_j^k}{\sqrt{2\pi\theta_j^k}} \exp\left\{-\frac{(u_j^k - v_i)^2}{2\theta_j^k}\right\} \tag{5.14}$$

The macro observables ρ_j^k , u_j^k , and θ_j^k are recovered by the numerical integration based on (5.7) and (5.8):

$$\begin{aligned} \Delta v \sum_{i=-M}^M f_{i,j}^k &= \rho_j^k \\ \Delta v \sum_{i=-M}^M v_i f_{i,j}^k &= \rho_j^k u_j^k \\ \Delta v \sum_{i=-M}^M v_i^2 f_{i,j}^k &= \rho_j^k (\theta_j^k + (u_j^k)^2) \end{aligned} \tag{5.15}$$

where Δv is the mesh step in the phase space. Similarly to (5.6) we define a discretized counterpart of the f -averages

$$\langle\langle \cdot \rangle\rangle_{\vec{f}} : \mathbb{R}^{2M+1} \longrightarrow \mathbb{R} \tag{5.16}$$

$$\langle\langle \vec{\phi} \rangle\rangle_{\vec{f}} = \Delta v \sum_{i=-M}^M f_i \phi_i, \quad \vec{f}, \vec{\phi} \in \mathbb{R}^{2M+1} \tag{5.17}$$

Chapter 5. Numerical Solution of the 1-D Bhatnagar–Gross–Krook Model

As before, whenever the subscript is not specified it is assumed to be f^k or \vec{f}^k depending on the context. In terms of notations above (5.17) takes form

$$\begin{aligned}\langle\langle \vec{1} \rangle\rangle_{f_j^k} &= \rho_j^k \\ \langle\langle \vec{v} \rangle\rangle_{f_j^k} &= \rho_j^k u_j^k \\ \langle\langle \vec{v}^2 \rangle\rangle_{f_j^k} &= \rho_j^k (\theta_j^k + (u_j^k)^2)\end{aligned}\tag{5.18}$$

which can be solved for discretized macro-observables ρ_j^k , u_j^k , and θ_j^k

$$\begin{aligned}\rho_j^k &= \langle\langle \vec{1} \rangle\rangle_{f_j^k} \\ u_j^k &= \frac{\langle\langle \vec{v} \rangle\rangle_{f_j^k}}{\langle\langle \vec{1} \rangle\rangle_{f_j^k}} \\ \theta_j^k &= \frac{\langle\langle \vec{v}^2 \rangle\rangle_{f_j^k}}{\langle\langle \vec{1} \rangle\rangle_{f_j^k}} - \frac{\langle\langle \vec{v} \rangle\rangle_{f_j^k}^2}{\langle\langle \vec{1} \rangle\rangle_{f_j^k}^2}\end{aligned}\tag{5.19}$$

For $\vec{v} \in \mathbb{R}^{2M+1}$ defined in (5.10) we used the following definitions

$$\vec{v} = [v_{-M}^2, v_{-M+1}^2, \dots, v_M^2]^T\tag{5.20}$$

and

$$\vec{1} = [1, 1, \dots, 1]^T \in \mathbb{R}^{2M+1}\tag{5.21}$$

Equation (5.11) is a finite volume explicit scheme that has a straightforward solution

$$f_{i,j}^{k+1} = f_{i,j}^k - \sigma_1 v_j \hat{\Delta} f_{i,j}^k - \sigma_3 (f_{i,j}^k - f_{i,j}^{e,k})\tag{5.22}$$

where σ_1 is the same as in (4.23) and

$$\sigma_3 = \frac{\Delta t}{\tau}\tag{5.23}$$

Let

$$\vec{f}_j^k = [f_{-M,j}^k, f_{-M+1,j}^k, \dots, f_{M,j}^k]^T \quad (5.24)$$

then formulae (5.11) and (5.22) can be written in the vector form

$$\frac{\vec{f}_j^{k+1} - \vec{f}_j^k}{\Delta x} + \mathbf{V} \frac{\hat{\Delta} \vec{f}_j^k}{\Delta x} = -\frac{1}{\tau} (\vec{f}_j^k - \vec{f}_j^{e,k}) \quad (5.25)$$

or equivalently

$$\vec{f}_j^{k+1} = \vec{f}_j^k - \sigma_1 \mathbf{V} \hat{\Delta} \vec{f}_j^k - \sigma_3 (\vec{f}_j^k - \vec{f}_j^{e,k}) \quad (5.26)$$

where \mathbf{V} is a diagonal matrix

$$\mathbf{V} = \begin{bmatrix} v_{-M} & & & & \\ & v_{-M+1} & & & \\ & & \ddots & & \\ & & & \ddots & \\ & & & & v_M \end{bmatrix} \quad (5.27)$$

and $\vec{f}_j^{e,k}$ is the vector whose components are $f_{i,j}^{e,k}$.

5.3 The Boundary Conditions

The boundary data for (5.1) must agree with the boundary data used to simulate the 1-D Navier-Stokes and Euler equations. Therefore we present boundary conditions for (5.1) in terms of ρ , u , and θ

$$\begin{aligned} \vec{w}(t, 0) &= [\rho_L, u_L, \theta_L]^T \\ \vec{w}(t, 1) &= [\rho_R, u_R, \theta_R]^T \end{aligned} \quad (5.28)$$

where

$$\vec{w} = [\rho, u, \theta]^T \quad (5.29)$$

and $\rho_L, u_L, \theta_L, \rho_R, u_R,$ and θ_R are the values satisfying the Rankine-Hugoniot conditions (3.3) in Section 3.1 (p.45) which we impose on the model. In order to transfer the boundary conditions given in terms of macroscopic variables (5.28) into an adequate description in terms of microscopic variables we assume that the distribution function is close to the Maxwellian Distribution (5.2). Therefore the distributions on the left and right boundaries can be obtained as

$$\begin{aligned} f(t, 0, v) &= f_L(t, v) = f_{(\rho_L, u_L, \theta_L)}^e(v) \\ f(t, 1, v) &= f_R(t, v) = f_{(\rho_R, u_R, \theta_R)}^e(v) \end{aligned} \quad (5.30)$$

where f^e is the Maxwellian Equilibrium given by (5.2). The discretized boundary conditions have the following form

$$\begin{aligned} f_{i,1}^k &= f_{(\rho_L, u_L, \theta_L)}^e(v_i) \\ f_{i,N}^k &= f_{(\rho_R, u_R, \theta_R)}^e(v_i) \end{aligned} \quad (5.31)$$

The numerical scheme (5.25) is a discretization of equation (5.1), which is a non-linear hyperbolic partial differential equation. Therefore in order to understand the behavior on the boundary one must analyze the characteristics of (5.1). Our task is simplified since the advection term of (5.11) is already in the diagonal form (5.27). The diagonal of matrix \mathbf{V} contains $2M+1$ diagonal elements with exactly M positive, exactly M negative and one zero element. Thus there are M positive and M negative characteristics traveling opposite directions with different speeds (see figure 5.3)

Assume that the data for time level t^k has been calculated i.e. $\vec{f}_j^k, \vec{f}_j^{e,k}, \rho_j^k, u_j^k,$ and θ_j^k are known. There are M inflowing characteristics for $v_j > 0$ and M outflowing

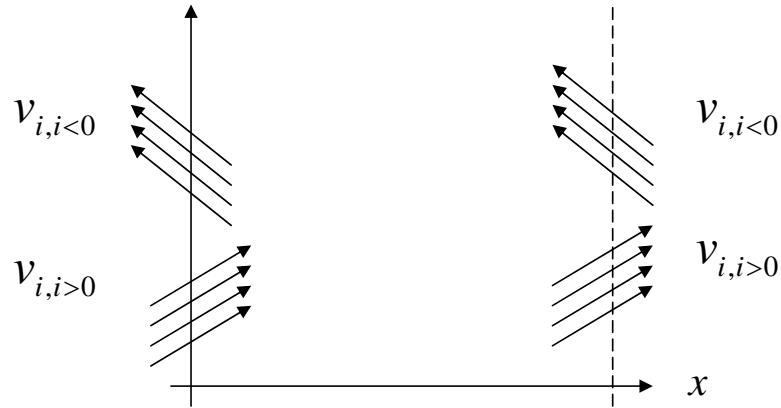


Figure 5.1: Inflowing and outflowing characteristics of the BGK model

ones for $v_j < 0$. Thus half of the components of \vec{v}_1^{k+1} is obtained from (5.30) and the other half must be advected from the interior of the domain using (5.26):

$$f_{i,1}^k = \begin{cases} f_{i,1}^k - \sigma_1 v_j (f_{1,j}^k - f_{2,j}^k) - \sigma_3 (f_{1,j}^k - f_{1,j}^{e,k}), & j > 0 \\ f_{(\rho_L, u_L, \theta_L)}^e(v_i), & j \leq 0 \end{cases} \quad (5.32)$$

A similar formula used for the right boundary:

$$f_{i,N}^k = \begin{cases} f_{(\rho_R, u_R, \theta_R)}^e(v_i), & j > 0 \\ f_{i,N}^k - \sigma_1 v_j (f_{N,j}^k - f_{N-1,j}^k) - \sigma_3 (f_{N,j}^k - f_{N,j}^{e,k}), & j \leq 0 \end{cases} \quad (5.33)$$

The components of each of the boundary distribution vectors are calculated differently depending upon the sign of the corresponding speed v_j . It is not important which part of the formulas (5.32) and (5.33) includes case $j = 0$ since $v_0 = 0$ and it can be treated as upwinding or downwinding with the same result. In the case $j = 0$ the advection term vanishes and the solution merely propagates based on the right hand side of (5.25).

5.4 The Truncation Error

For numerical computations of the integrals in (5.7) the domain of integration must be truncated. This will result in the truncation error defined by

$$\mathcal{E}_T^n[f, V] = \left| \int_{\mathbb{R}} v^n f(v) dv - \int_{-V}^{+V} v^n f(v) dv \right| \quad (5.34)$$

Let \mathcal{E} be the error due to discretization of (5.1) by (5.11). It is essential to ensure that the truncation error is negligible with respect to the structural error of the numerical scheme (5.11):

$$\mathcal{E}_T^n[f, V] \ll \mathcal{E} \quad (5.35)$$

The inequality above will provide the range for admissible values of V . Since a priori information about distribution f is not available, the best way we can address this problem is to approximate $\mathcal{E}_T^n[f, V]$ by $\mathcal{E}_T^n[f^e, V]$ assuming that distribution f is close enough to a Maxwellian equilibrium f^e given by (5.2):

$$\mathcal{E}_T^n[f^e, V] \ll \mathcal{E} \quad (5.36)$$

After substituting (5.2) into (5.34) we obtain

$$\left| \int_{B(V)} v^n \frac{\rho}{\sqrt{2\pi\theta}} \exp \left\{ -\frac{(u-v)^2}{2\theta} \right\} dv \right| < \mathcal{E} \quad (5.37)$$

where

$$B(V) = \mathbb{R} \setminus [-V, V] \quad (5.38)$$

Let

$$\tilde{\mathcal{E}} = \frac{\mathcal{E} \sqrt{2\pi\theta}}{\rho} \quad (5.39)$$

then (5.37) will take form

$$\left| \int_{B(V)} v^n \exp \left\{ -\frac{(u-v)^2}{2\theta} \right\} dv \right| < \tilde{\mathcal{E}} \quad (5.40)$$

To find acceptable values of V satisfying (5.40) we consider the following theorem.

Theorem 2. *Let $\rho > 0$, $u > 0$, $\theta > 0$ be positive constants. Then for $n = 0, 1, 2, \dots$ and for V satisfying*

$$V \geq \max \{1, 2u, u + \sqrt{2\theta}\} \quad (5.41)$$

the following estimate holds:

$$\left| \int_{B(V)} v^n \exp \left\{ -\frac{(v-u)^2}{2\theta} \right\} dv \right| \leq \alpha_n \exp \left\{ -\frac{V-u}{2\sqrt{2\theta}} \right\} \quad (5.42)$$

where

$$\alpha_n = 2^{\frac{5(n+1)}{2}} \theta^{\frac{n+1}{2}} n^n e^{-n} \quad (5.43)$$

and 0^0 should be treated as 1.

Proof of Theorem 2 is provided in Appendix C.1 on page 142.

It follows from Theorem 2 that in order to satisfy (5.40) it suffices to choose V large enough so that (5.41) is satisfied together with

$$\alpha_n e^{-\frac{V-u}{2\sqrt{2\theta}}} < \tilde{\mathcal{E}} \quad (5.44)$$

or equivalently

$$V \geq u + \log \frac{\alpha_n \rho}{\sqrt{2\pi\theta}} + \log \frac{1}{\mathcal{E}} \quad (5.45)$$

Finally by including the condition of Theorem 2 we obtain a bound on V

$$V \geq V_n^*(\mathcal{E}) = \max \left\{ 1, 2u, u + \sqrt{2\theta}, u + \log \frac{\rho}{\sqrt{2\pi\theta}} + \log \alpha_n + \log \frac{1}{\mathcal{E}} \right\} \quad (5.46)$$

5.5 The Reassembling Error

The numerical approach to solve the 1-D BGK model (5.1) discussed in Section 5.1 requires numerical integration to recover the macroscopic observables from distribution function f . The reassembling error is introduced by the numerical integration we use in (5.15,5.18). Similarly to the truncation error, one has to make sure that the numerical integration does not introduce an error exceeding the structural error \mathcal{E} of the numerical scheme (5.25):

$$\mathcal{E}_R \leq \mathcal{E} \quad (5.47)$$

In order to control the reassembling error we test the following protocol. Assume that the discretized macroscopic variables are

$$\begin{aligned} \rho_j &= \rho(x_j) \\ u_j &= u(x_j) \\ \theta_j &= \theta(x_j) \end{aligned} \quad (5.48)$$

and the equilibrium distribution is calculated using (5.14):

$$f_{i,j} = f_{(\rho_j, u_j, \theta_j)}^e(v_i) \quad (5.49)$$

Based on distribution (5.49) one can reassemble the macro-variables ρ , u , and θ using (5.19). Since a numerical integration procedure has been used, one should not expect to obtain exactly the same values as we started with in (5.48). Therefore we will refer to the recovered macro-variables as $\hat{\rho}$, \hat{u} , and $\hat{\theta}$:

$$\begin{aligned} \hat{\rho}_j &= \langle\langle \vec{1} \rangle\rangle_{f_j} \\ \hat{u}_j &= \frac{\langle\langle \vec{v} \rangle\rangle_{f_j}}{\langle\langle \vec{1} \rangle\rangle_{f_j}} \\ \hat{\theta}_j &= \frac{\langle\langle \vec{v}^2 \rangle\rangle_{f_j}}{\langle\langle \vec{1} \rangle\rangle_{f_j}} - \frac{\langle\langle \vec{v} \rangle\rangle_{f_j}^2}{\langle\langle \vec{1} \rangle\rangle_{f_j}^2} \end{aligned} \quad (5.50)$$

Although the values (ρ, u, θ) are not exactly the same as $(\hat{\rho}, \hat{u}, \hat{\theta})$, it is reasonable to require them to be sufficiently close. Otherwise it is unknown how much of an error has been introduced into a solution by the numerical integration technique. Thus we define the following quantities

$$\begin{aligned} \mathcal{E}_R^M[\rho] &= \max_{1 \leq j \leq N} |\rho_j - \hat{\rho}_j| \\ \mathcal{E}_R^M[u] &= \max_{1 \leq j \leq N} |u_j - \hat{u}_j| \\ \mathcal{E}_R^M[\theta] &= \max_{1 \leq j \leq N} |\theta_j - \hat{\theta}_j| \end{aligned} \quad (5.51)$$

where M is the number related to the step size of the phase space mesh of $[-V, V]$. There are $2M + 1$ nodes in the mesh, therefore M and δv are related by

$$\Delta v = \frac{V}{M}$$

By adjusting M we can make sure that

$$\mathcal{E}_R^M[\rho, u, \theta] = \max \{ \mathcal{E}_R^M[\rho], \mathcal{E}_R^M[u], \mathcal{E}_R^M[\theta] \} \leq \mathcal{E} \quad (5.52)$$

Chapter 5. Numerical Solution of the 1-D Bhatnagar–Gross–Krook Model

where \mathcal{E} is the structural error of the numerical scheme (5.25).

Since M must be chosen before the numerical procedure is executed, the macroscopic data is not available except for the initial conditions. Therefore we make a choice of M based upon the initial data only:

$$M \geq M^* = \inf \{ \mathcal{E}_R^M[\rho_0, u_0, \theta_0] \leq \mathcal{E} \} \quad (5.53)$$

Chapter 6

Numerical Simulations and Results

6.1 Numerical Problem Setup

In order to compare how the kinetic theory agrees with the continuum mechanics we compare numerical stationary solutions of one-dimensional continuum model and the simplest one-dimensional approximation of the Boltzmann equation. For the continuum model we chose to solve the 1-D Navier-Stokes system given by (2.1)-(2.3):

$$\begin{aligned}\rho_t + (\rho u)_x &= 0 \\ (\rho u)_t + (\rho u^2)_x &= \sigma_x \\ (\frac{1}{2}\rho u^2 + \rho e)_t + (\rho u(\frac{1}{2}u^2 + e))_x + q_x &= (\sigma u)_x\end{aligned}\tag{6.1}$$

We chose the simplest possible equations of state given by (2.10) and (2.11). After the nondimensionalization process and expressing all variable in terms of three non-conservative variables ρ , u , and θ and three unitless parameters γ , $\mathcal{R}e$, and $\mathcal{P}r$ we arrive to the system of partial differential equations (2.48). For numerical purposes

Chapter 6. Numerical Simulations and Results

we set

$$\mathcal{Pr} = 1 \tag{6.2}$$

As discussed in Section 1.2) the adiabatic ratio γ has to be 3 to agree with a corresponding kinetic model:

$$\gamma = 3.0 \tag{6.3}$$

The final system of equations to be solved numerically is given by

$$\begin{bmatrix} \rho \\ \rho u \\ \frac{1}{2}\rho u^2 + \frac{1}{2}\rho\theta \end{bmatrix}_t + \begin{bmatrix} \rho u \\ \rho u^2 + \rho\theta \\ \frac{1}{2}\rho u^3 + \frac{3}{2}\gamma\rho u\theta \end{bmatrix}_x = \frac{1}{\mathcal{Re}} \begin{bmatrix} 0 \\ u \\ \frac{3}{2}\theta + \frac{1}{2}u^2 \end{bmatrix}_{xx} \tag{6.4}$$

The numerical scheme for solving (6.4) is given by (4.27) and its detailed discussion is included in Section (4.4). Equation (6.4) is solved on $[0,1]$. The number of space steps $N = 1000$ therefore $\Delta x = 10^{-3}$. Time discretization step will vary depending on the value of the Reynolds number

$$\Delta t = \frac{5}{\mathcal{Re}}\Delta x \tag{6.5}$$

We choose a set of boundary conditions that are consistent with the Rankine-Hugoniot equations (3.3) on page 46. Implementation of the boundary conditions for 1-D Navier-Stokes system is discussed in Sections 4.5.2. The values are provided in Tables 6.1 and 6.2. There are 5 sets of trials for each of the boundary conditions referred by NS_0 , NS_1 , NS_2 , NS_3 , and NS_4 .

Chapter 6. Numerical Simulations and Results

Set #	ρ_L	u_L	θ_L	ρ_R	u_R	θ_R
BC ₀	$\frac{3}{2}$	2	$\frac{2}{3}$	2	$\frac{3}{2}$	$\frac{5}{4}$
BC ₁	$\frac{9}{2}$	$\frac{7}{6}$	$\frac{7}{18}$	$\frac{63}{13}$	$\frac{13}{12}$	$\frac{65}{144}$
BC ₂	$\frac{7}{3}$	$\frac{4}{3}$	$\frac{8}{27}$	$\frac{28}{9}$	1	$\frac{5}{9}$
BC ₃	$\frac{8}{3}$	$\frac{3}{2}$	$\frac{1}{4}$	4	1	$\frac{2}{3}$
BC ₄	6	$\frac{5}{3}$	$\frac{5}{27}$	10	1	$\frac{7}{9}$

Table 6.1: Examples of the exact values of shock forming boundary data

Set #	ρ_L	u_L	θ_L	ρ_R	u_R	θ_R
BC ₀	1.500	2.000	0.667	2.000	1.500	1.250
BC ₁	4.500	1.667	0.389	4.846	1.083	0.451
BC ₂	2.333	1.333	0.296	3.111	1.000	0.555
BC ₃	2.667	1.500	0.250	4.000	1.000	0.667
BC ₄	6.000	1.667	0.185	10.000	1.000	0.778

Table 6.2: Examples of the approximate values of shock forming boundary data

System (6.4) depends on Reynolds Number \mathcal{Re} , which corresponds to viscosity $\tilde{\mu}$ provided by (2.32). For each of the sets of boundary conditions we will consider five trials for different values of $\mathcal{Re} = 32, 64, 128, 256, 512$ denoted by RE_{32} , RE_{64} , RE_{128} , RE_{256} , and RE_{512} correspondingly. Thus there will be total of 25 experiments: five values of the Reynolds Number for each of the 5 sets of boundary conditions. Abbreviation NS_nRE_r will refer to a numerical solution of 1-D Navier-Stokes system with n^{th} set of boundary conditions given in Table 6.1 and Reynolds Number $\mathcal{Re} = r$.

Summary of all parameters used in solving the Navier-Stokes system is provided in Table 6.3.

Chapter 6. Numerical Simulations and Results

Trial	$\mathcal{R}e$	N	Δx	Δt
NS _n RE ₃₂	32	1000	10 ⁻³	1.563 ⁻⁴
NS _n RE ₆₄	64	-	-	7.812 ⁻⁵
NS _n RE ₁₂₈	128	-	-	3.906 ⁻⁵
NS _n RE ₂₅₆	256	-	-	1.953 ⁻⁵
NS _n RE ₅₁₂	512	-	-	9.766 ⁻⁶

Table 6.3: Parameters used in the numerical scheme to solve the 1-D Navier-Stokes system

For the kinetic model we choose the 1-D Bhatnagar–Gross–Krook equation (5.1):

$$\frac{\partial f}{\partial t} + v \frac{\partial f}{\partial x} = -\frac{1}{\tau}(f - f^e) \quad (6.6)$$

Equation (6.6) depends on relaxation time τ . We will vary the relaxation time and investigate its affect on the stationary solution of (6.6). Numerical solution of (6.6) is discussed in Section 5.2. Similarly to the Navier-Stokes trials there will be 5 numerical experiments for solving the 1-D Bhatnagar–Gross–Krook model refereed by **BGK_nT_t** where n corresponds the n^{th} set boundary condition from Table 6.1 and $\tau = t \in \{32^{-1}, 64^{-1}, 128^{-1}, 256^{-1}, 512^{-1}\}$. In addition to space and time discretization the BGK model requires the phase space discretization (5.10) with $2M + 1$ nodes:

$$v_j = -V + (j + M)\Delta v, \quad j = -M, -M + 1, \dots, M \quad (6.7)$$

To find suitable values of Δv and M we use the Truncation Error (Section 5.4) and reassembling Error (Section 5.5) estimates.

According to (5.46) we have

$$V \geq V_n^*(\mathcal{E}) = \max \left\{ 1, 2u, u + \sqrt{2\theta}, u + \log \frac{\rho}{\sqrt{2\pi\theta}} + \log \alpha_n + \log \frac{1}{\mathcal{E}} \right\} \quad (6.8)$$

Chapter 6. Numerical Simulations and Results

where \mathcal{E} is an admissible error and α_n is defined by (5.43):

$$\alpha_n = 2^{\frac{5(n+1)}{2}} \theta^{\frac{n+1}{2}} n^n e^{-n} \quad (6.9)$$

For the 1-D BGK model, the highest moment used is of order 2 (5.4). Therefore we will only need to take into account α_n for $n = 0, 1, 2$. According to (5.43) $\alpha_n = \alpha_n(\theta)$ is an increasing function of θ . In order to use estimate (5.46) it is enough to consider $\alpha_n(\theta^*)$ where θ^* is the largest value used for numerical simulations. Tables 6.1 and 6.2 provide the exact and approximate values of macroscopic observables that are used as boundary condition for the numerical simulations. Due to a specific structure of the viscous shock profile (see Fig. 6.3(a) on page 98 for instance) it is reasonable to expect that

$$\begin{aligned} \rho_* &\leq \rho \leq \rho^* \\ u_* &\leq u \leq u^* \\ \theta_* &\leq \theta \leq \theta^* \end{aligned} \quad (6.10)$$

where ρ_* , ρ^* , u_* , u^* , θ_* , and θ^* can be obtained from Tables 6.1 and 6.2:

$$\begin{aligned} \rho_* &= \frac{3}{2}, & \rho^* &= 10 \\ u_* &= 1, & u^* &= 2 \\ \theta_* &= \frac{5}{27}, & \theta^* &= \frac{5}{4} \end{aligned} \quad (6.11)$$

n	α_n	$\log \alpha_n$
0	6.3246×10^0	1.8444
1	1.4715×10^1	2.6889
2	1.3695×10^2	4.9196

Table 6.4: Determining α_n^*

Chapter 6. Numerical Simulations and Results

To find a suitable value of V we apply formula (6.8) in the form

$$V \geq V^*(\mathcal{E}) = \max \left\{ 1, 2u^*, u^* + \sqrt{2\theta^*}, u^* + \log \frac{\rho^*}{\sqrt{2\pi\theta^*}} + \log \alpha^* + \log \frac{1}{\mathcal{E}} \right\} \quad (6.12)$$

where (see Table 6.4)

$$\alpha^* = \max_{n=0,1,2} \alpha_n(\theta^*) = 4.9196 \quad (6.13)$$

Since $\Delta x = 10^{-3}$ and the numerical scheme used to solve the BGK model is of the first order it is enough to take $\mathcal{E} = 10^{-4}$. After substituting (6.13) and (6.11) into (6.12) we arrive to an estimate on V :

$$V \geq V^*(10^{-4}) = 16.54 \quad (6.14)$$

Since there is no available estimate for the reassembling error defined by (5.52) we can establish the number of subintervals on $[-V, V]$ experimentally only. Numerical computations on the initial data indicate that value

$$M = 50 \quad (6.15)$$

will satisfy (5.52) for $\mathcal{E} \ll 10^{-3}$. Parameters used in the numerical scheme to calculate a stationary solution of the 1-D BGK model are summarized in Table (6.5).

Trial	τ	N	Δx	Δt	V	Δv
BGK _n T ₃₂	32^{-1}	1000	10^{-3}	5^{-5}	20	0.4
BGK _n T ₆₄	64^{-1}	-	-	-	-	-
BGK _n T ₁₂₈	128^{-1}	-	-	-	-	-
BGK _n T ₂₅₆	256^{-1}	-	-	-	-	-
BGK _n T ₅₁₂	512^{-1}	-	-	-	-	-

Table 6.5: Parameters used in the numerical scheme to solve the 1-D Bhatnagar–Gross–Krook equation

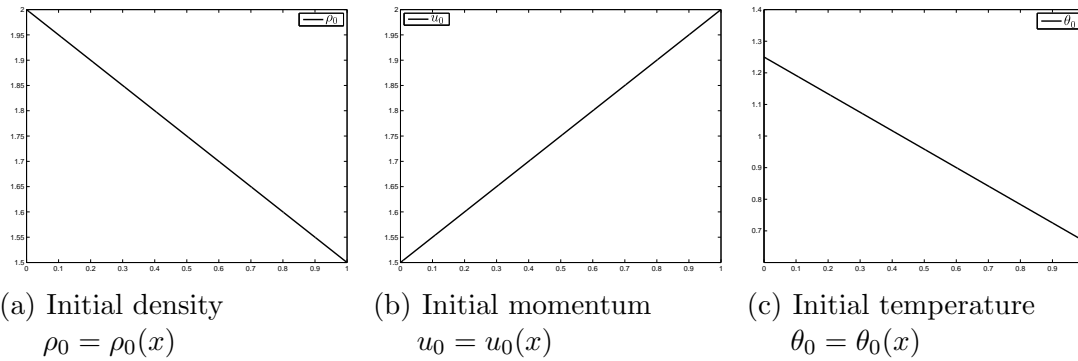


Figure 6.1: Initial conditions for the 1-D Navier-Stokes and the 1-D BGK models

The initial conditions for both Navier-Stokes and BGK equations are constructed as follows. For ρ_L , ρ_R , u_L , u_R , θ_L , and θ_R values we build linear functions spanning these values (see Figure 6.1)

$$\begin{aligned}
 \rho_0(x) &= \rho_R x + \rho_L(1 - x) \\
 u_0(x) &= u_R x + u_L(1 - x) \\
 \theta_0(x) &= \theta_R x + \theta_L(1 - x)
 \end{aligned} \tag{6.16}$$

Whereas the initial conditions (6.16) are ready to be implemented in the numerical scheme for the Navier-Stokes system, the BGK model requires converting (6.16) into microscopic variable domain using the Maxwellian equilibrium (5.2):

$$f_0^j(x) = \frac{\rho_0(x)}{\sqrt{2\pi\theta_0(x)}} \exp \left\{ -\frac{(u_0(x) - v_j)^2}{2\theta_0(x)} \right\} \tag{6.17}$$

where ρ_0 , u_0 , and θ_0 are defined by (6.16). The resulting initial conditions for the BGK equations are given in Figure 6.2.

6.2 Simulation Results

Stationary solutions of the 1-D Navier-Stokes system with different boundary conditions are presented on Figures 6.3, 6.4, 6.5, 6.6, and 6.7. Each of the figures contains

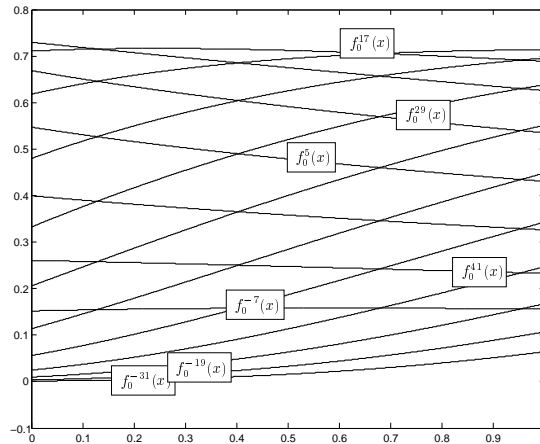


Figure 6.2: Initial distributions $f_0^j = f_0^j(x)$ based on ρ_0 , u_0 , and θ_0

three graphs corresponding to stationary density ρ , stationary velocity u , and stationary temperature θ given for different values of the Reynolds Number $\mathcal{R}e$. We start with the initial value of Reynolds number $\mathcal{R}e_0 = 32$ and vary it to confirm the stationary solution response. The Reynolds Number for each set of boundary conditions is changed according to

$$\mathcal{R}e_r = 2^{r-1}\mathcal{R}e_0, \quad r = 1, \dots, 5 \quad (6.18)$$

Numerical simulations of the 1-D BGK model produce stationary distributions f , which correspond to microscopic observable of the system. In order to obtain the macroscopic variables we use the reconstruction procedure given by (5.19) (see discussion in Section 5.2). The reconstructed stationary density, velocity and solutions are provided on Figures 6.8, 6.9, 6.10, 6.11, and 6.12. Similarly to the Navier-Stokes simulations, the BGK figures contain graphs of the density, velocity, and temperature for different values of parameter τ (relaxation time, see formula (5.1) for example).

The Relaxation time is varied according to

$$\tau_t = 2^{t-1}\tau_0, \quad t = 1, \dots, 5 \tag{6.19}$$

where $\tau_0 = \frac{1}{512}$. For the demonstration purposes we provide stationary distributions for the case of boundary conditions BC_0 only (for references see Tables 6.1 and 6.2). These results are listed on Figures 6.13 and they correspond to the reconstructed macroscopic stationary variables given on Figure 6.8.

Table 6.6 references to the graphical results of the Navier-Stokes and BGK simulations.

BoundaryConditions	NS	BGK
BC_0	Fig. 6.3 p.98	Fig. 6.8 p.103
BC_1	Fig. 6.4 p.99	Fig. 6.9 p.104
BC_2	Fig. 6.5 p.100	Fig. 6.10 p.105
BC_3	Fig. 6.6 p.101	Fig. 6.11 p.106
BC_4	Fig. 6.7 p.102	Fig. 6.12 p.107

Table 6.6: References to the figures and corresponding pages for results of numerical simulations of the Navier-Stokes and Bhatnagar–Gross–Krook models. The first column contains sets of boundary conditions that can be found in Tables 6.1 and 6.2

6.3 Analysis of Simulation Results

As one can see that the Kinetic model ¹ has successfully demonstrated shock forming capabilities. It would be beneficial to understand how exactly the stationary solution of the Navier-Stokes systems relates to the corresponding solution of the BGK model. However at this time we will provide only indirect comparison in the sense of identifying common trends in behavior of shock profiles with respect to changing parameters.

¹on the example of the 1-D BGK equation

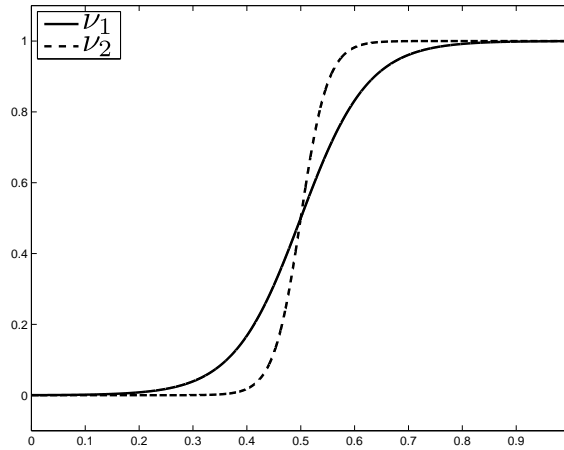


Figure 6.14: Two shock profiles correspond to two values of viscosity ν_1 and ν_2 , $\nu_1 < \nu_2$

It is known [19] that for the Burgers' equation² the steepness of the shock profile is directly related to the viscosity of the system. A less steep shock profile corresponds to a less viscous case (Fig.6.14). Moreover if we introduce a measure of steepness of a shock profile, such as the shock width, this dependence must be linear for the Navier-Stokes shock profiles [19]. Let us visually compare solutions of the Navier-Stokes model and Bhatnagar–Gross–Krook model in the case of boundary condition set BC₃. Stationary solutions for the both models are presented on Figure (6.15). One can see that both results exhibit similar behaviors³.

In the discussion below we take the following steps:

1. We introduce the Shock Width Measure and apply it to the solutions obtained from the Navier-Stokes and BGK simulations.
2. We confirm that Navier-Stokes stationary solutions the shock width is a linear function of Reynolds Number \mathcal{Re} , which, according to (2.32), controls the

² $\frac{\partial u}{\partial t} - \frac{\partial}{\partial x}(u^2) = \nu \frac{\partial^2 u}{\partial x^2}$
³at least visually

viscosity of the system

3. We examine how the relaxation time depends upon the shock width for the stationary solutions of the BGK model

6.3.1 Shock Width

To measure the steepness of a viscous shock profile we introduce the shock width measure ω . Consider a viscous shock profile f given on Figure 6.16. Let f^- and f^+ represent the terminal states of the shock

$$\begin{aligned} f^- &= f(0) \\ f^+ &= f(1) \end{aligned} \tag{6.20}$$

and let Δf be the total terminal span of the shock

$$\Delta f = |f^+ - f^-| \tag{6.21}$$

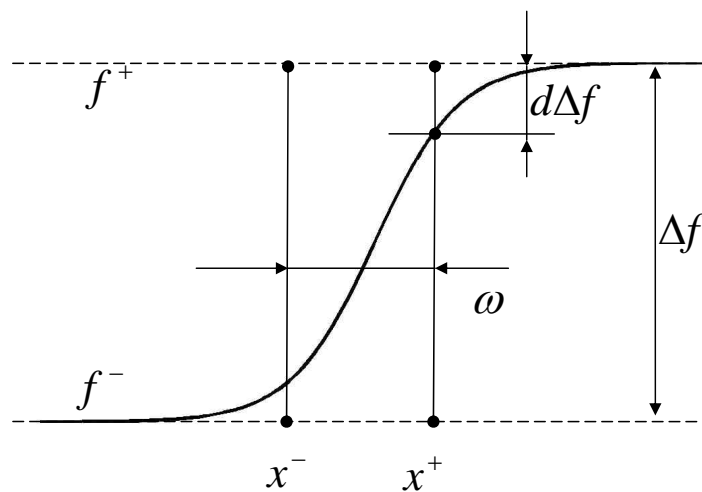


Figure 6.16: Shock width definition

Chapter 6. Numerical Simulations and Results

For simplicity we assume that $f^- < f^+$. In the case when $f^- > f^+$ the computations are very similar. To measure the width of the shock we must measure the largest coordinate x^+ where the shock profile deviates from its right terminal value and smallest coordinate x^- at which the shock profile deviates from its left terminal states. Let d be the shock tolerance or the deviation level with respect to the total terminal span of the shock Δf (see Figure 6.16) then we have

$$\begin{aligned} x^+ &= \sup_{0 \leq x \leq 1} \{|f(x) - f^+| \geq d\Delta f\} \\ x^- &= \inf_{0 \leq x \leq 1} \{|f(x) - f^-| \geq d\Delta f\} \end{aligned} \tag{6.22}$$

Since the shock profile is not defined as a continuous function but rather as a set of nodes, definitions (6.22) translate into discrete form as

$$\begin{aligned} x^+ &= \sup_{1 \leq i \leq N} \{|f_i - f^+| \geq d\Delta f\} \\ x^- &= \inf_{1 \leq i \leq N} \{|f_i - f^-| \geq d\Delta f\} \end{aligned} \tag{6.23}$$

We define the shock width as

$$\omega = x^+ - x^- \tag{6.24}$$

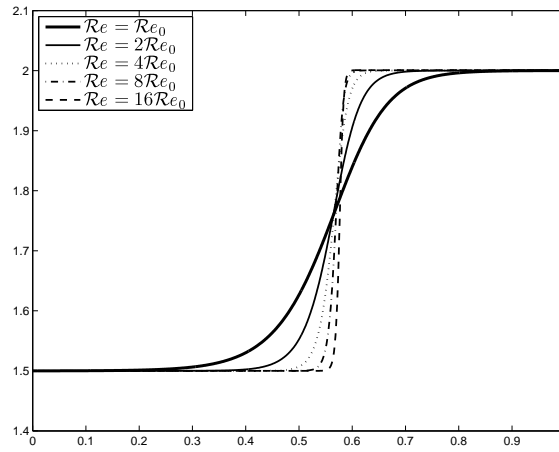
Shock width measurements with shock tolerance $d = 10^{-2}$ for solutions of the 1-D Navier-Stokes and BGK equations are provided in Table 6.7.

Chapter 6. Numerical Simulations and Results

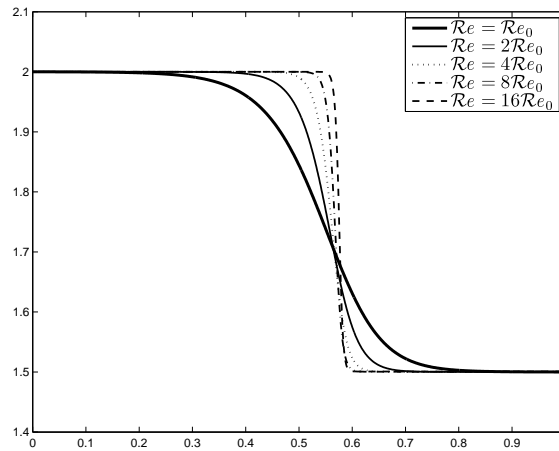
Shock width values for the 1-D Navier-Stokes system						
		BC ₀	BC ₁	BC ₂	BC ₃	BC ₄
$Re = Re_0$	ρ	3.65×10^{-1}	4.18×10^{-1}	3.52×10^{-1}	2.17×10^{-1}	7.41×10^{-2}
	u	3.66×10^{-1}	4.18×10^{-1}	3.53×10^{-1}	2.18×10^{-1}	7.51×10^{-2}
	θ	4.46×10^{-1}	5.79×10^{-1}	4.47×10^{-1}	2.83×10^{-1}	1.02×10^{-1}
$Re = 2Re_0$	ρ	1.84×10^{-1}	2.26×10^{-1}	1.78×10^{-1}	1.10×10^{-1}	3.90×10^{-2}
	u	1.85×10^{-1}	2.26×10^{-1}	1.78×10^{-1}	1.11×10^{-1}	4.05×10^{-2}
	θ	2.34×10^{-1}	3.20×10^{-1}	2.26×10^{-1}	1.44×10^{-1}	5.44×10^{-2}
$Re = 4Re_0$	ρ	9.41×10^{-2}	1.14×10^{-1}	9.11×10^{-2}	5.66×10^{-2}	2.00×10^{-2}
	u	9.41×10^{-2}	1.14×10^{-1}	9.11×10^{-2}	5.71×10^{-2}	2.10×10^{-2}
	θ	1.19×10^{-1}	1.62×10^{-1}	1.15×10^{-1}	7.41×10^{-2}	2.80×10^{-2}
$Re = 8Re_0$	ρ	4.90×10^{-2}	5.81×10^{-2}	4.70×10^{-2}	3.00×10^{-2}	1.10×10^{-2}
	u	4.90×10^{-2}	5.81×10^{-2}	4.72×10^{-2}	3.10×10^{-2}	1.20×10^{-2}
	θ	6.21×10^{-2}	8.31×10^{-2}	6.01×10^{-2}	4.00×10^{-2}	1.60×10^{-2}
$Re = 16Re_0$	ρ	2.60×10^{-2}	3.00×10^{-2}	2.50×10^{-2}	1.70×10^{-2}	7.01×10^{-3}
	u	2.70×10^{-2}	3.00×10^{-2}	2.60×10^{-2}	1.80×10^{-2}	7.01×10^{-3}
	θ	3.30×10^{-2}	4.30×10^{-2}	3.20×10^{-2}	2.24×10^{-2}	1.00×10^{-2}
Shock width values for the 1-D BGK equation						
		BC ₀	BC ₁	BC ₂	BC ₃	BC ₄
$\tau = \tau_0$	ρ	4.71×10^{-1}	5.11×10^{-1}	3.24×10^{-1}	3.09×10^{-1}	3.16×10^{-1}
	u	4.66×10^{-1}	5.09×10^{-1}	3.23×10^{-1}	3.08×10^{-1}	3.14×10^{-1}
	θ	5.09×10^{-1}	6.79×10^{-1}	3.57×10^{-1}	3.32×10^{-1}	3.45×10^{-1}
$\tau = 2\tau_0$	ρ	2.45×10^{-1}	3.01×10^{-1}	1.66×10^{-1}	1.58×10^{-1}	1.61×10^{-1}
	u	2.46×10^{-1}	3.01×10^{-1}	1.66×10^{-1}	1.59×10^{-1}	1.61×10^{-1}
	θ	2.73×10^{-1}	4.19×10^{-1}	1.85×10^{-1}	1.71×10^{-1}	1.78×10^{-1}
$\tau = 4\tau_0$	ρ	1.26×10^{-1}	1.58×10^{-1}	8.51×10^{-2}	8.11×10^{-2}	8.31×10^{-2}
	u	1.27×10^{-1}	1.58×10^{-1}	8.61×10^{-2}	8.21×10^{-2}	8.31×10^{-2}
	θ	1.41×10^{-1}	2.21×10^{-1}	9.61×10^{-2}	8.81×10^{-2}	9.11×10^{-2}
$\tau = 8\tau_0$	ρ	6.51×10^{-2}	8.41×10^{-2}	4.50×10^{-2}	4.30×10^{-2}	4.40×10^{-2}
	u	6.61×10^{-2}	8.51×10^{-2}	4.60×10^{-2}	4.30×10^{-2}	4.30×10^{-2}
	θ	7.41×10^{-2}	1.18×10^{-1}	5.11×10^{-2}	4.70×10^{-2}	4.90×10^{-2}
$\tau = 16\tau_0$	ρ	3.50×10^{-2}	4.70×10^{-2}	2.60×10^{-2}	2.40×10^{-2}	2.40×10^{-2}
	u	3.60×10^{-2}	4.80×10^{-2}	2.60×10^{-2}	2.40×10^{-2}	2.40×10^{-2}
	θ	4.10×10^{-2}	6.71×10^{-2}	2.90×10^{-2}	2.60×10^{-2}	2.70×10^{-2}

Table 6.7: Shock width measurements of viscous shock profiles computed for the 1-D Navier-Stokes and BGK models for different sets of boundary conditions and different values of parameters Re and τ . Shock tolerance has been chosen to be $d = 10^{-2}$ (see Figure 6.16 for details)

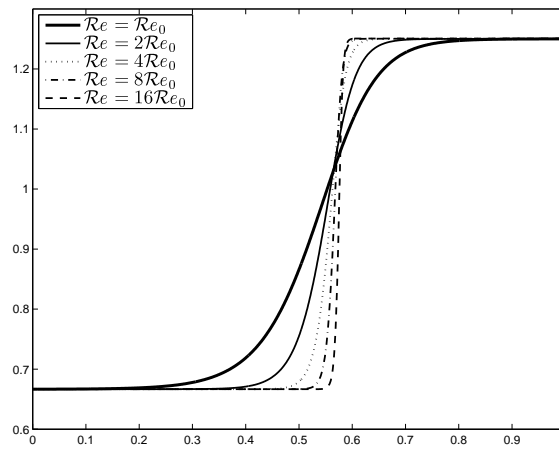
Chapter 6. Numerical Simulations and Results



(a) Density ρ NS_0RE_r



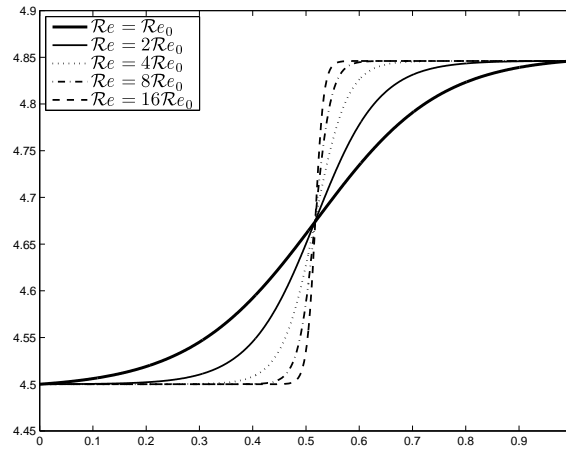
(b) Velocity u NS_0RE_r



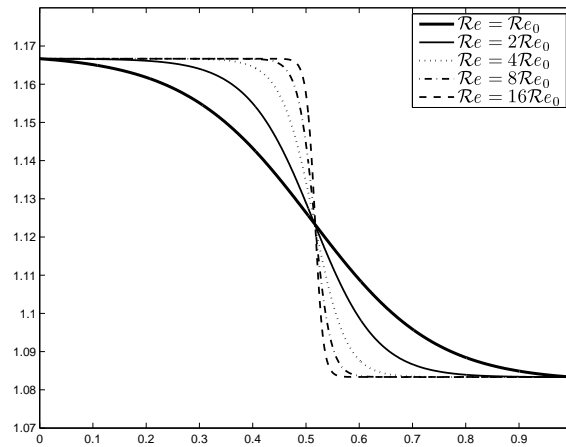
(c) Temperature θ NS_0RE_r

Figure 6.3: Numerical stationary solution NS_0RE_r case

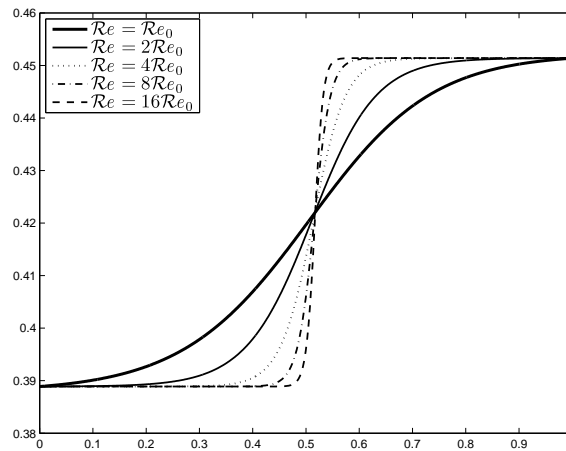
Chapter 6. Numerical Simulations and Results



(a) Density ρ NS_1RE_r



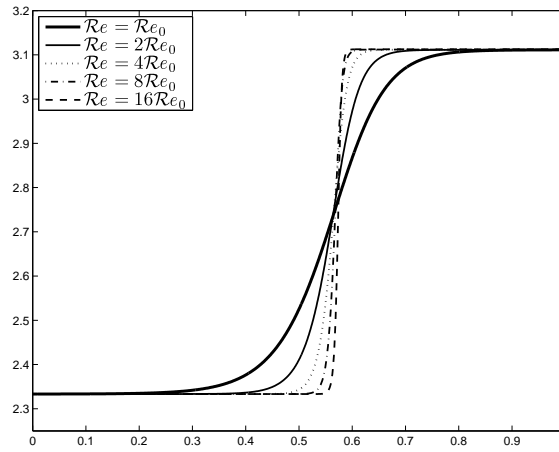
(b) Velocity u NS_1RE_r



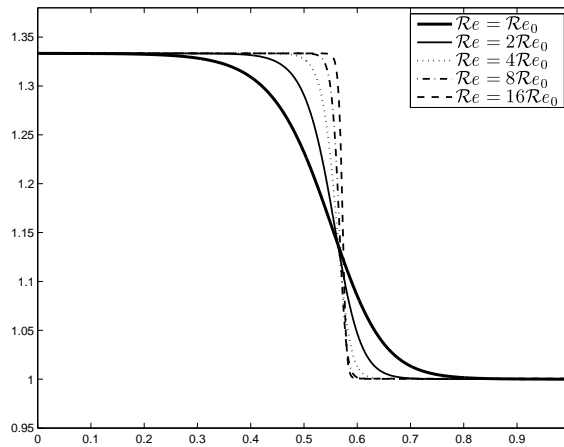
(c) Temperature θ NS_1RE_r

Figure 6.4: Numerical stationary solution NS_1RE_r case

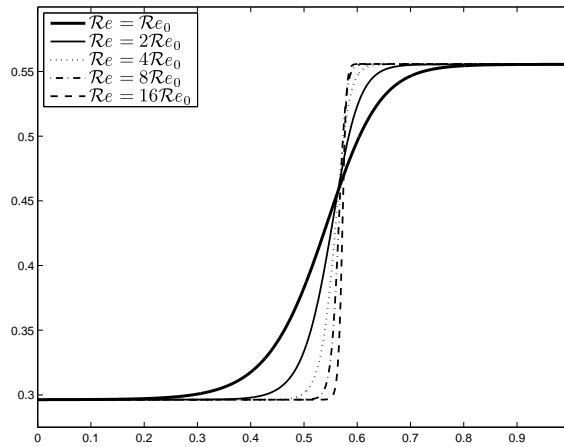
Chapter 6. Numerical Simulations and Results



(a) Density ρ NS_2RE_r



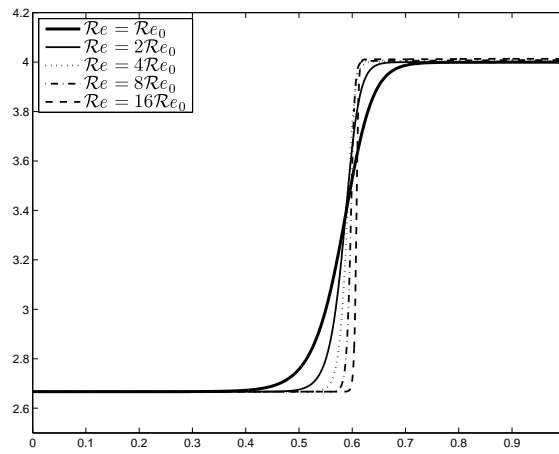
(b) Velocity u NS_2RE_r



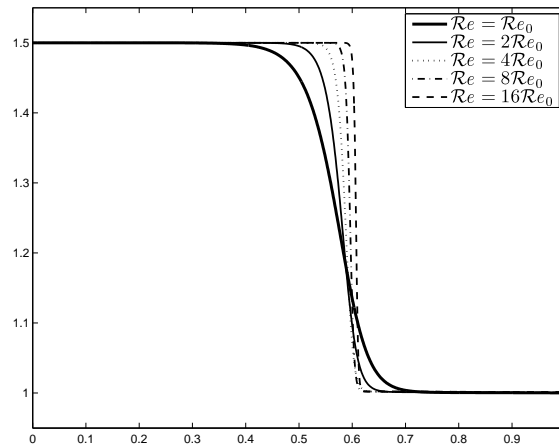
(c) Temperature θ NS_2RE_r

Figure 6.5: Numerical stationary solution NS_2RE_r case

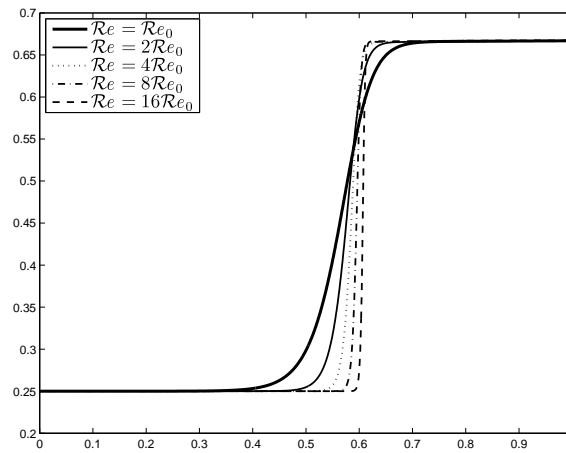
Chapter 6. Numerical Simulations and Results



(a) Density ρ NS_3RE_r



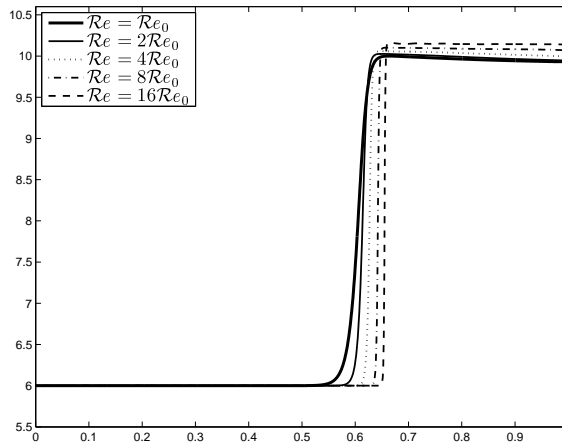
(b) Velocity u NS_3RE_r



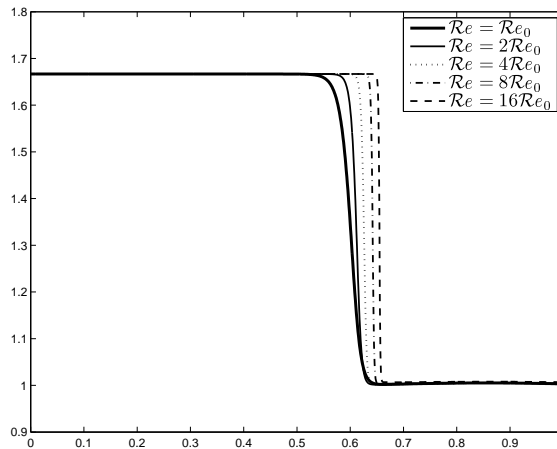
(c) Temperature θ NS_3RE_r

Figure 6.6: Numerical stationary solution NS_3RE_r case

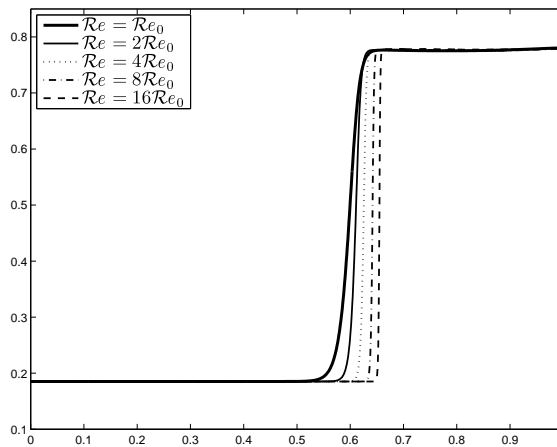
Chapter 6. Numerical Simulations and Results



(a) Density ρ NS_4RE_r



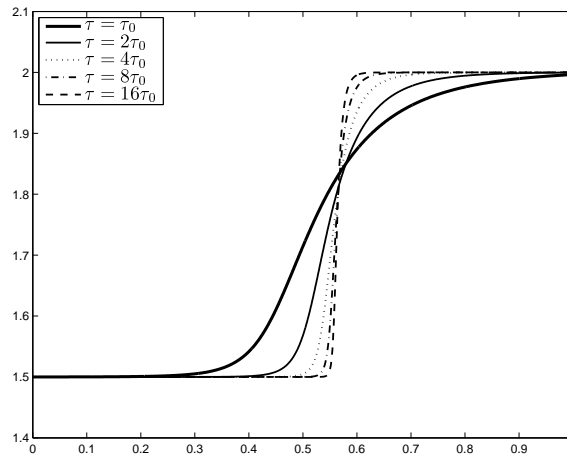
(b) Velocity u NS_4RE_r



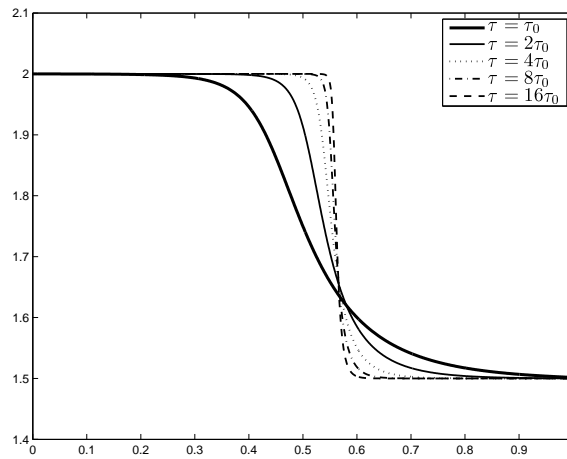
(c) Temperature θ NS_4RE_r

Figure 6.7: Numerical stationary solution NS_4RE_r case

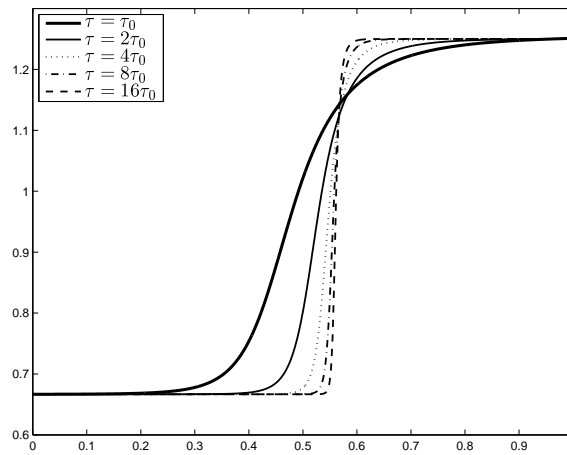
Chapter 6. Numerical Simulations and Results



(a) Density ρ $BGK_0 T_t$



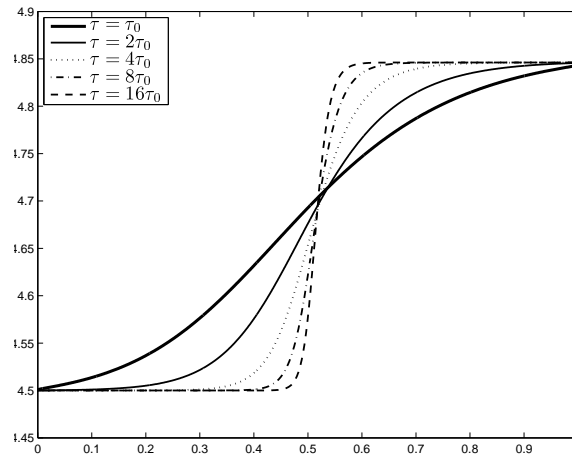
(b) Velocity u $BGK_0 T_t$



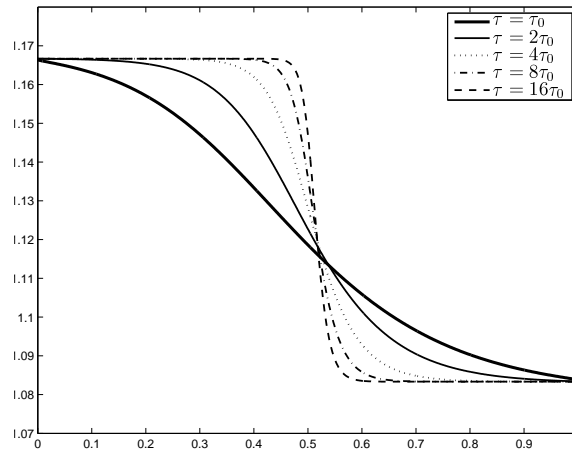
(c) Temperature θ $BGK_0 T_t$

Figure 6.8: Numerical stationary solution $BGK_0 T_t$ case

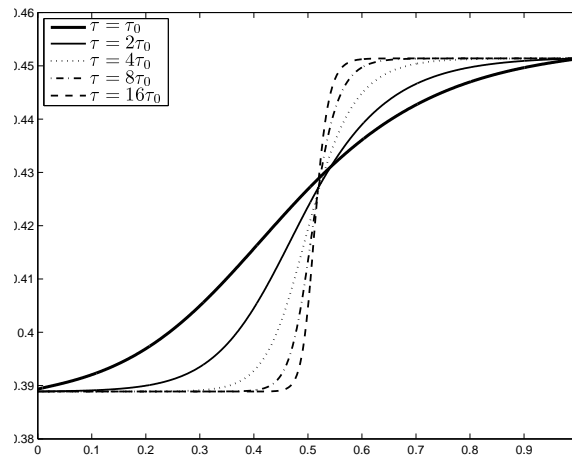
Chapter 6. Numerical Simulations and Results



(a) Density ρ $BGK_1 T_t$



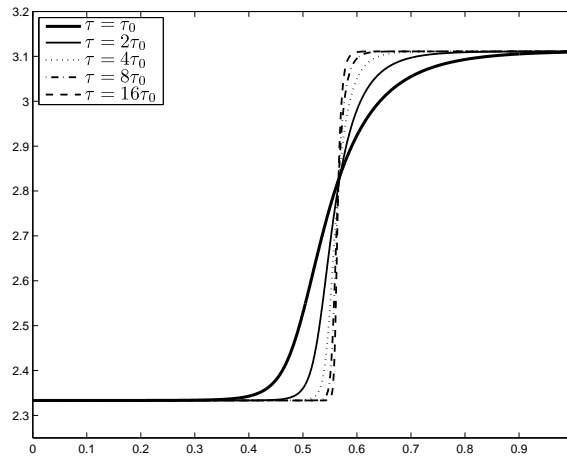
(b) Velocity u $BGK_1 T_t$



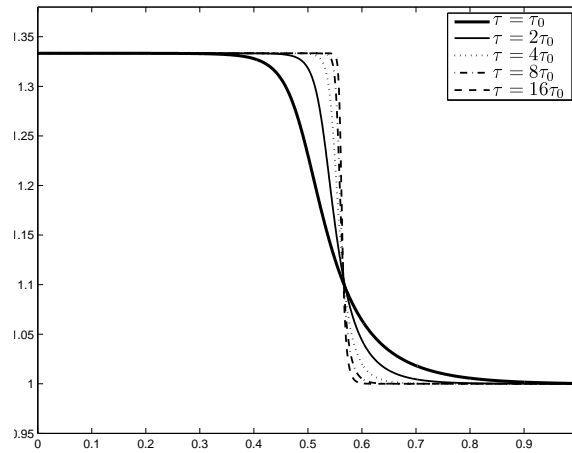
(c) Temperature θ $BGK_1 T_t$

Figure 6.9: Numerical stationary solution $BGK_1 T_t$ case

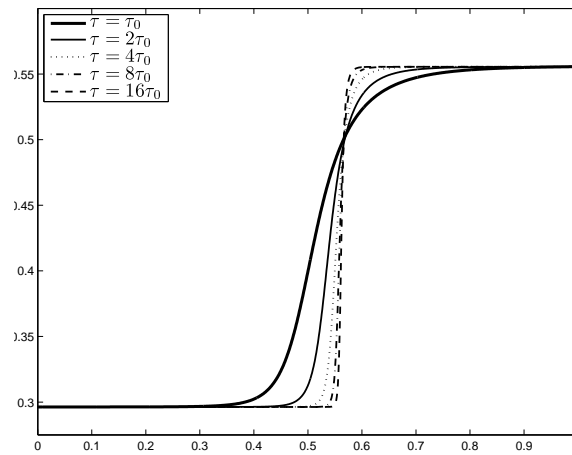
Chapter 6. Numerical Simulations and Results



(a) Density ρ $BGK_2 T_t$



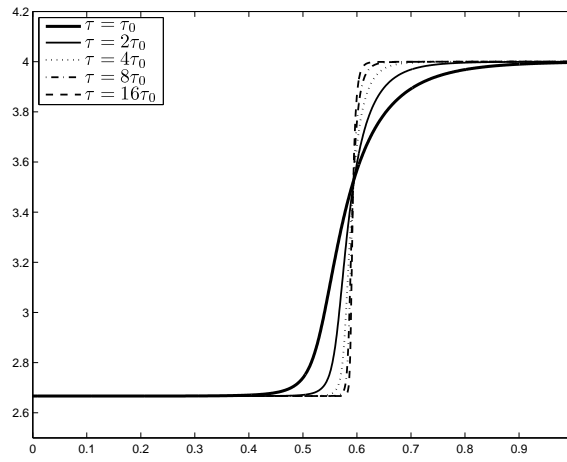
(b) Velocity u $BGK_2 T_t$



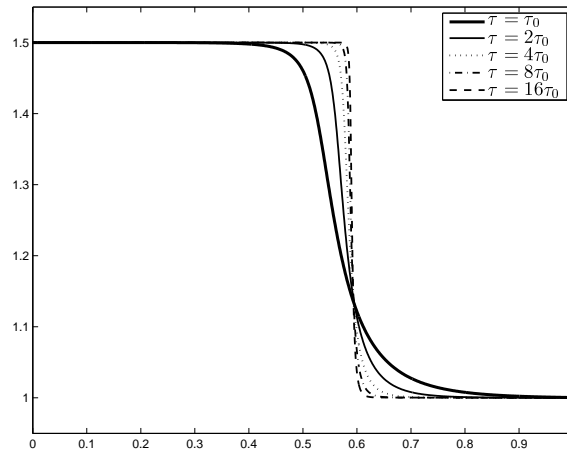
(c) Temperature θ $BGK_2 T_t$

Figure 6.10: Numerical stationary solution $BGK_2 T_t$ case

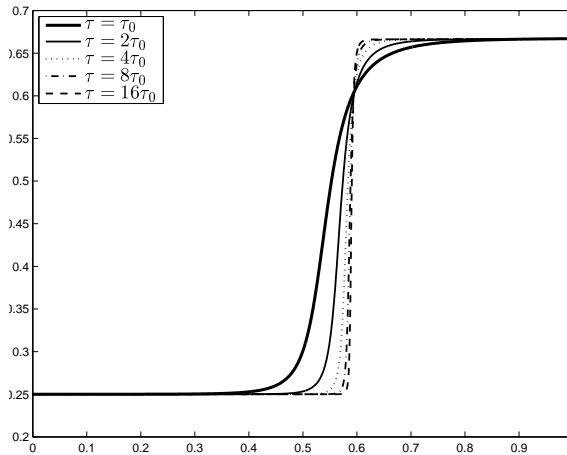
Chapter 6. Numerical Simulations and Results



(a) Density ρ BGK_3T_t



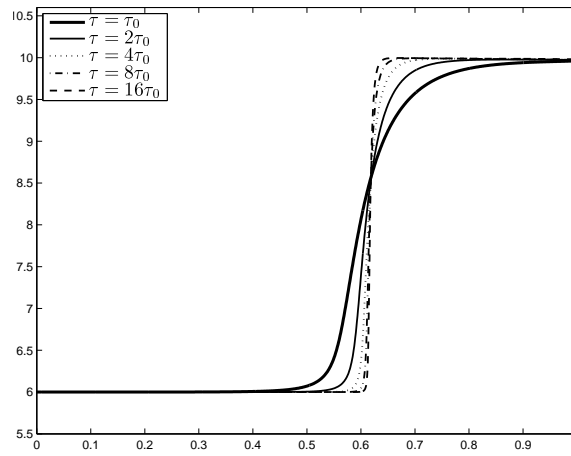
(b) Velocity u BGK_3T_t



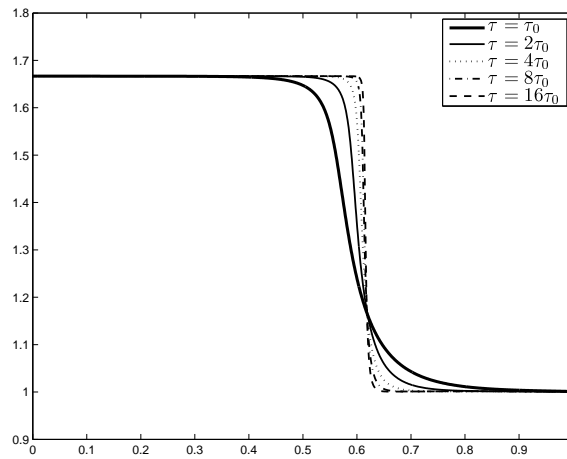
(c) Temperature θ BGK_3T_t

Figure 6.11: Numerical stationary solution BGK_3T_t case

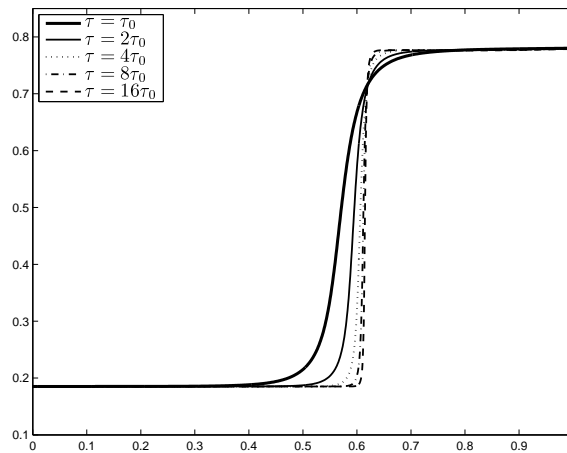
Chapter 6. Numerical Simulations and Results



(a) Density ρ $BGK_4 T_t$



(b) Velocity u $BGK_4 T_t$



(c) Temperature θ $BGK_4 T_t$

Figure 6.12: Numerical stationary solution $BGK_4 T_t$ case

Chapter 6. Numerical Simulations and Results

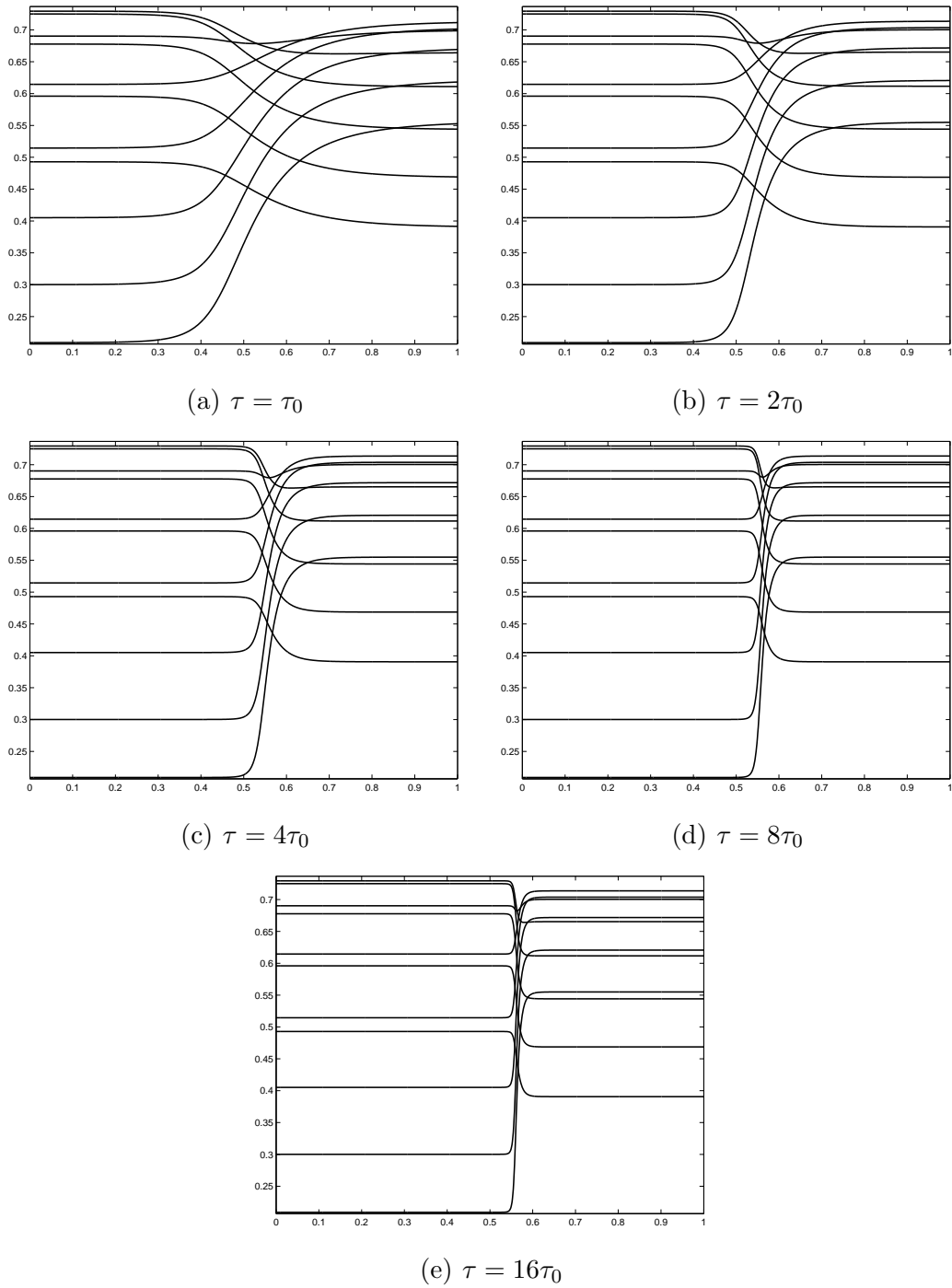


Figure 6.13: Stationary distributions $f_j(x)$ for BGK_0T_t case

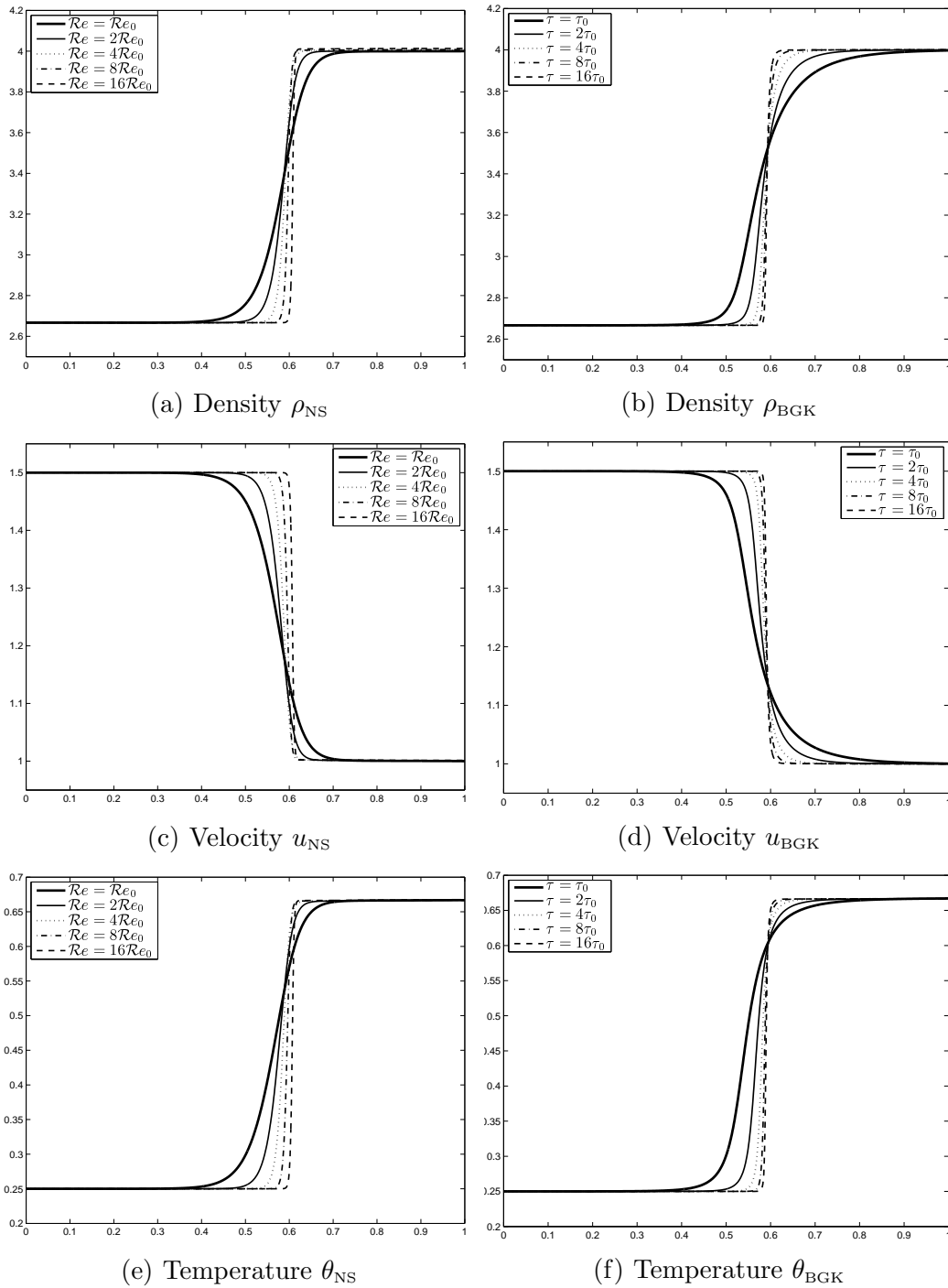


Figure 6.15: Side by side comparison of the macroscopic observables obtained by Navier-Stokes and Bhatnagar–Gross–Krook simulations in the case of BC_3 set of boundary conditions

6.3.2 Regression Analysis of the Shock Width

In this section we will perform a linear regression analysis to understand how the shock width depends on a parameter of a model considered. For the Navier-Stokes system, based on the analysis of the Burgers' equation[19], one should expect that the shock width is a linear function of the viscosity, which is inversely proportional to the Reynolds Number. Numerical simulations performed on the Navier-Stokes model will test this. A side-by-side comparison of numerical solutions of Navier-Stokes and Bhatnagar–Gross–Krook models provided on Figure 6.15 suggests that both models feature the same trend as far as dependence on corresponding model parameters⁴ are concerned. Thus we will test the linear hypothesis for the BGK model as well.

Let p_1, p_2, \dots, p_r be values of a parameter ($\mathcal{R}e$ or τ), and $\omega_1, \omega_2, \dots, \omega_r$ be the corresponding values of the shock width. We accept the following hypothesis

$$\omega(p) = Cp^{-m} \tag{6.25}$$

Its linearized version reads

$$\log \omega(p) = \log C - m \log p \tag{6.26}$$

Equations (6.25) and (6.27) must be satisfied by the empirical data:

$$\begin{cases} \log \omega_1 = \log C - m \log p_1 \\ \dots \\ \log \omega_r = \log C - m \log p_r \end{cases} \tag{6.27}$$

Solving (6.27) will provide the best fitted values of C and m . System (6.27) is overdetermined and therefore we use the Least Square Method to solve it:

$$\begin{bmatrix} \log C \\ m \end{bmatrix} = (A^T A)^{-1} A^T \begin{bmatrix} \log \omega_1 \\ \dots \\ \log \omega_r \end{bmatrix} \tag{6.28}$$

⁴Reynolds number $\mathcal{R}e$ for NS and relaxation time τ for BGK

where

$$A = \begin{bmatrix} 1 & -\log p_1 \\ \cdots & \\ 1 & -\log p_r \end{bmatrix} \quad (6.29)$$

BC set	θ -shock width
BC ₀	$\omega_\theta \sim 0.00169\tau^{-1}$
BC ₁	$\omega_\theta \sim 0.00352\tau^{-1}$
BC ₂	$\omega_\theta \sim 0.00119\tau^{-1}$
BC ₃	$\omega_\theta \sim 0.00103\tau^{-1}$
BC ₄	$\omega_\theta \sim 0.00107\tau^{-1}$

Table 6.8: Proportionality coefficients of θ -associated shock width for different sets of boundary conditions (BGK model)

6.3.3 Conclusions

We apply the regression analysis described by (6.25)-(6.29) to the shock width measurements for the stationary solutions of the Navier-Stokes and BGK equations for each of the sets of boundary conditions BC₀, BC₁, . . . , BC₄. The shock width measurements are provided in Table 6.7. The results of the fitting process are presented in Table 6.9 as well as in Figures 6.17– 6.22.

One can see from Figures 6.17–6.19 that for the 1-D Navier-Stokes system the shock width is proportional to the inverse of the Reynolds number which is essentially the viscosity. This behavior is similar to the one observed in the properties of the shock width for shock solutions of the Burgers' equation which maybe viewed as a prototype of the 1-D Navier-Stokes system [19].

From the simulation results discussed in this chapter we can draw the following conclusions.

Chapter 6. Numerical Simulations and Results

1. We have chosen five sets of shock forming boundary conditions (Tables 6.1 and 6.2) that satisfy Rankine-Hugoniot equations (Chapter 3). The 1-D Navier-Stokes system of equations was nondimensionalized (Chapter 2) and solved (Chapter 4). We observed viscous shock profiles associated with the stationary solutions of the 1-D NS system (Section 6.2, Figures 6.3-6.7). The same sets of boundary conditions were used to solve the 1-D Bhatnagar–Gross–Krook model (Chapter 5). Similarly to the Navier-Stokes case, the simulation results exhibit viscous shock features in stationary solutions of the 1-D BGK model (Figures 6.8-6.12). This enables us to conclude that kinetic models are capable of producing shock features as the continuum models. Moreover a direct visual comparison of viscous shock profiles (Figure 6.15) suggests that the relaxation time parameter (τ) has the same influence on the stationary solution of the BGK model as Reynolds number does on the stationary solution of the NS system.

2. A numerical measure such as the shock width was introduced (Section 6.3.1) and applied (Section 6.3.2) to both the 1-D Navier-Stokes (Figures 6.17–6.19) and 1-D BGK (Figures 6.20–6.22) simulations. In both cases essentially a linear trend was observed. Therefore it has been established that the relaxation time parameter (τ) in the BGK model plays the same role as the Reynolds number ($\mathcal{R}e$) in the Navier-Stokes system. Namely, since the Reynolds number is the inverse viscosity, the relaxation time must have the same meaning in the kinetic model.

3. Conducted analysis indicates that the shock width and hence viscosity are inversely proportional to the Reynolds number in the case of the Navier-Stokes system and the relaxation time τ in the case of the Bhatnagar–Gross–Krook model:

$$\omega \sim A\mathcal{R}e^{-1}, \tag{6.30}$$

$$\omega \sim B\tau^{-1}. \tag{6.31}$$

Chapter 6. Numerical Simulations and Results

One should expect that there are universal constants A and B such that the identities (6.30) and (6.31) would hold regardless of the boundary conditions. However the numerical simulations demonstrated that constants A and B depend on the boundary conditions (Table 6.9). Indeed, one can see from Table 6.8 that the proportionality constant varies significantly depending on the boundary conditions. The nature of this phenomenon must be further investigated in future work.

Navier-Stokes shock widths					
	BC ₀	BC ₁	BC ₂	BC ₃	BC ₄
ρ	$\omega_\rho = 9.772\mathcal{R}e^{-0.95}$	$\omega_\rho = 11.75\mathcal{R}e^{-0.96}$	$\omega_\rho = 9.517\mathcal{R}e^{-0.96}$	$\omega_\rho = 5.144\mathcal{R}e^{-0.92}$	$\omega_\rho = 1.408\mathcal{R}e^{-0.86}$
u	$\omega_u = 9.426\mathcal{R}e^{-0.94}$	$\omega_u = 11.75\mathcal{R}e^{-0.96}$	$\omega_u = 9.091\mathcal{R}e^{-0.94}$	$\omega_u = 4.808\mathcal{R}e^{-0.9}$	$\omega_u = 1.439\mathcal{R}e^{-0.86}$
θ	$\omega_\theta = 12.43\mathcal{R}e^{-0.95}$	$\omega_\theta = 15.81\mathcal{R}e^{-0.95}$	$\omega_\theta = 11.91\mathcal{R}e^{-0.95}$	$\omega_\theta = 6.585\mathcal{R}e^{-0.92}$	$\omega_\theta = 1.833\mathcal{R}e^{-0.85}$
BGK shock widths					
	BC ₀	BC ₁	BC ₂	BC ₃	BC ₄
ρ	$\omega_\rho = 0.00132\tau^{-0.94}$	$\omega_\rho = 0.002286\tau^{-0.87}$	$\omega_\rho = 0.001036\tau^{-0.92}$	$\omega_\rho = 0.0009404\tau^{-0.93}$	$\omega_\rho = 0.0009304\tau^{-0.93}$
u	$\omega_u = 0.001417\tau^{-0.93}$	$\omega_u = 0.002401\tau^{-0.86}$	$\omega_u = 0.001063\tau^{-0.91}$	$\omega_u = 0.0009434\tau^{-0.93}$	$\omega_u = 0.0009183\tau^{-0.93}$
θ	$\omega_\theta = 0.00169\tau^{-0.91}$	$\omega_\theta = 0.003525\tau^{-0.85}$	$\omega_\theta = 0.001193\tau^{-0.91}$	$\omega_\theta = 0.001038\tau^{-0.92}$	$\omega_\theta = 0.001079\tau^{-0.92}$

Table 6.9: Navier-Stokes and BGK shock width regression results for different boundary condition sets.

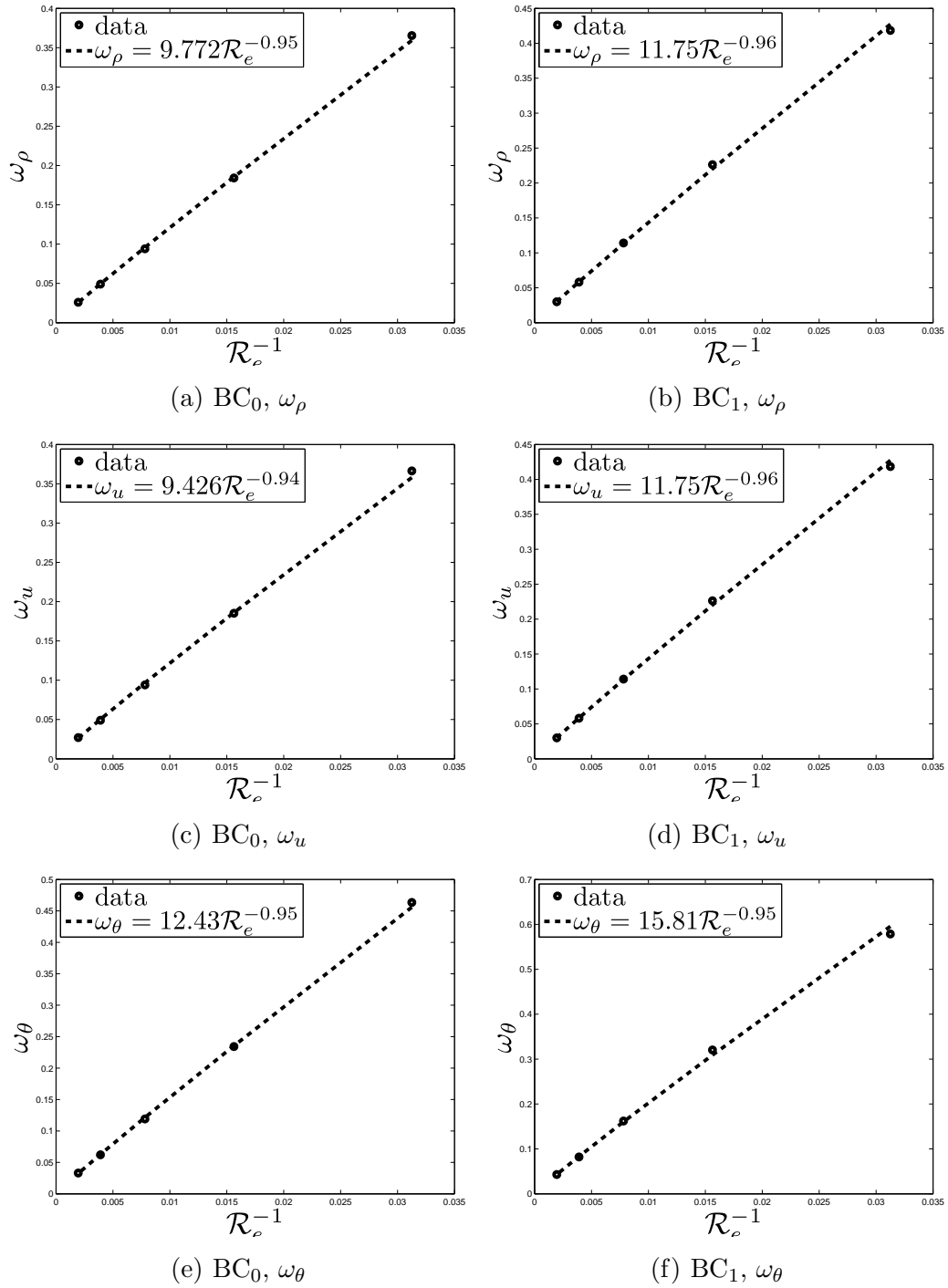


Figure 6.17: Navier-Stokes shock width regression for BC₀ and BC₁ sets of boundary conditions. Horizontal axis is reciprocal of Reynolds number \mathcal{R}_e^{-1}

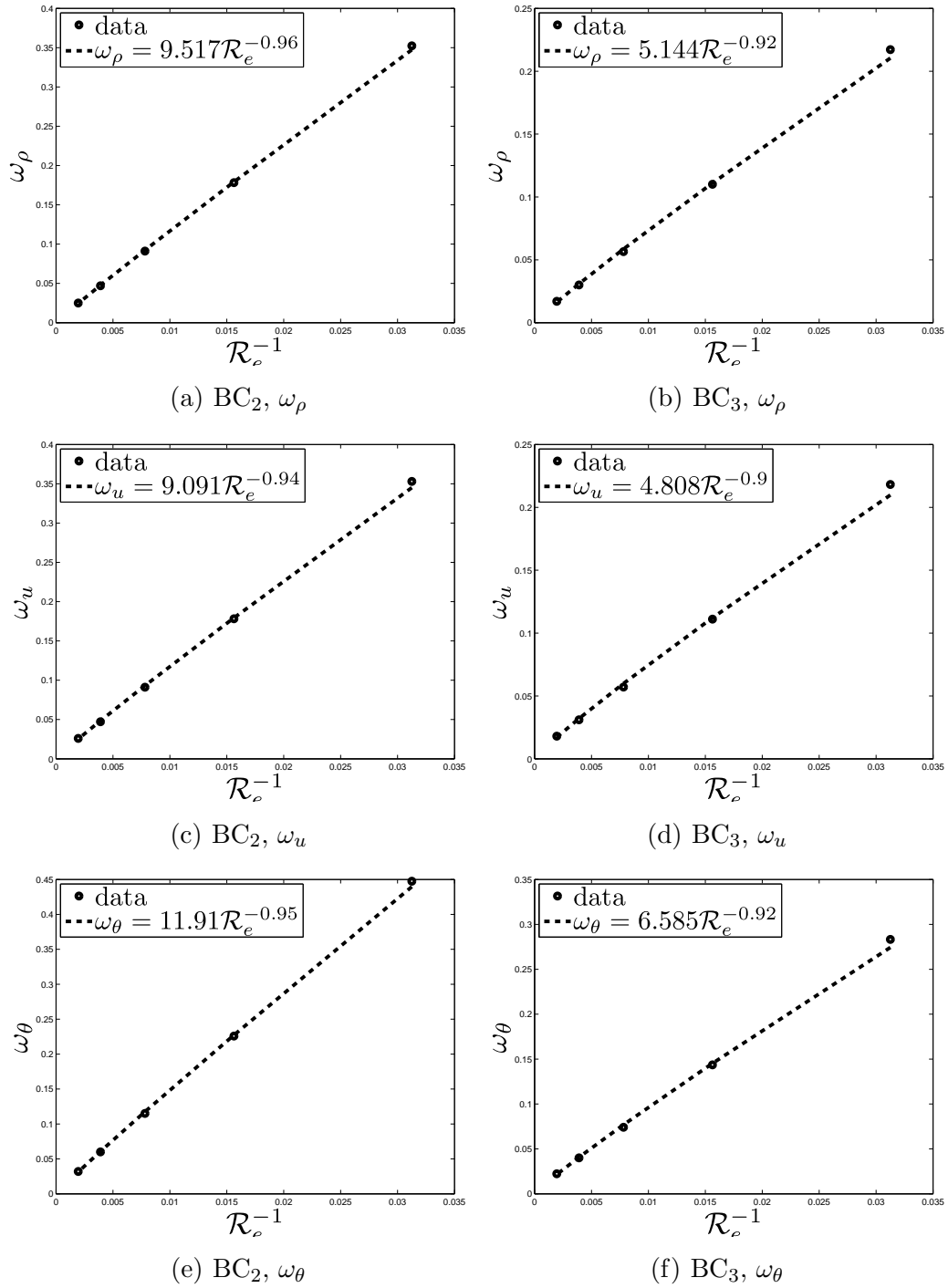
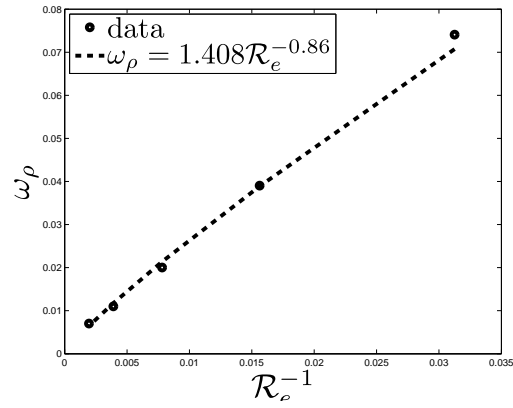
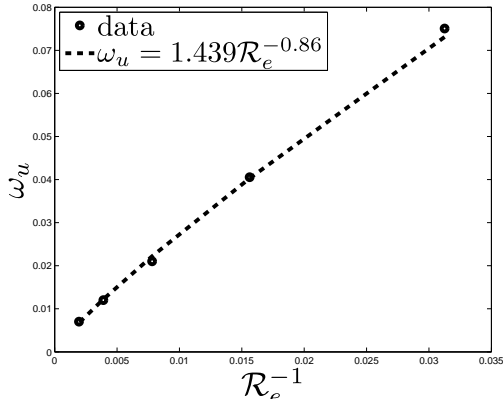


Figure 6.18: Navier-Stokes shock width regression for BC_2 and BC_3 sets of boundary conditions. Horizontal axis is reciprocal of Reynolds number $\mathcal{R}e^{-1}$

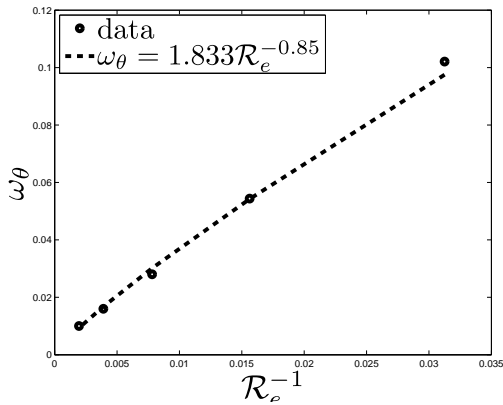
Chapter 6. Numerical Simulations and Results



(a) BC₄, ω_ρ



(b) BC₄, ω_u



(c) BC₄, ω_θ

Figure 6.19: Navier-Stokes shock width regression for BC₄ sets of boundary conditions. Horizontal axis is reciprocal of Reynolds number \mathcal{R}_e^{-1}

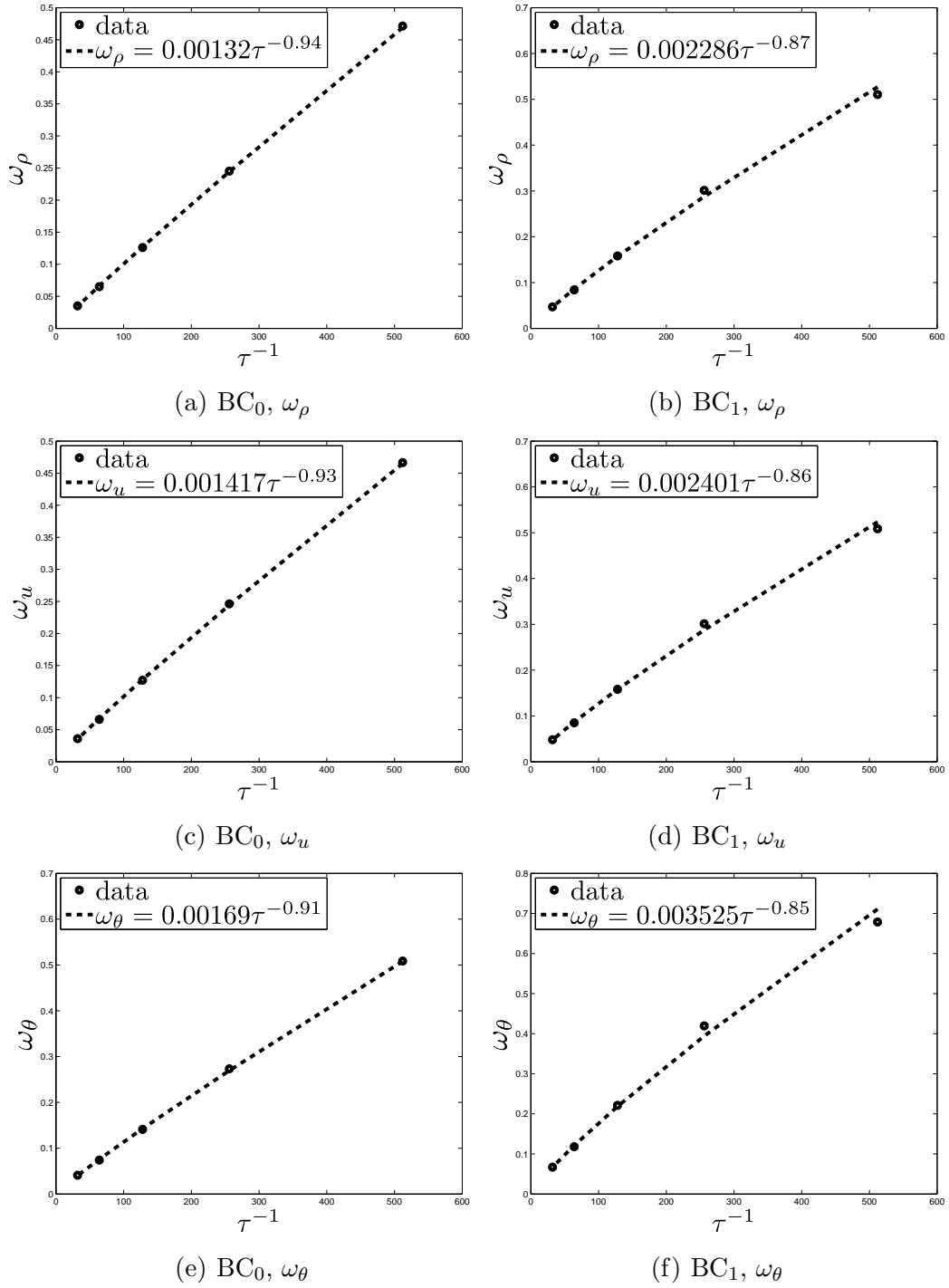


Figure 6.20: BGK shock width regression for BC_0 and BC_1 sets of boundary conditions. Horizontal axis is reciprocal of relaxation time τ^{-1}

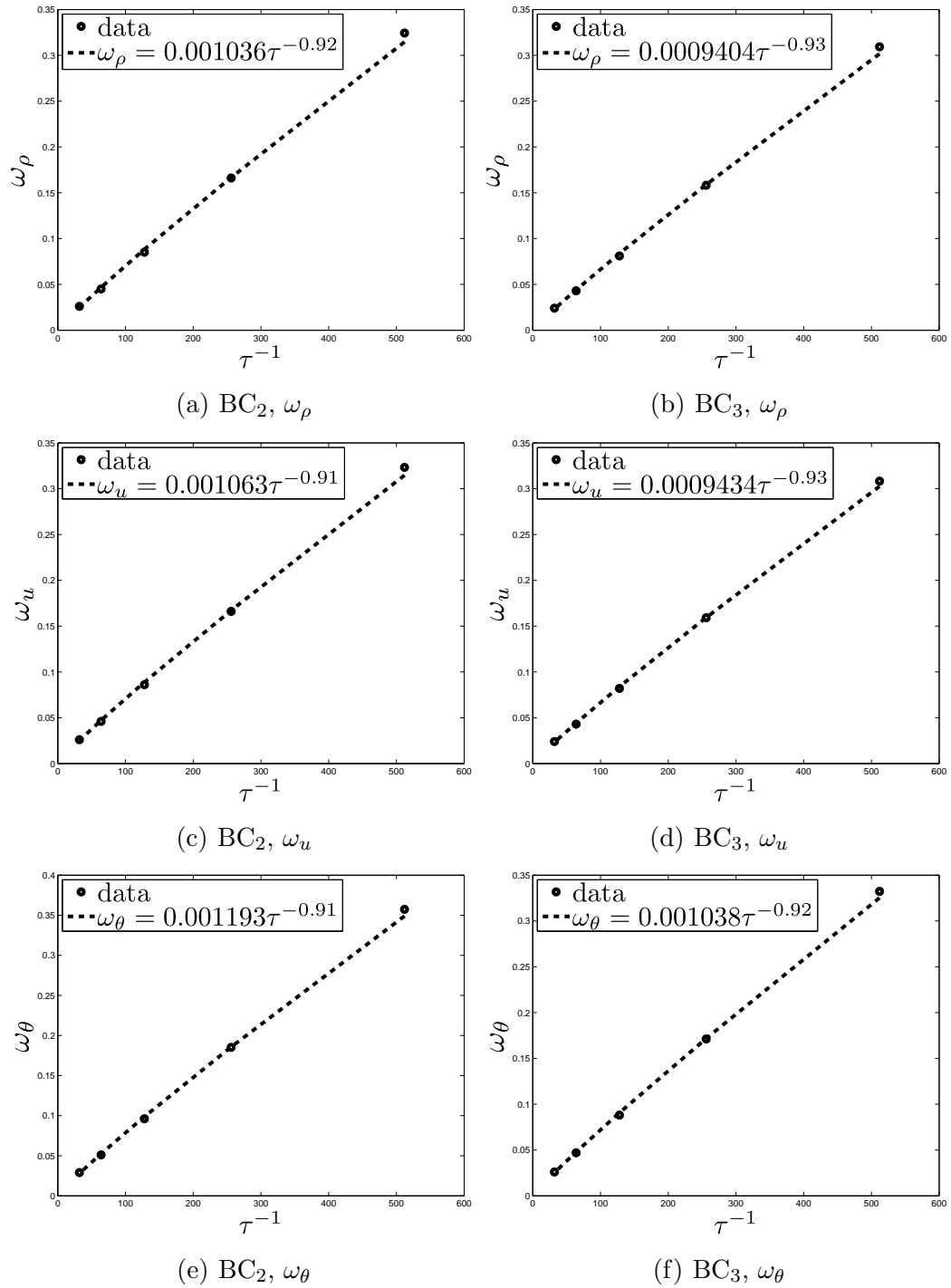
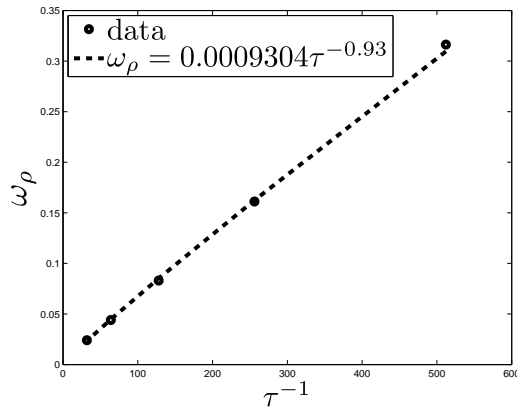
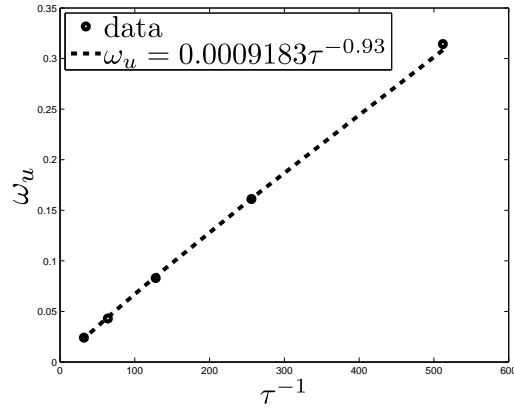


Figure 6.21: BGK shock width regression for BC₂ and BC₃ sets of boundary conditions. Horizontal axis is reciprocal of relaxation time τ^{-1}

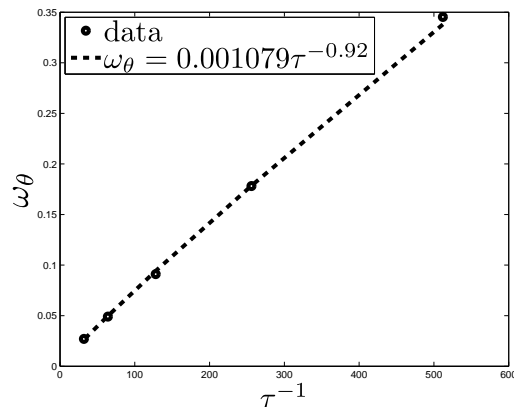
Chapter 6. Numerical Simulations and Results



(a) BC_4 , ω_ρ



(b) BC_4 , ω_u



(c) BC_4 , ω_θ

Figure 6.22: BGK shock width regression for BC_4 sets of boundary conditions. Horizontal axis is reciprocal of relaxation time τ^{-1}

Appendix A

Integration Procedures

A.1 Moments of the 1-D Maxwellian Distribution

Consider the n^{th} moment of the Gaussian 1-D distribution

$$I_n(u, \theta) = \int_{\mathbb{R}} v^n \exp \left\{ -\frac{(u-v)^2}{2\theta} \right\} dv \quad (\text{A.1})$$

Integration by parts yields

$$\begin{aligned} I_n &= \underbrace{\frac{1}{n+1} \exp \left\{ -\frac{(u-v)^2}{2\theta} \right\} \Big|_{v=-\infty}^{v=+\infty}}_0 - \\ &\quad - \frac{1}{n+1} \int_{\mathbb{R}} v^{n+1} \frac{d}{dv} \exp \left\{ -\frac{(u-v)^2}{2\theta} \right\} dv = \\ &= -\frac{1}{\theta(n+1)} \int_{\mathbb{R}} v^{n+1} (u-v) \exp \left\{ -\frac{(u-v)^2}{2\theta} \right\} dv = -\frac{1}{\theta(n+1)} [uI_{n+1} - I_{n+2}] \end{aligned}$$

Thus we get

$$I_{n+2} = \theta(n+1)I_n + uI_{n+1} \quad (\text{A.2})$$

Appendix A. Integration Procedures

The recursive equation (A.2) requires two initial conditions I_0 and I_1 which must be addressed separately. Using a trivial substitution

$$\xi = (u - v)\theta^{-\frac{1}{2}} \quad (\text{A.3})$$

we get

$$I_0 = \sqrt{\theta} \int_{\mathbb{R}} e^{-\xi^2} d\xi \quad (\text{A.4})$$

or equivalently

$$\theta^{-1} I_0^2 = \iint_{\mathbb{R}^2} e^{-\xi_1^2 - \xi_2^2} d\xi_1 d\xi_2 = \int_0^{2\pi} d\phi \int_{\mathbb{R}} r e^{-r^2} dr = 2\pi \quad (\text{A.5})$$

To obtain (A.5) from (A.4) we used iterative integration and polar coordinates. After solving (A.5) for $I_0 > 0$ we obtained

$$I_0 = \sqrt{2\pi\theta} \quad (\text{A.6})$$

Similarly for I_1 :

$$uI_0 - I_1 = \int_{\mathbb{R}} \exp\left\{-\frac{(u-v)^2}{2\theta}\right\} (u-v)dv = \sqrt{\theta} \int_{\mathbb{R}} e^{-\xi^2} \xi d\xi = 0 \quad (\text{A.7})$$

Here we used substitution (A.3). Therefore we obtain

$$I_1 = u\sqrt{2\pi\theta} \quad (\text{A.8})$$

Appendix A. Integration Procedures

Formulae (A.2), (A.6), and (A.8) imply the general rule for calculating the n^{th} moment:

$$I_n = \int_{\mathbb{R}} v^n \exp \left\{ -\frac{(u-v)^2}{2\theta} \right\} dv = \begin{cases} \sqrt{2\pi\theta}, & n = 0 \\ u\sqrt{2\pi\theta}, & n = 1 \\ \theta(n-1)I_{n-2} + uI_{n-1}, & n \geq 2 \end{cases} \quad (\text{A.9})$$

The expression for I_2 follows from (A.9):

$$I_2 = \int_{\mathbb{R}} v^2 \exp \left\{ -\frac{(u-v)^2}{2\theta} \right\} dv \theta I_0 + uI_1 = \sqrt{2\pi\theta}(\theta + u^2) \quad (\text{A.10})$$

A special case when $u = 0$ will be used in Section A.2.1. In this case formula (A.9) reduces to

$$I_n = \theta(n-1)I_{n-2} \quad (\text{A.11})$$

Clearly for odd values of n $I_n = 0$. For even n the recursive equation (A.11) results in

$$I_{2k} = \theta^k (2k-1)!! \sqrt{2\pi\theta}, \quad (\text{A.12})$$

where $n!!$ is the product of all numbers between 1 and n that have the same parity as n .

A.2 Moments of the 3-D Maxwellian Distribution

In this section we compute first three moments m_0 , \vec{m}_1 , and m_2 of Maxwellian distribution defined by (1.65) corresponding to the collision invariants (1.40).

Appendix A. Integration Procedures

$$1. \quad m_0 = \frac{\rho}{(2\pi\theta)^{\frac{3}{2}}} \iiint_{\mathbb{R}^3} \exp\left\{-\frac{|\vec{v} - \vec{u}|^2}{2\theta}\right\} d\vec{v} \quad (\text{A.13})$$

After translation by \vec{u} we get $m_0 = \frac{\rho}{(2\pi\theta)^{\frac{3}{2}}} \iiint_{\mathbb{R}^3} \exp\left\{-\frac{|\vec{v}|^2}{2\theta}\right\} d\vec{v}$

$$m_0(2\pi\theta)^{\frac{3}{2}}\rho^{-1} = \int_0^\pi \int_0^{2\pi} \int_0^{+\infty} e^{-\frac{r^2}{2\theta}} r^2 \sin\phi dr d\psi d\phi \quad (\text{A.14})$$

Spherical coordinates (r, ψ, ϕ) were used in (A.14). Furthermore

$$m_0(2\pi\theta)^{\frac{3}{2}}\rho^{-1} = 4\pi \int_0^{+\infty} r^2 e^{-\frac{r^2}{2\theta}} dr = 2\pi I_2(0, \theta) \quad (\text{A.15})$$

where $I_n(u, \theta)$ is defined by (A.1) in Appendix A.1. Formula A.10 for $u = 0$ produces $m_0(2\pi\theta)^{\frac{3}{2}}\rho^{-1} = 2\pi\theta\sqrt{2\pi\theta}$ and therefore the zeroth moment of the Maxwellian is

$$m_0 = \frac{\rho}{(2\pi\theta)^{\frac{3}{2}}} \iiint_{\mathbb{R}^3} \exp\left\{-\frac{|\vec{v} - \vec{u}|^2}{2\theta}\right\} d\vec{v} = \rho \quad (\text{A.16})$$

$$2. \quad \vec{m}_1 = \frac{\rho}{(2\pi\theta)^{\frac{3}{2}}} \iiint_{\mathbb{R}^3} \exp\left\{-\frac{|\vec{v} - \vec{u}|^2}{2\theta}\right\} \vec{v} d\vec{v} \quad (\text{A.17})$$

After adding and subtracting \vec{u} from \vec{v} and after translation by \vec{u} we get

$$\begin{aligned} \vec{m}_1 &= \frac{\rho}{(2\pi\theta)^{\frac{3}{2}}} \iiint_{\mathbb{R}^3} \exp\left\{-\frac{|\vec{v}|^2}{2\theta}\right\} \vec{v} d\vec{v} + \\ &+ \frac{\rho\vec{u}}{(2\pi\theta)^{\frac{3}{2}}} \iiint_{\mathbb{R}^3} \exp\left\{-\frac{|\vec{v} - \vec{u}|^2}{2\theta}\right\} d\vec{v} = \\ &= \frac{\rho}{(2\pi\theta)^{\frac{3}{2}}} \iiint_{\mathbb{R}^3} \exp\left\{-\frac{|\vec{v}|^2}{2\theta}\right\} \vec{v} d\vec{v} + m_0\vec{u} \end{aligned} \quad (\text{A.18})$$

The remaining triple integral is 0 since $\vec{v} \mapsto \exp\left\{-\frac{|\vec{v}|^2}{2\theta}\right\} \vec{v}$ is odd and the integration is performed over whole space \mathbb{R}^3 . Therefore we get

$$\vec{m}_1 = \frac{\rho}{(2\pi\theta)^{\frac{3}{2}}} \iiint_{\mathbb{R}^3} \exp\left\{-\frac{|\vec{v} - \vec{u}|^2}{2\theta}\right\} \vec{v} d\vec{v} = \rho\vec{u} \quad (\text{A.19})$$

Appendix A. Integration Procedures

3. In order to calculate

$$m_2 = \frac{\rho}{(2\pi\theta)^{\frac{3}{2}}} \iiint_{\mathbb{R}^3} \exp\left\{-\frac{|\vec{v} - \vec{u}|^2}{2\theta}\right\} |\vec{v}|^2 d\vec{v} \quad (\text{A.20})$$

we use $|\vec{v}|^2 = |\vec{v} - \vec{u}|^2 + |\vec{u}|^2 + 2(\vec{v} - \vec{u}) \cdot \vec{u}$. Therefore

$$m_2 = \frac{\rho}{(2\pi\theta)^{\frac{3}{2}}} \iiint_{\mathbb{R}^3} \exp\left\{-\frac{|\vec{v}|^2}{2\theta}\right\} |\vec{v}|^2 d\vec{v} + |\vec{u}|^2 m_0 + 2\vec{u} \cdot \vec{0} \quad (\text{A.21})$$

$$\begin{aligned} (m_2 - \rho|\vec{u}|^2)(2\pi\theta)^{\frac{3}{2}}\rho^{-1} &= \iiint_{\mathbb{R}^3} \exp\left\{-\frac{|\vec{v}|^2}{2\theta}\right\} |\vec{v}|^2 d\vec{v} = \\ &= \int_0^\pi \int_0^{2\pi} \int_0^{+\infty} e^{-\frac{r^2}{2\theta}} r^4 \sin\phi dr d\psi d\phi = 2\pi I_4(0, \theta), \end{aligned} \quad (\text{A.22})$$

where $I_4(u, \theta)$ is defined by (A.1) and it can be computed by (A.9) and (A.10). Namely $I_4 = 3I_2 = 3\theta^2\sqrt{2\pi\theta}$ and thus we get

$$(m_2 - \rho|\vec{u}|^2)(2\pi\theta)^{\frac{3}{2}}\rho^{-1} = 3\theta(2\pi\theta)^{\frac{3}{2}} \quad (\text{A.23})$$

Finally

$$m_2 = \frac{\rho}{(2\pi\theta)^{\frac{3}{2}}} \iiint_{\mathbb{R}^3} \exp\left\{-\frac{|\vec{v} - \vec{u}|^2}{2\theta}\right\} |\vec{v}|^2 d\vec{v} = \rho(|\vec{u}|^2 + 3\theta) \quad (\text{A.24})$$

A.2.1 Additional Moments of Maxwellian Distribution

In this section we compute additional moment required to establish orthogonality relationships (1.123,1.124) in Section (1.3.6). The definitions of the moments and their values are provided in Table A.1 below.

Appendix A. Integration Procedures

Notation	Definition	Value
$\mathcal{G}_k(\theta)$	$= \alpha \iiint_{\mathbb{R}^3} e^{-\frac{ \vec{\xi} ^2}{2\theta}} \vec{\xi} ^k d\vec{\xi}$	$= \begin{cases} 1, & k = 0 \\ 3\theta, & k = 2 \\ 15\theta^2, & k = 4 \end{cases}$
$\mathcal{G}_{j,k}(\theta)$	$= \alpha \iiint_{\mathbb{R}^3} e^{-\frac{ \vec{\xi} ^2}{2\theta}} \xi_j \xi_k d\vec{\xi}$	$= \theta \delta_{jk} = \frac{1}{3} \delta_{j,k} \mathcal{G}_2(\theta)$
$\mathcal{G}_{i,j,k}(\theta)$	$= \alpha \iiint_{\mathbb{R}^3} e^{-\frac{ \vec{\xi} ^2}{2\theta}} \xi_i \xi_j \xi_k d\vec{\xi}$	$= 0$
$\mathcal{G}_j^k(\theta)$	$= \alpha \iiint_{\mathbb{R}^3} e^{-\frac{ \vec{\xi} ^2}{2\theta}} \vec{\xi} ^k \xi_j d\vec{\xi}$	$= 0$
$\mathcal{G}_{j,k}^2(\theta)$	$= \alpha \iiint_{\mathbb{R}^3} e^{-\frac{ \vec{\xi} ^2}{2\theta}} \vec{\xi} ^2 \xi_j \xi_k d\vec{\xi}$	$= 5\theta^2 \delta_{jk} = \frac{5}{\theta} \mathcal{G}_{j,k}(\theta)$

Table A.1: Moments of Maxwellian Distribution. Constant $\alpha = \frac{1}{\sqrt{(2\pi\theta)^3}}$

Values for $\mathcal{G}_0(\theta)$ and $G_2(\theta)$ have already been calculated in this section. To obtain $\mathcal{G}_0(\theta) = 1$ we set $\vec{u} = 0$ in (A.16) and it follows from (A.24) that $G_2(\theta) = 3\theta$. In order to calculate $G_4(\theta)$ we use spherical coordinates (r, ψ, ϕ) :

$$G_4(\theta) = \alpha \int_0^\pi \int_0^{2\pi} \int_0^{+\infty} e^{-\frac{r^2}{2\theta}} r^6 \sin \phi dr d\psi d\phi = 4\pi\alpha \int_0^{+\infty} e^{-\frac{r^2}{2\theta}} r^6 dr. \quad (\text{A.25})$$

Since¹

$$\int_0^{+\infty} e^{-\frac{r^2}{2\theta}} r^5 dr = 4\sqrt{2}\theta^{\frac{7}{2}} \int_0^{+\infty} e^{-z} z^{\frac{5}{2}} dz = 4\sqrt{2}\theta^{\frac{7}{2}} \Gamma\left(\frac{7}{2}\right) = 15\sqrt{\frac{\pi}{2}}\theta^{\frac{7}{2}} \quad (\text{A.26})$$

the value for $G_4(\theta) = 5\theta\mathcal{G}_{j,j}(\theta) = 15\theta^2$ and the result follows.

In order to calculate $\mathcal{G}_{j,k}$ we observe that for $j \neq k$ the integral is zero since the

¹ $\Gamma(z) = \int_0^{+\infty} e^{-s} s^{z-1} dz, \Gamma\left(\frac{7}{2}\right) = \frac{15\sqrt{\pi}}{8}$

Appendix A. Integration Procedures

integrand is odd. In the case when $j = k$ we have

$$G_{k,k}(\theta) = \alpha \iiint_{\mathbb{R}^3} e^{-\frac{|\vec{\xi}|^2}{2\theta}} \xi_k^2 d\vec{\xi} = \frac{\alpha}{3} \iiint_{\mathbb{R}^3} e^{-\frac{|\vec{\xi}|^2}{2\theta}} |\vec{\xi}|^2 d\vec{\xi} = \frac{1}{3} G_2(\theta). \quad (\text{A.27})$$

Regardless of values of (i, j, k) functions $\vec{\xi} \mapsto e^{-\frac{|\vec{\xi}|^2}{2\theta}} \xi_i \xi_j \xi_k$ and $\vec{\xi} \mapsto \vec{\xi} \mapsto e^{-\frac{|\vec{\xi}|^2}{2\theta}} |\vec{\xi}|^k \xi_i$ are odd and hence the resulting integrals $\mathcal{G}_{i,j,k}(\theta) = \mathcal{G}_j^k(\theta) = 0$ due to integration over \mathbb{R}^3 .

Lastly, in order to calculate $\mathcal{G}_{j,k}^2$ we use the same approach as the one used for $\mathcal{G}_{j,k}$. In the case when $j = k$ the integral is zero. Due to symmetry, for $j = k$, we have

$$\mathcal{G}_{k,k}^2(\theta) = \frac{1}{3} \mathcal{G}_4(\theta). \quad (\text{A.28})$$

Appendix B

Continuum and Kinetic Theory

B.1 The Nondimensionalized 3-D Euler System

Consider the 3-D Euler system of partial differential equations as given by (1.7) equipped with equations of state (1.7):

$$\begin{aligned}\partial_t \rho + \operatorname{div}(\rho \vec{u}) &= 0, \\ \partial_t(\rho \vec{u}) + \operatorname{Div}(\rho \vec{u} \otimes \vec{u}) + \vec{\nabla} p &= 0, \\ \partial_t \left(\frac{1}{2} \rho |\vec{u}|^2 + \rho e \right) + \operatorname{div} \left[\rho \vec{u} \left(\frac{1}{2} |\vec{u}|^2 + e \right) + p \vec{u} \right] &= 0.\end{aligned}\tag{B.1}$$

First we nondimensionalize equations of state (1.7). According to (2.17) on page 35

$$\frac{R}{C_V} = \frac{C_P - C_V}{C_V} = \gamma - 1.\tag{B.2}$$

$$p_0 \hat{p} = \frac{R \theta_0}{M u_0^2} \rho_0 u_0^2 \hat{\rho} \hat{\theta}\tag{B.3}$$

$$e_0 \hat{e} = \frac{C_V \theta_0}{M} \hat{\theta} = \frac{C_V}{R} \frac{R \theta_0}{M} \hat{\theta}\tag{B.4}$$

Appendix B. Continuum and Kinetic Theory

Equations (1.10), (1.11) and (1.12) imply

$$\hat{p} = \hat{\rho}\hat{\theta} \quad (\text{B.5})$$

$$\hat{e} = (\gamma - 1)^{-1}\hat{\theta} \quad (\text{B.6})$$

Equations (B.5) and (B.6) represent nondimensionalized equations of state.

From the equations of state (1.7) we have $\frac{p}{e} = \frac{R}{C_V}\rho$ and therefore

$$p = (\gamma - 1)^{-1}\rho e \quad (\text{B.7})$$

After substituting (B.7) into (B.1), the Euler system takes form

$$\begin{aligned} \partial_t \rho + \text{div}(\rho \vec{u}) &= 0, \\ \partial_t(\rho \vec{u}) + \text{Div}(\rho \vec{u} \otimes \vec{u}) + (\gamma - 1)\vec{\nabla}[\rho e] &= 0, \\ \partial_t\left(\frac{1}{2}\rho |\vec{u}|^2 + \rho e\right) + \text{div}\left[\rho \vec{u}\left(\frac{1}{2}|\vec{u}|^2 + \gamma e\right)\right] &= 0. \end{aligned} \quad (\text{B.8})$$

Rescaling of system (B.8) is achieved by using (1.10) and substituting (1.8) into (B.8). The differential operators are transformed according to

$$\begin{aligned} \partial_t &= t_0^{-1}\partial_{\hat{t}} \\ \text{div}_{\vec{x}} &= L^{-1}\text{div}_{\hat{x}} \\ \vec{\nabla}_{\vec{x}} &= L^{-1}\vec{\nabla}_{\hat{x}} \end{aligned} \quad (\text{B.9})$$

After removing the hat notations above the rescaled variables the resulting system takes form

$$\begin{aligned} \frac{\rho_0}{t_0}\partial_t \rho + \frac{\rho_0 u_0}{L}\text{div}(\rho \vec{u}) &= 0, \\ \frac{\rho_0 u_0}{t_0}\partial_t(\rho \vec{u}) + \text{Div}(\rho \vec{u} \otimes \vec{u}) + \frac{(\gamma - 1)\rho_0 u_0^2}{L}\vec{\nabla}[\rho e] &= 0, \\ \frac{\rho_0 u_0^2}{t_0}\partial_t\left(\frac{1}{2}\rho |\vec{u}|^2 + \rho e\right) + \frac{\rho_0 u_0^3}{L}\text{div}\left[\rho \vec{u}\left(\frac{1}{2}|\vec{u}|^2 + \gamma e\right)\right] &= 0. \end{aligned} \quad (\text{B.10})$$

Appendix B. Continuum and Kinetic Theory

In order to obtain the final nondimensionalized Euler system (B.11) we use (B.6):

$$\begin{aligned}
 \partial_t \rho + \operatorname{div}(\rho \vec{u}) &= 0, \\
 \partial_t(\rho \vec{u}) + \operatorname{Div}(\rho \vec{u} \otimes \vec{u}) + \vec{\nabla}[\rho \theta] &= 0, \\
 \partial_t \left(\frac{1}{2} \rho |\vec{u}|^2 + \frac{1}{\gamma-1} \rho \theta \right) + \operatorname{div} \left[\rho \vec{u} \left(\frac{1}{2} |\vec{u}|^2 + \frac{\gamma}{\gamma-1} \theta \right) \right] &= 0.
 \end{aligned} \tag{B.11}$$

B.2 Proof of Identities (1.56)-(1.58) in Section 1.3.2

In this section we prove that identities (1.56)-(1.58) on page 17 hold. Before we get to the proof we adopt some convenient notations as well as establish some useful tensor identities.

Let $\langle \phi \rangle$ denote $\int_{\mathbb{R}} \phi(\vec{v}) f(\vec{v}) d\vec{v}$, where $\vec{v} \mapsto \phi(\vec{v})$ can be a function or a vector or matrix field, depending upon context. In the light of the introduced notations, identities (1.52)-(1.55) can be rewritten as

$$\rho = \langle 1 \rangle \tag{B.12}$$

$$\rho \vec{u} = \langle \vec{v} \rangle \tag{B.13}$$

$$P = \langle (\vec{v} - \vec{u})^{\otimes 2} \rangle \tag{B.14}$$

$$C = \langle (\vec{v} - \vec{u}) |\vec{v} - \vec{u}|^2 \rangle \tag{B.15}$$

Consider

$$\langle (\vec{v} - \vec{u})^{\otimes 2} \rangle = \langle \vec{v}^{\otimes 2} \rangle + \langle \vec{u}^{\otimes 2} \rangle - \langle \vec{u} \otimes \vec{v} \rangle - \langle \vec{u} \otimes \vec{v} \rangle = \langle \vec{v}^{\otimes 2} \rangle + \langle \vec{u}^{\otimes 2} \rangle - \vec{u} \otimes \langle \vec{v} \rangle - \langle \vec{v} \rangle \otimes \vec{u}$$

Since $\rho \vec{u} \otimes \vec{u} = \vec{u} \otimes \rho \vec{u}$ and

$$\langle \vec{u}^{\otimes 2} \rangle = \vec{u}^{\otimes 2} \langle 1 \rangle = \rho \vec{u}^{\otimes 2} \tag{B.16}$$

Appendix B. Continuum and Kinetic Theory

we have

$$P = \langle (\vec{v} - \vec{u})^{2\otimes} \rangle = \langle \vec{v}^{\otimes 2} \rangle - \rho \vec{u}^{\otimes 2}, \quad (\text{B.17})$$

which implies (1.56)

In order to establish (1.57) we observe that $\text{tr}\langle A \rangle = \langle \text{tr} A \rangle$ as well as

$$\text{tr}\langle \vec{V}^{\otimes 2} \rangle = \langle \text{tr} \vec{V}^{\otimes 2} \rangle = \langle |\vec{V}|^2 \rangle. \quad (\text{B.18})$$

Therefore after using (B.14) as a definition of P we have $\rho|\vec{u}|^2 + \text{tr} P = \rho|\vec{u}|^2 + \text{tr}\langle (\vec{v} - \vec{u})^{\otimes 2} \rangle = \rho|\vec{u}|^2 + \langle |\vec{v} - \vec{u}|^2 \rangle = \rho|\vec{u}|^2 + \langle |\vec{v}|^2 \rangle + \langle |\vec{u}|^2 \rangle - 2\vec{u} \cdot \langle \vec{v} \rangle$ and thusly implementing (B.16) and (B.13) we have $\rho|\vec{u}|^2 + \text{tr} P = \langle |\vec{v}|^2 \rangle$ which is no more than (1.57).

In order to prove (1.58) we consider the following property

$$\vec{V}^{\otimes 2} \vec{W} = (\vec{V} \vec{V}^{\text{T}}) \vec{W} = \vec{V} (\vec{V}^{\text{T}} \vec{W}) = \vec{V} (\vec{V} \cdot \vec{W}), \quad (\text{B.19})$$

which for $\vec{V} = \vec{W}$ implies

$$\vec{V}^{\otimes 2} \vec{V} = \vec{V} |\vec{V}|^2 \quad (\text{B.20})$$

By utilizing (1.57), (B.17), and (B.20) the right hand side of (1.58) transforms into

$$[\rho|\vec{u}|^2 + \text{tr} P] \vec{u} + 2P\vec{u} + C = -2\rho|\vec{u}|^2 \vec{u} + \langle |\vec{v}|^2 \rangle \vec{u} + 2\langle \vec{v}(\vec{v} \cdot \vec{u}) \rangle + C \quad (\text{B.21})$$

The definition of C (B.15) implies that

$$C = 2\rho|\vec{u}|^2 \vec{u} + \langle |\vec{v}|^2 \rangle \vec{v} - 2\langle \vec{v}(\vec{v} \cdot \vec{u}) \rangle - \langle |\vec{v}|^2 \rangle \vec{u} \quad (\text{B.22})$$

Substituting (B.22) into (B.21) yields desired result (1.58).

B.3 Some Details of the Proof of the H-Theorem

Here we provide detailed computations required for establishing implication (c) \implies (a) in the H-Theorem.

Since $f = f^e$, where f^e is defined by (1.65), we have

$$\begin{aligned} f &= f(\vec{v}) = \alpha e^{-\sigma|\vec{u}-\vec{v}|^2}, \\ f_* &= f(\vec{v}_*) = \alpha e^{-\sigma|\vec{u}-\vec{v}_*|^2}, \end{aligned} \quad (\text{B.23})$$

where $\alpha = \frac{\rho}{\sqrt{2\pi\theta}}$ and $\sigma = \frac{1}{2\theta}$. Let

$$\delta = \delta(\vec{v}, \vec{v}_*, \vec{\omega}) = (\vec{v} - \vec{v}_*) \cdot \vec{\omega} \quad (\text{B.24})$$

for $\omega \in \mathbb{S}^2$. Then we have

$$f f_* = \alpha^2 e^{-\sigma[(\vec{u}-\vec{v})^2 - (\vec{u}-\vec{v}_*)^2]} \quad (\text{B.25})$$

Let $\vec{p}, \vec{q} \in \mathbb{R}^3$ and let $p = |\vec{p}|$ and $q = |\vec{q}|$, then we have

$$f(\vec{p} + \vec{q}) = \alpha e^{-\sigma|\vec{u}-\vec{p}-\vec{q}|^2} = \alpha e^{-\sigma[(\vec{u}-\vec{p})^2 - 2\vec{q} \cdot (\vec{u}-\vec{p}) + q^2]} = \alpha e^{-\sigma|\vec{u}-\vec{p}|^2} e^{2\sigma\vec{q} \cdot (\vec{u}-\vec{p}) - \sigma q^2}$$

Therefore

$$f(\vec{p} + \vec{q}) = f(\vec{p}) e^{-\sigma[q^2 - 2\vec{q} \cdot (\vec{u}-\vec{p})]} \quad (\text{B.26})$$

We use (1.33), (B.26) and the fact that $|\delta\vec{\omega}| = |\delta|$ to obtain

$$\begin{aligned} f' &= f(\vec{v} - \delta\vec{\omega}) = f e^{-\sigma[\delta^2 + 2\delta\vec{\omega} \cdot (\vec{u}-\vec{v})]} \\ f'_* &= f(\vec{v}_* + \delta\vec{\omega}) = f_* e^{-\sigma[\delta^2 - 2\delta\vec{\omega} \cdot (\vec{u}-\vec{v}_*)]} \end{aligned}$$

Appendix B. Continuum and Kinetic Theory

The expression inside the collision integral (1.36) becomes

$$f' f'_* - f f_* = f f_* \left[e^{-\sigma(2\delta^2 + 2\delta\vec{\omega} \cdot (\vec{v}_* - \vec{v}))} - 1 \right]. \quad (\text{B.27})$$

We observe that $2\delta^2 + 2\delta\vec{\omega} \cdot (\vec{v}_* - \vec{v}) = 0$ due to (B.24) and therefore $f' f'_* - f f_* = 0 \implies \mathcal{B}(f^e, f^e) = 0$. This finalizes the proof.

B.4 Calculation of $D_t \log f_0$

This section we provide verification of (1.112) for A and B defined by (1.113) and (1.114) and f_0 defined by (1.65).

Let

$$\begin{aligned} D &= \frac{1}{\rho} \underbrace{\left[\partial_t \rho + \vec{u} \cdot \vec{\nabla} \rho + \rho \operatorname{div} \vec{u} \right]}_{E_1} + \\ &+ \frac{\vec{v} - \vec{u}}{\theta} \cdot \underbrace{\left[\partial_t \vec{u} + \vec{u} * \vec{\nabla} \vec{u} + \vec{\nabla} \theta + \frac{\theta}{\rho} \vec{\nabla} \rho \right]}_{\vec{E}_2} + \\ &+ \frac{1}{2\theta} \left[\frac{|\vec{v} - \vec{u}|^2}{\theta} - 3 \right] \underbrace{\left[\partial_t \theta + \vec{u} \cdot \vec{\nabla} \theta + \frac{2}{3} \theta \operatorname{div} \vec{u} \right]}_{E_3} + \\ &+ \underbrace{A \left(\frac{\vec{v} - \vec{u}}{\sqrt{\theta}} \right) : \vec{\nabla} \vec{u}}_{\mathcal{A}} + \underbrace{2B \left(\frac{\vec{v} - \vec{u}}{\sqrt{\theta}} \right) \cdot \vec{\nabla} \sqrt{\theta}}_{\mathcal{B}} \end{aligned} \quad (\text{B.28})$$

In the notation introduced above D take a more consist form D :

$$D = \frac{1}{\rho} E_1 + \frac{\vec{v} - \vec{u}}{\theta} \cdot \vec{E}_2 + \frac{1}{2\theta} \left[\frac{|\vec{v} - \vec{u}|^2}{\theta} - 3 \right] E_3 + \mathcal{A} + \mathcal{B} \quad (\text{B.29})$$

First we calculate $\log f_0$:

$$\log f_0 = \log \rho - \frac{3}{2} \log \theta - \frac{|\vec{v} - \vec{u}|^2}{2\theta} - \log \sqrt{(2\pi)^3}, \quad (\text{B.30})$$

Appendix B. Continuum and Kinetic Theory

$$\begin{aligned}
D_t \log f_0 &= \left(\partial_t + \vec{v} \cdot \vec{\nabla} \right) \left[\log \rho - \frac{3}{2} \log \theta - \frac{|\vec{v} - \vec{u}|^2}{2\theta} \right] = \\
&= \frac{1}{\rho} \partial_t \rho + \frac{1}{\rho} \vec{v} \cdot \vec{\nabla} \rho - \frac{3}{2\theta} \partial_t \theta - \frac{3}{2\theta} \vec{v} \cdot \vec{\nabla} \theta + \frac{|\vec{v} - \vec{u}|^2}{2\theta^2} \partial_t \theta + \\
&+ \frac{|\vec{v} - \vec{u}|^2}{2\theta^2} \vec{v} \cdot \vec{\nabla} \theta + \frac{1}{\theta} (\vec{v} - \vec{u}) \cdot \partial_t \vec{u} + \frac{1}{\theta} \sum_{j,k=1}^3 v_k (v_j - u_j) \frac{\partial u_j}{\partial x_k}
\end{aligned} \tag{B.31}$$

One has to establish that $D = D_t \log f_0$. First we rearrange terms of $D_t \log f_0$ as shown below:

$$\begin{aligned}
D_t \log f_0 &= \\
&= \underbrace{\left[\frac{1}{\rho} \partial_t \rho + \frac{1}{\rho} \vec{v} \cdot \vec{\nabla} \rho \right]}_{D_1} + \underbrace{\left[\frac{1}{\theta} (\vec{v} - \vec{u}) \cdot \partial_t \vec{u} - \frac{3}{2\theta} \vec{v} \cdot \vec{\nabla} \theta \right]}_{D_2} + \\
&+ \underbrace{\left[\frac{|\vec{v} - \vec{u}|^2}{2\theta^2} \partial_t \theta - \frac{3}{2\theta} \partial_t \theta \right]}_{D_3} + \\
&+ \frac{|\vec{v} - \vec{u}|^2}{2\theta^2} \vec{v} \cdot \vec{\nabla} \theta + \frac{1}{\theta} \sum_{j,k=1}^3 v_k (v_j - u_j) \frac{\partial u_j}{\partial x_k}
\end{aligned} \tag{B.32}$$

Equivalently

$$D_t \log f_0 = D_1 + D_2 + D_3 + \frac{|\vec{v} - \vec{u}|^2}{2\theta^2} \vec{v} \cdot \vec{\nabla} \theta + \frac{1}{\theta} \sum_{j,k=1}^3 v_k (v_j - u_j) \frac{\partial u_j}{\partial x_k} \tag{B.33}$$

We establish by observation that

$$\frac{1}{\rho} E_1 = \left[\frac{1}{\rho} \partial_t \rho + \frac{1}{\rho} \vec{v} \cdot \vec{\nabla} \rho \right] + \operatorname{div} \vec{u} + \frac{\vec{u} - \vec{v}}{\rho} \cdot \vec{\nabla} \rho \tag{B.34}$$

$$\begin{aligned}
\frac{\vec{v} - \vec{u}}{\theta} \cdot \vec{E}_2 &= \left[\frac{\vec{v} - \vec{u}}{\theta} \cdot \partial_t \vec{u} - \frac{3\vec{v}}{2\theta} \cdot \vec{\nabla} \theta \right] + \frac{5\vec{v}}{2\theta} \cdot \vec{\nabla} \theta - \frac{\vec{u}}{\theta} \cdot \vec{\nabla} \theta + \\
&+ \frac{\vec{v} - \vec{u}}{\rho} \cdot \vec{\nabla} \rho + \frac{\vec{v} - \vec{u}}{\theta} \cdot (\vec{u} * \vec{\nabla} \vec{u})
\end{aligned} \tag{B.35}$$

Appendix B. Continuum and Kinetic Theory

$$\begin{aligned} \frac{1}{2\theta} \left[\frac{|\vec{v} - \vec{u}|^2}{\theta} - 3 \right] E_3 &= \left[\frac{|\vec{v} - \vec{u}|^2}{2\theta^2} - \frac{3}{2\theta} \right] \partial_t \theta - \operatorname{div} \vec{u} + \\ &+ \frac{|\vec{v} - \vec{u}|^2}{2\theta^2} \vec{u} \cdot \vec{\nabla} \theta - \frac{3\vec{u}}{2\theta} \cdot \vec{\nabla} \theta + \frac{|\vec{v} - \vec{u}|^2}{3\theta} \operatorname{div} \vec{u} \end{aligned} \quad (\text{B.36})$$

The terms in the brackets in (B.34), (B.35), and (B.36) are exactly D_1 , D_2 , and D_3 defined by (B.32). Therefore, after cancelation of $\operatorname{div} \vec{u}$ and $\frac{\vec{u} - \vec{v}}{\rho} \cdot \vec{\nabla} \rho$, expression (B.28) is reduced to

$$\begin{aligned} D &= D_1 + D_2 + D_3 + \frac{5(\vec{v} - \vec{u})}{2\theta} \cdot \vec{\nabla} \theta + \frac{\vec{v} - \vec{u}}{\theta} \cdot (\vec{u} * \vec{\nabla} \vec{u}) + \\ &+ \frac{|\vec{v} - \vec{u}|^2}{2\theta^2} \vec{u} \cdot \vec{\nabla} \theta + \frac{|\vec{v} - \vec{u}|^2}{3\theta} \operatorname{div} \vec{u} + \mathcal{A} + \mathcal{B} \end{aligned} \quad (\text{B.37})$$

After comparing (B.33) to (B.37) it becomes evident that in order to establish that $D = D_t \log f_0$ it remains to verify that the identity below holds:

$$\begin{aligned} \frac{|\vec{v} - \vec{u}|^2}{2\theta^2} \vec{v} \cdot \vec{\nabla} \theta + \frac{1}{\theta} \sum_{j,k=1}^3 v_k (v_j - u_j) \frac{\partial u_j}{\partial x_k} &= \frac{5(\vec{v} - \vec{u})}{2\theta} \cdot \vec{\nabla} \theta + \\ + \frac{\vec{v} - \vec{u}}{\theta} \cdot (\vec{u} * \vec{\nabla} \vec{u}) + \frac{|\vec{v} - \vec{u}|^2}{2\theta^2} \vec{u} \cdot \vec{\nabla} \theta + \frac{|\vec{v} - \vec{u}|^2}{3\theta} \operatorname{div} \vec{u} + \mathcal{A} + \mathcal{B} \end{aligned} \quad (\text{B.38})$$

The next three terms need to be clarified:

$$\begin{aligned} \frac{\vec{v} - \vec{u}}{\theta} \cdot (\vec{u} * \vec{\nabla} \vec{u}) &= \sum_j \frac{v_j - u_j}{\theta} (\vec{u} \cdot \vec{\nabla} u_j) = \sum_j \frac{v_j - u_j}{\theta} \sum_k u_k \frac{\partial u_j}{\partial x_k} = \\ &= \frac{1}{\theta} \sum_{j,k} (v_j - u_j) u_k \frac{\partial u_j}{\partial x_k} \end{aligned} \quad (\text{B.39})$$

$$\begin{aligned} \mathcal{A} &= \frac{1}{\theta} \sum_{j,k} \left[(v_j - u_j)(v_k - u_k) - \frac{1}{3} |\vec{v} - \vec{u}|^2 \delta_{jk} \right] \frac{\partial u_j}{\partial x_k} = \\ &= \frac{1}{\theta} \sum_{j,k} (v_j - u_j)(v_k - u_k) \frac{\partial u_j}{\partial x_k} - \frac{|\vec{v} - \vec{u}|^2}{3\theta} \sum_j \frac{\partial u_j}{\partial x_j} = \\ &= \frac{1}{\theta} \sum_{j,k} (v_j - u_j)(v_k - u_k) \frac{\partial u_j}{\partial x_k} - \frac{|\vec{v} - \vec{u}|^2}{3\theta} \operatorname{div} \vec{u} \end{aligned} \quad (\text{B.40})$$

Appendix B. Continuum and Kinetic Theory

$$\begin{aligned}
\mathcal{B} &= \left[\frac{|\vec{v} - \vec{u}|^2}{\theta} - 5 \right] \frac{\vec{v} - \vec{u}}{\sqrt{\theta}} \cdot \frac{1}{2\sqrt{\theta}} \vec{\nabla} \theta = \\
&= \frac{1}{2\theta} \left[\frac{|\vec{v} - \vec{u}|^2}{\theta} - 5 \right] (\vec{v} - \vec{u}) \cdot \vec{\nabla} \theta = \\
&= \frac{|\vec{v} - \vec{u}|^2}{2\theta^2} (\vec{v} - \vec{u}) \cdot \vec{\nabla} \theta - \frac{5}{2\theta} (\vec{v} - \vec{u}) \cdot \vec{\nabla} \theta
\end{aligned} \tag{B.41}$$

After substituting (B.39), (B.40), and (B.41) into the right hand side of (B.38) the expression $D_t \log f_0 = D$ becomes verified.

$$\begin{aligned}
RHS^1 &= \left(\frac{5(\vec{v} - \vec{u})}{2\theta} \cdot \vec{\nabla} \theta \right) + \left[\frac{1}{\theta} \sum_{j,k} (v_j - u_j) u_k \frac{\partial u_j}{\partial x_k} \right] + \left\{ \frac{|\vec{v} - \vec{u}|^2}{2\theta^2} \vec{u} \cdot \vec{\nabla} \theta \right\} + \\
&+ \frac{|\vec{v} - \vec{u}|^2}{3\theta} \operatorname{div} \vec{u} + \left[\frac{1}{\theta} \sum_{j,k} (v_j - u_j) (v_k - u_k) \frac{\partial u_j}{\partial x_k} \right] - \frac{|\vec{v} - \vec{u}|^2}{3\theta} \operatorname{div} \vec{u} + \\
&+ \left\{ \frac{|\vec{v} - \vec{u}|^2}{2\theta^2} (\vec{v} - \vec{u}) \cdot \vec{\nabla} \theta \right\} - \left(\frac{5}{2\theta} (\vec{v} - \vec{u}) \cdot \vec{\nabla} \theta \right) = \\
&= \left\{ \frac{|\vec{v} - \vec{u}|^2}{2\theta^2} \vec{v} \cdot \vec{\nabla} \theta \right\} + \left(\frac{1}{\theta} \sum_{j,k=1}^3 v_k (v_j - u_j) \frac{\partial u_j}{\partial x_k} \right) = LHS^1
\end{aligned} \tag{B.42}$$

B.5 Certain Orthogonality Relations for Tensors A and B

In this sections we verify that orthogonality relations for (1.123) and (1.124) hold. Since $\mathcal{Ker} L_{f_0}$ is a finite dimensional subspace of \mathcal{W}_{f_0} we have to verify that

$$\langle a_{ij}, \phi_k \rangle = 0, \tag{B.43}$$

$$\langle b_i, \phi_k \rangle = 0, \tag{B.44}$$

where ϕ_k are the collision invariants defined by (1.40) and the scalar product in \mathcal{W}_{f_0} is defined by (1.101)

¹RHS=right hand side, LHS=left hand side

Appendix B. Continuum and Kinetic Theory

We recall that $a_{i,j} = A_{i,j} \left(\frac{\vec{v} - \vec{u}}{\sqrt{\theta}} \right)$ and $b_i = B_i \left(\frac{\vec{v} - \vec{u}}{\sqrt{\theta}} \right)$ for A and B defined in (1.113) and (1.114):

$$A_{i,j}(\vec{V}) = V_i V_j - \frac{1}{3} |\vec{V}|^2 \delta_{i,j} \quad (\text{B.45})$$

$$B_i(\vec{V}) = \frac{1}{2} (|\vec{V}|^2 - 5) V_i \quad (\text{B.46})$$

Let $\alpha = \frac{1}{\sqrt{(2\pi\theta)^3}}$, let ϕ' be a collision invariant of a general form

$$\phi'(\vec{v}) = c'_0 + \vec{c}'_2 \cdot \vec{v} + c'_4 |\vec{v}|^2 \quad (\text{B.47})$$

and let ϕ be a translation of ϕ'

$$\phi(\vec{v}) = \phi'(\vec{v} + \vec{u}) = c_0(\vec{u}) + \vec{c}_2(\vec{u}) \cdot \vec{v} + c_4(\vec{u}) |\vec{v}|^2. \quad (\text{B.48})$$

It suffices to demonstrate that $\langle a_{ij}, \phi \rangle = 0$ and $\langle b_i, \phi \rangle = 0$ for ϕ defined by (B.46).

$$\langle a_{ij}, \phi \rangle = \frac{\alpha}{\theta} \int_{\mathbb{R}^3} e^{-\frac{|\vec{v}-\vec{u}|^2}{2\theta}} \left[(v_i - u_i)(v_j - u_j) - \frac{1}{3} |\vec{u} - \vec{v}|^2 \delta_{ij} \right] \phi'(\vec{v}) d\vec{v}. \quad (\text{B.49})$$

We use change of variables $\vec{\xi} = \vec{u} - \vec{v}$ and translation property of collision invariants (B.48)

$$\langle a_{ij}, \phi \rangle = \frac{\alpha}{\theta} \int_{\mathbb{R}^3} e^{-\frac{|\vec{\xi}|^2}{2\theta}} \left[\xi_i \xi_j - \frac{1}{3} |\vec{\xi}|^2 \delta_{ij} \right] \phi(\vec{\xi}) d\vec{\xi}. \quad (\text{B.50})$$

Utilizing the notations of the moments from Table A.1 on page 126, the expression above can be rewritten as

$$\begin{aligned} \theta \langle a_{ij}, \phi \rangle &= c_0(\vec{u}) \left[\mathcal{G}_{i,j}(\theta) - \frac{\delta_{ij}}{3} \mathcal{G}_2(\theta) \right] + \sum_{k=1}^3 c_2^k(\vec{u}) \left[\mathcal{G}_{i,j,k}(\theta) - \frac{\delta_{ij}}{3} \mathcal{G}_k^2(\theta) \right] + \\ &+ c_3(\vec{u}) \left[\mathcal{G}_{i,j}^2(\theta) - \frac{\delta_{ij}}{3} \mathcal{G}_4(\theta) \right] \end{aligned} \quad (\text{B.51})$$

Appendix B. Continuum and Kinetic Theory

According to Table A.1 we have

$$\mathcal{G}_{i,j}(\theta) - \frac{\delta_{ij}}{3}\mathcal{G}_2(\theta) = \mathcal{G}_{i,j,k}(\theta) = \frac{\delta_{ij}}{3}\mathcal{G}_k^2(\theta) = \mathcal{G}_{i,j}^2(\theta) - \frac{\delta_{ij}}{3}\mathcal{G}_4(\theta) = 0 \quad (\text{B.52})$$

and hence the orthogonality (B.43) has been proven. We proceed in a similar way to prove (B.44).

$$\begin{aligned} \langle b_i, \phi \rangle &= \frac{\alpha}{2\sqrt{\theta}} \int_{\mathbb{R}^3} e^{-\frac{|\vec{\xi}|^2}{2\theta}} \left[\frac{|\vec{\xi}|^2}{\theta} - 5 \right] \xi_i \phi(\vec{\xi}) d\vec{\xi} = \\ &= \frac{c_0(\vec{u})}{2\sqrt{\theta}} \left[\frac{\mathcal{G}_i^2(\theta)}{\theta} - 5\mathcal{G}_i^0(\theta) \right] + \\ &+ \frac{1}{2\sqrt{\theta}} \sum_{k=1}^3 c_2^k(\vec{u}) \left[\frac{\mathcal{G}_{i,k}^2(\theta)}{\theta} - 5\mathcal{G}_{i,k}(\theta) \right] + \frac{c_3(\vec{u})}{2\sqrt{\theta}} \left[\frac{\mathcal{G}_i^4(\theta)}{\theta} - 5\mathcal{G}_i^2(\theta) \right] \end{aligned} \quad (\text{B.53})$$

By looking up the corresponding values of moments $\mathcal{G}(\theta)$ in Table A.1 we establish that

$$\frac{\mathcal{G}_i^2(\theta)}{\theta} = 5\mathcal{G}_i^0(\theta) = \frac{\mathcal{G}_{i,k}^2(\theta)}{\theta} - 5\mathcal{G}_{i,k}(\theta) = \frac{\mathcal{G}_i^4(\theta)}{\theta} = 5\mathcal{G}_i^2(\theta) = 0 \quad (\text{B.54})$$

and therefore (B.44) is verified.

B.6 A Transformation of the Compressible Euler System

In this section we will demonstrate that the following two systems are equivalent.

$$\begin{aligned} \partial_t \rho + \vec{u} \cdot \vec{\nabla} \rho + \rho \operatorname{div} \vec{u} &= 0, \\ \partial_t \vec{u} + \vec{u} * \vec{\nabla} \vec{u} + \vec{\nabla} \theta + \frac{\theta}{\rho} \vec{\nabla} \rho &= 0, \\ \partial_t \theta + \vec{u} \cdot \vec{\nabla} \theta + \frac{2}{3} \theta \operatorname{div} \vec{u} &= 0; \end{aligned} \quad (\text{B.55})$$

Appendix B. Continuum and Kinetic Theory

$$\begin{aligned}
\partial_t \rho + \operatorname{div}(\rho \vec{u}) &= 0, \\
\partial_t(\rho \vec{u}) + \operatorname{Div}(\rho \vec{u} \otimes \vec{u}) + \vec{\nabla}(\rho \theta) &= 0, \\
\partial_t \left(\frac{1}{2} \rho |\vec{u}|^2 + \frac{3}{2} \rho \theta \right) + \operatorname{div} \left[\rho \vec{u} \left(\frac{1}{2} |\vec{u}|^2 + \frac{5}{2} \theta \right) \right] &= 0.
\end{aligned} \tag{B.56}$$

First we provide several differential identities that will be useful and further considerations. It is assumed that all mapping in this section are smooth and have sufficient number of partial derivatives. It is trivial to establish that for scalar fields $\rho, \theta : \mathbb{R}^3 \rightarrow \mathbb{R}$ and for a vector field $\vec{u} : \mathbb{R}^3 \rightarrow \mathbb{R}^3$ the following differentiation rules hold:

$$\operatorname{div}(\rho \vec{u}) = \vec{\nabla} \rho \cdot \vec{u} + \rho \operatorname{div} \vec{u} \tag{B.57}$$

$$\vec{\nabla}(\rho \theta) = \theta \vec{\nabla} \rho + \rho \vec{\nabla} \theta. \tag{B.58}$$

The gradient $\vec{\nabla}$ is extended to vector fields by (1.115) on page 30. Operations Div and $*$ were defined by (1.44) on page 15 and (1.116) on page 29 correspondingly. We observe that

$$\begin{bmatrix} \operatorname{div}(\rho u_1 \vec{u}) \\ \operatorname{div}(\rho u_2 \vec{u}) \\ \operatorname{div}(\rho u_3 \vec{u}) \end{bmatrix} = \begin{bmatrix} \rho \vec{u} \cdot \vec{\nabla} u_1 + u_1 \operatorname{div}(\rho \vec{u}) \\ \rho \vec{u} \cdot \vec{\nabla} u_2 + u_2 \operatorname{div}(\rho \vec{u}) \\ \rho \vec{u} \cdot \vec{\nabla} u_3 + u_3 \operatorname{div}(\rho \vec{u}) \end{bmatrix}, \tag{B.59}$$

therefore

$$\operatorname{Div}(\rho \vec{u} \otimes \vec{u}) = \rho \vec{u} * \vec{\nabla} \vec{u} + \vec{u} \operatorname{div}(\rho \vec{u}). \tag{B.60}$$

Property (B.57) immediately implies that the first equations of (B.55) and (B.56) are equivalent.

The second equation of (B.56) takes form

$$\rho \partial_t \vec{u} + \vec{u} \partial_t \rho + \rho \vec{u} * \vec{\nabla} \vec{u} + \vec{u} \operatorname{div}(\rho \vec{u}) + \vec{\nabla}(\rho \theta) = 0 \tag{B.61}$$

Appendix B. Continuum and Kinetic Theory

Since $\vec{u}(\partial_t \rho + \text{div} \rho \vec{u}) = 0$ because of the continuity equation and since $\vec{\nabla}(\rho \theta) = \theta \vec{\nabla} \rho + \rho \vec{\nabla} \theta$, equation (B.61) becomes

$$\rho \partial_t \vec{u} + \rho \vec{u} * \vec{\nabla} \vec{u} + \theta \vec{\nabla} \rho + \rho \vec{\nabla} \theta = 0, \quad (\text{B.62})$$

which is equivalent to the second equation of (B.55). Thus the equivalence of the first two equations of (B.55) and (B.56) has been established.

To establish equivalence of the third equations we assume that

$$\partial_t \left(\frac{1}{2} \rho |\vec{u}|^2 + \frac{3}{2} \rho \theta \right) + \text{div} \left[\rho \vec{u} \left(\frac{1}{2} |\vec{u}|^2 + \frac{5}{2} \theta \right) \right] = 0 \quad (\text{B.63})$$

is true. We observe that $\vec{u} \cdot \partial_t \vec{u} = \frac{1}{2} \partial_t |\vec{u}|^2$ and

$$\begin{aligned} \rho \vec{u} \cdot (\vec{u} * \vec{\nabla} \vec{u}) &= \rho \sum_{j=1}^3 u_j (\vec{u} \cdot \vec{\nabla} u_j) = \rho \sum_{j=1}^3 \vec{u} \cdot (u_j \vec{\nabla} u_j) = \\ &= \rho \vec{u} \cdot \sum_{j=1}^3 u_j \vec{\nabla} u_j = \rho \vec{u} \cdot \sum_{j=1}^3 \vec{\nabla} \frac{u_j^2}{2} = \frac{1}{2} \rho \vec{u} \cdot \vec{\nabla} |\vec{u}|^2 \end{aligned} \quad (\text{B.64})$$

We multiply the second equation of (B.55) by $\rho \vec{u}$ and use (B.64):

$$\frac{1}{2} \rho \partial_t |\vec{u}|^2 + \frac{1}{2} \rho \vec{u} \cdot \vec{\nabla} |\vec{u}|^2 + \rho \vec{u} \cdot \vec{\nabla} \theta + \theta \vec{u} \cdot \vec{\nabla} \rho = 0, \quad (\text{B.65})$$

equivalently, since $\frac{1}{2} \partial_t (\rho |\vec{u}|^2) = \frac{1}{2} \rho \partial_t |\vec{u}|^2 + \frac{1}{2} |\vec{u}|^2 \partial_t \rho$, we have that

$$\frac{1}{2} \partial_t (\rho |\vec{u}|^2) + \left[-\frac{1}{2} |\vec{u}|^2 \partial_t \rho + \frac{1}{2} \rho \vec{u} \cdot \vec{\nabla} |\vec{u}|^2 \right] + \rho \vec{u} \cdot \vec{\nabla} \theta + \theta \vec{u} \cdot \vec{\nabla} \rho = 0. \quad (\text{B.66})$$

Since the continuity equation holds $-\frac{1}{2} |\vec{u}|^2 \partial_t \rho = \frac{1}{2} |\vec{u}|^2 \text{div}(\rho \vec{u})$ and therefore after applying (B.57) the term in brackets reduces to

$$-\frac{1}{2} |\vec{u}|^2 \partial_t \rho + \frac{1}{2} \rho \vec{u} \cdot \vec{\nabla} |\vec{u}|^2 = \frac{1}{2} |\vec{u}|^2 \text{div}(\rho \vec{u}) + \frac{1}{2} \rho \vec{u} \cdot \vec{\nabla} |\vec{u}|^2 = \frac{1}{2} \text{div}(\rho |\vec{u}|^2 \vec{u}). \quad (\text{B.67})$$

Appendix B. Continuum and Kinetic Theory

After noticing that $\rho \vec{u} \cdot \vec{\nabla} \theta + \theta \vec{u} \cdot \vec{\nabla} \rho = \vec{u} \cdot \vec{\nabla}(\rho \theta)$, equation (B.66) transforms to

$$\frac{1}{2} \partial_t (\rho |\vec{u}|^2) + \frac{1}{2} \operatorname{div} (\rho |\vec{u}|^2 \vec{u}) + \vec{u} \cdot \vec{\nabla}(\rho \theta) = 0. \quad (\text{B.68})$$

Now we subtract (B.68) from the equation we assumed was correct (B.63):

$$\frac{3}{2} \partial_t (\rho \theta) + \frac{5}{2} \operatorname{div}(\rho \theta \vec{u}) - \vec{u} \cdot \vec{\nabla}(\rho \theta) = 0 \quad (\text{B.69})$$

The following chain of transformations finalizes the proof.

$$\frac{3}{2} \partial_t (\rho \theta) + \frac{3}{2} \operatorname{div}(\rho \theta \vec{u}) + \underbrace{\operatorname{div}(\rho \theta \vec{u}) - \vec{u} \cdot \vec{\nabla}(\rho \theta)}_{\rho \theta \operatorname{div} \vec{u}} = 0 \quad (\text{B.70})$$

$$\partial_t (\rho \theta) + \operatorname{div}(\rho \theta \vec{u}) + \frac{2}{3} \rho \theta \operatorname{div} \vec{u} = 0. \quad (\text{B.71})$$

Applying the continuity equation:

$$(\rho \partial_t \theta + \underbrace{\theta \partial_t \rho}_0) + (\theta \operatorname{div}(\rho \vec{u}) + \rho \vec{u} \cdot \vec{\nabla} \theta) + \frac{2}{3} \rho \theta \operatorname{div} \vec{u} = 0. \quad (\text{B.72})$$

Dividing by ρ :

$$\partial_t \theta + \vec{u} \cdot \vec{\nabla} \theta + \frac{2}{3} \theta \operatorname{div} \vec{u} = 0, \quad (\text{B.73})$$

which is the third equation in system (B.55).

Thus it has been proven that (B.55) is equivalent to (B.56).

Appendix C

Technical Calculations for Numerical Solutions

C.1 Truncation Error Estimation Theorem

Theorem 2 Let $\rho, u, \theta > 0$ be positive constants and $B(V) = (-\infty, -V) \cup (V, +\infty)$.

Then for $n = 0, 1, 2, \dots$ and for V satisfying

$$V \geq \max \left\{ 1, 2u, u + \sqrt{2\theta} \right\} \quad (\text{C.1})$$

the following inequality holds :

$$\left| \int_{B(V)} v^n \exp \left\{ -\frac{(v-u)^2}{2\theta} \right\} dv \right| \leq \alpha_n \exp \left\{ -\frac{V-u}{2\sqrt{2\theta}} \right\} \quad (\text{C.2})$$

where

$$\alpha_n = 2^{\frac{5(n+1)}{2}} \theta^{\frac{n+1}{2}} n^n e^{-n} \quad (\text{C.3})$$

Appendix C. Technical Calculations for Numerical Solutions

and 0^0 should be treated as 1.

Proof. Assume (C.1) holds and let

$$J_n(u, \theta, V) = \int_{B(V)} v^n e^{-\frac{(v-u)^2}{2\theta}} dv \quad (\text{C.4})$$

then

$$|J_n(u, \theta, V)| \leq \int_V^{+\infty} v^n e^{-\frac{(v-u)^2}{2\theta}} dv + \int_{-\infty}^{-V} |v|^n e^{-\frac{(v-u)^2}{2\theta}} dv \quad (\text{C.5})$$

After substitution $v \mapsto -v$ in the second integral in (C.5) we obtain

$$\int_V^{+\infty} v^n \left[e^{-\frac{(v-u)^2}{2\theta}} + e^{-\frac{(u+v)^2}{2\theta}} \right] dv = 2 \int_V^{+\infty} v^n e^{-\frac{u^2+v^2}{2\theta}} \cosh \frac{uv}{\theta} dv \quad (\text{C.6})$$

Since $\cosh x \leq e^x$ for $x \geq 0$ we have

$$|J_n(u, \theta, V)| \leq 2 \int_V^{+\infty} v^n e^{-\frac{(v-u)^2}{2\theta}} dv \quad (\text{C.7})$$

Assume that $n \geq 1$ and let $\xi = \frac{v-u}{\sqrt{2\theta}}$ then

$$\int_V^{+\infty} v^n e^{-\frac{(v-u)^2}{2\theta}} dv = \sqrt{2\theta} \int_{\frac{V-u}{\sqrt{2\theta}}}^{+\infty} (\xi\sqrt{2\theta} + u)^n e^{-\xi^2} d\xi \quad (\text{C.8})$$

Since we assumed that (C.1) is true we have

$$V \geq 2u \iff \frac{u}{\sqrt{2\theta}} \leq \frac{V-u}{\sqrt{2\theta}} \leq \xi \implies u \leq \xi\sqrt{2\theta} \implies \xi\sqrt{2\theta} + u \leq 2\xi\sqrt{2\theta} \quad (\text{C.9})$$

Appendix C. Technical Calculations for Numerical Solutions

furthermore by (C.1)

$$1 \leq V \leq \xi\sqrt{2\theta} + u \leq 2\xi\sqrt{2\theta} \quad (\text{C.10})$$

and thus

$$(\xi\sqrt{2\theta} + u)^n \leq (2\xi\sqrt{2\theta})^n \quad (\text{C.11})$$

$$|J_n(u, \theta, V)| \leq (2\sqrt{2\theta})^{n+1} \int_{\frac{V-u}{\sqrt{2\theta}}}^{+\infty} \xi^n e^{-\xi^2} d\xi \quad (\text{C.12})$$

According to the assumption (C.1)

$$\xi \geq \frac{V-u}{\sqrt{2\theta}} \geq 1 \implies e^{-\xi^2} \leq e^{-\xi} \quad (\text{C.13})$$

and therefore

$$|J_n(u, \theta, V)| \leq 2^{n+1}(2\theta)^{\frac{n+1}{2}} \int_{\frac{V-u}{\sqrt{2\theta}}}^{+\infty} \xi^n e^{-\xi} d\xi \quad (\text{C.14})$$

Consider function

$$\psi_n(\xi) = \xi^n e^{-\frac{1}{2}\xi}, \quad \xi \geq 0 \quad (\text{C.15})$$

Its derivative is given by

$$\psi'_n(\xi) = \xi^{n-1} e^{-\frac{1}{2}\xi} \left(n - \frac{1}{2}\xi \right) \quad (\text{C.16})$$

Function ψ_n attains its absolute maximum

$$\psi_n^* = (2n)^n e^{-n} \quad (\text{C.17})$$

Appendix C. Technical Calculations for Numerical Solutions

at $\xi_n^* = 2n$ and therefore

$$\psi_n(\xi) \leq \psi_n^* \quad \forall \xi \geq 0 \quad (\text{C.18})$$

It follows from (C.18) that

$$\xi^n \leq (2n)^n e^{-n} e^{\frac{1}{2}\xi} \quad \forall \xi \geq 0 \quad (\text{C.19})$$

Applying (C.19) to (C.15) we obtain

$$|J_n(u, \theta, V)| \leq 2^{\frac{5n+1}{2}} \theta^{\frac{n+1}{2}} \left(\frac{n}{e}\right)^n \int_{\frac{V-u}{\sqrt{2\theta}}}^{+\infty} e^{-\frac{1}{2}\xi} d\xi = 2^{\frac{5n+3}{2}} \theta^{\frac{n+1}{2}} \left(\frac{n}{e}\right)^n e^{-\frac{V-u}{2\sqrt{2\theta}}} \quad (\text{C.20})$$

After defining¹ $\alpha_n = 2^{\frac{5(n+1)}{2}} \theta^{\frac{n+1}{2}} n^n e^{-n}$ the result follows for $n \geq 1$.

Consider case $n = 0$. All calculations prior to and including (C.8) are valid and therefore we have

$$|J_0(u, \theta, V)| \leq 2\sqrt{2\theta} \int_{\frac{V-u}{\sqrt{2\theta}}}^{+\infty} e^{-\xi^2} d\xi \leq 2\sqrt{2\theta} \int_{\frac{V-u}{\sqrt{2\theta}}}^{+\infty} e^{-\frac{1}{2}\xi} d\xi = 4\sqrt{2\theta} e^{-\frac{V-u}{2\sqrt{2\theta}}} \quad (\text{C.21})$$

We notice that according to (C.3) $\alpha_0 = 4\sqrt{2\theta}$ and this finalizes the proof. \square

C.2 Computation of the Determinant of M

Let M be as in (4.63). Then after substituting the expression for transformation T (2.66) we obtain

¹ α_n was taken twice the coefficient in (C.20) to insure that case $n = 0$ conforms to the formula (C.3) provided 0^0 is treated as 1.

Appendix C. Technical Calculations for Numerical Solutions

$$\begin{aligned}
 \det M &= \det \left[\begin{array}{ccc|cc} 1 & 0 & 0 & * & * & \rho\theta^{-1} \\ 0 & 1 & 0 & * & * & 0 \\ 0 & 0 & 1 & * & * & 1 \\ \hline \phi_1 & \phi_2 & \phi_3 & 0 & 0 & 0 \\ 0 & 0 & 0 & 1 & 0 & 0 \\ 0 & 0 & 0 & 0 & 1 & 0 \end{array} \right] = \det \left[\begin{array}{ccc|cc} 1 & 0 & 0 & * & * & \rho\theta^{-1} \\ 0 & 1 & 0 & * & * & 0 \\ 0 & 0 & 1 & * & * & 1 \\ \hline \phi_1 & \phi_2 & \phi_3 & 0 & 0 & 0 \\ 0 & 0 & 0 & 1 & 0 & 0 \\ \hline 0 & 0 & 0 & 0 & 1 & 0 \end{array} \right] \\
 &= -\det \left[\begin{array}{ccc|c} 1 & 0 & 0 & * \\ 0 & 1 & 0 & * \\ 0 & 0 & 1 & * \\ \hline \phi_1 & \phi_2 & \phi_3 & 0 \\ 0 & 0 & 0 & 1 \end{array} \right] \rho\theta^{-1} = +\det \left[\begin{array}{ccc|c} 1 & 0 & 0 & \rho\theta^{-1} \\ 0 & 1 & 0 & 0 \\ 0 & 0 & 1 & 1 \\ \hline \phi_1 & \phi_2 & \phi_3 & 0 \end{array} \right] = -(\phi_3 + \phi_1\rho\theta^{-1})
 \end{aligned}$$

C.3 Expressions for $\mathcal{J}\mathcal{F}_{NL}(W)$ and $\mathcal{J}\mathcal{F}'_{NL}(W)$

The expression for \vec{F}_{NL} is provided in (4.45)

Based on (4.38) \mathcal{F}_{NL} has the form of

$$\mathcal{F}_{NL}(\vec{w}_1, \vec{w}_2, \dots, \vec{w}_N) = \frac{1}{2} \begin{bmatrix} 0 \\ 0 \\ \frac{w_{2,1}^2}{0} \\ 0 \\ \frac{w_{2,2}^2}{0} \\ 0 \\ \frac{w_{2,3}^2}{\dots} \\ 0 \\ 0 \\ \frac{w_{2,N-1}^2}{0} \\ 0 \\ w_{2,N}^2 \end{bmatrix} \quad (\text{C.22})$$

Let

$$\partial_{i,j} = \frac{\partial}{\partial w_{i,j}}, \quad (\text{C.23})$$

References

- [1] P. L. Bhatnagar, E. P. Gross, M. Krook, *A Model for Collision Processes in Gases. I. Small Amplitude Processes in Charged and Neutral One-Component Systems*, Physical Review, Volume 94, Number 3, May 1954, pp.511-525.
- [2] L. Boltzmann, *Weitere Studien über das Wärmegleichgewicht unter Gasmolekülen*, Wiener Berichte 66, 1872, pp.275-371.
- [3] F. Bouchut, F. Golse, M. Pulvirenti, *Kinetic Equations and Asymptotic Theory*; L.Desvillettes & B.Perthame ed., Editions scientifiques et médicales Elsevier, Paris, 2000.
- [4] J. A. Bittencourt, *Fundamentals of plasma physics*, Springer, 2004 ISBN 0387209751, 9780387209753.
- [5] T. Carleman, Acta Math. 60:91, 1933.
- [6] T. Carleman, *Problèmes Mathématiques dans la théorie cinétique des gaz*, Notes written by Carleson and Frostman, Uppsala, Almqvist and Wikselles, 1957.
- [7] C. Cercignani, A. Palczewski, *Existence and Uniqueness for Nonlinear Boundary Value Problems in Kinetic Theory*, Journal of Statistical Physics, Volume 46, Numbers 1-2, January, 1987, pp.273-281.
- [8] C. Cercignani, R. Illner, M. Pulvirenti, *The Mathematical Theory of Dilute Gases*, Springer Verlag, New York, NY 1994.
- [9] S. Chapman, T. G. Cowling, *The Mathematical Theory of Nonuniform Gases*, Cambridge University Press, London, 1960.
- [10] C. F. Delale, *The Hilbert Expansion to the Boltzmann Equation for Steady Flow*, Journal of Statistical Physics, Volume 28, pp.589-602.

References

- [11] P. Ehrenfest, T. Ehrenfest, *Begriffliche Grundlagen der statistischen Auffassung in der Mechanik*, Encyklopädie der mathematischen Wissenschaften, mit Einschluß ihrer Anwendungen, Vol. 4, eds. Felix Klein and Conrad Müller, 1911, (Leipzig: Teubner, 1907-1914), pp. 190. English translation: M. J. Moravcsik, *The Conceptual Foundations of the Statistical Approach in Mechanics*, Cornell University Press, 1959. ISBN 0486495043.
- [12] D. Enskog, *Theorie der Vorgänge in Massing Verdumten Gasen*, Ph.D thesis, University of Uppsala, Sweden, 1917.
- [13] S. Friedlander, D. Serre, *Handbook of Mathematical Fluid Dynamics*, Elsevier, 2004 ISBN 0444515569, 9780444515568.
- [14] J. Goodrich, T. Hagstrom, J. Lorenz, *Explicit Solution of the Equations for a Viscous Shock Layer*, Department of Mathematics and Statistics, UNM, Albuquerque, NM 87131, August 2003.
- [15] H. Grad, *On the Kinetic Theory of Rarefied Gases*, Communications on Pure and Applied Mathematics, 2:331, 1949.
- [16] V. Garzó, A. Santos, *Kinetic Theory of Gases in Shear Flows: Nonlinear Transport* Springer, 2003 ISBN 1402014368, 9781402014369.
- [17] B. Gustafsson, H.O. Kreiss, J. Oliger, *Time Dependent Problems and Difference Methods*, Wiley-Interscience, 1996 ISBN 0471507342, 9780471507345.
- [18] F. Golse, C.D. Levermore, *Hydrodynamic Limits of Kinetic Models* in *Topics in Kinetic Theory*, T. Passot et al. eds.; Fields Institute Communications 46, American Mathematical Society, Providence, 2005.
- [19] H. O. Kreiss, J. Lorenz, *Initial-Boundary Value Problems and the Navier-Stokes Equations*, ACADEMIC PRESS, INC., San Diego, CA, 1989, ISBN 0-12-426125-6.
- [20] P. A. Lagerstrom, F. K. Moore, *Laminar Flow Theory*, Princeton University Press, 1996, ISBN 0-69-102598-3.
- [21] C. B. Laney, *Computational gasdynamics*, Cambridge University Press, 1998 ISBN 0521625580, 9780521625586.
- [22] P. D. Lax, *Hyperbolic Systems of Conservation Laws and Mathematical Theory of Shock Waves*, SIAM, Philadelphia, 1973.
- [23] B. Perthame, P. Souganidis, *Intorduction to the collision models in the Boltzmann's theory*, in *Modeling of Collisions*, P.-A. Raviart ed., Masson, Paris, 1997.
- [24] L. A. Santalò, *Sobre la distribución probable de corpúsculos en un cuerpo, deducida de la distribución en sus secciones y problemas analogos*, Revista Unión Mat. Argentina 9 1943, pp.145-164.

References

- [25] Y. Sone, *Kinetic Theory and Fluid Dynamics*, Birkhäuser, Boston 2002.
- [26] P. Wesseling, *Principles of Computational Fluid Dynamics*, Springer, 2001 ISBN 3540678530, 9783540678533.